Τ.Ε.Ι. ΚΡΗΤΗΣ
ΤΜΗΜΑ ΦΥΣΙΚΩΝ ΠΟΡΩΝ ΚΑΙ ΠΕΡΙΒΑΛΛΟΝΤΟΣ

ΠΤΥΧΙΑΚΗ ΕΡΓΑΣΙΑ

ΟΝΟΜΑ: ***ΑΘΑΝΑΣΙΟΣ***
ΕΠΩΝΥΜΟ: ***ΑΡΓΥΡΙΟΥ***

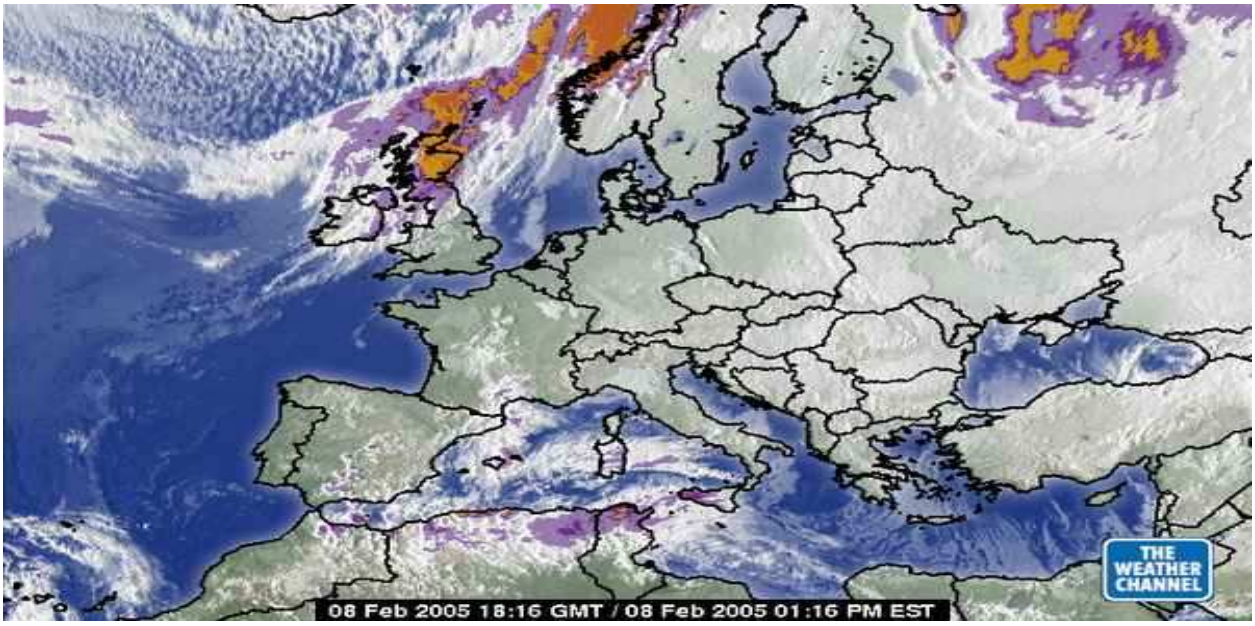

ΘΕΜΑ :
"Development of an integrated GIS for the interpretation of satellite derived Thermal Infra-Red (TIR) anomalies possibly related to impending earthquakes"

ΕΠΙΒΛΕΠΟΝΤΕΣ ΚΑΘΗΓΗΤΕΣ :
ΒΑΛΛΙΑΝΑΤΟΣ ΦΙΛΙΠΠΟΣ
TRAMUTOLI VALERIO

ΧΑΝΙΑ2005

INTRODUCTION

In the work that has been made below we will have the chance to learn some basic things about the Geographic Information Systems(GIS) , a tool which the last years with the spreadsheet development of technology and science has become useful all over the world. The GIS can find applications in many sectors of our life and could be helpful to reach important conclusions and have a clearest picture of any sector that they occupy.

Remote sensing is an inseparable piece of geographic infomation systems and by his turn the benefits that we can obtain are significant for our lives.

GIS and remote sensing have found great application in geologic science and specially in the sector of earthquakes . It is an important tool in order to collect many informations and have a better overview and better conclusions over the features and the seismicity of a seismic area that interests us .

In the eighties, satellite techniques have been proposed for the observation of pre and co-seismic events, just as for the estimation of the following years over the seismic events .

Between these , those that today are considered to be more promising for the study of pre and co-seismic phenomena are : The analyse of crystal deformations, with the use of interferometria SAR differential , the analyse of motion, the ionosferic heating and the instability of the plasma, causes the emission of the electromagnetic potentially correlated with the pre-seismic events, analyse of the radiation emissions from the Earth of the infrared thermal , potentially correlabile with the preparation phases of the seismic events .

In this job of thesis we occupying the last phenomenologia , that is the study of possible pre and co-seismic events, on the base of measures of the infrared thermal , of the radiation emitted from the land surface . For that purpose we are going to view a robust approach called RAT (Robust AVHHR Technique) which is proposed for the identification of space time thermal anomalies . In this technique, long term satellite records are used in order to evaluate the possible correlation,in the space-time domain,between TIR anomalies and pre/co-seismic phenomena by using different methologies in different geographic scenarios.Independent measurements based on GPS ,seismometric ,multi-parametric (geothermal , geochemical,geoelectrical)networks, as well as systematic campaigns of magnetotelluric and electromagnetic tomographic survey are analysed in order to verify explanatory physical models which can justify satellite observations.All significant changes in the measured parameters are compared with both satellite TIR anomaly fields and earthquake occurences, in order to confirm or reject, the proposed models for thermal anomaly occurence explanation. The above have been applied to the Irpinia-Basilicata(Southern Italy)earthquake of November 23rd,1980(Ms=6.9)in order to obtain a preliminary estimate of the signal-to-noise ratio associated to the TIR signal measured by NOAA/AVHRR before,during and after the seismic event.

1° CAPITAL

1.1. Introduction GIS

GIS through history

Some 35,000 years ago, Cro-Magnon hunters drew pictures of the animals they hunted on the walls of caves near Lascaux, France. Associated with the animal drawings are track lines and tallies thought to depict migration routes. These early records followed the two-element structure of modern geographic information systems (GIS): a graphic file linked to an attribute database.

If we look back to the first observations made by Galileo in 1610 when he turned a telescope to the heavens and caught a glimpse of the surface complexities exhibited on our nearest neighbour, the Moon, and then later confirmed the Copernican Revolution with his discoveries of moons, or orbiting satellites, around Jupiter.

Since then, first with telescopes and, after the opening of the Space Age, with orbiting spacecraft, flyby, probe, and lander missions to the Moon and the planets, most of the same instruments that survey the electromagnetic spectrum interacting with the Earth have been the principal tools used in exploring our planetary associates and beyond - searching well into outer space to look at stars and other members of the Universe.

The science of 'remote sensing' in its broadest sense has been developing since the 19th century with the invention of photography and the first aerial photographs taken from captive balloons. Throughout the 20th century, technological advances in a number of areas - the development of colour and infrared sensitive films,

aircraft and satellite platforms - enlarged the sphere of remote sensing with the development of applications such as mapping, geological exploration and meteorology making use of remotely sensed images.

Remote sensing as it is currently practised, however, began with two major advances in technology - the launch of high resolution digital imaging systems (starting with Landsat-1 in 1972) and the development of minicomputers and image-display terminals in the 1970s.

With these advances, image processing systems rapidly evolved. By the early 1980s, a typical system would have functionality for image input, geometric correction, classification (supervised and unsupervised), image enhancement, convolution, arithmetic functions (e.g. band rationing) and principal components analysis. These would be performed as batch or interactive operations, with special frame-store hardware used for image display.

The evolution continued throughout the 1980s, with an increased range of processing functions, data from new sensors (Landsat TM, SPOT, radar, airborne multispectral scanners), faster processors, higher resolution displays and user-friendly menu interfaces. Interfaces to vector data are provided by most systems, although functionality is largely limited to overlay of the data over imagery.

As the computer spreadsheet changed the way people organized and used information in the 1980s, so is GIS doing the same thing today, in an even more powerful way. GIS facilitates wise use of limited resources by clarifying characteristics and patterns over space. It's especially useful for problem-solving situations.

GIS has found great application in geologic science and specially in the sector of earthquakes . It is an important tool in order to collect many informations and have a better overview and better conclusions over the features and the seismicity of a seismic area that interests us.

Though most of the data, like geologic features, seismic features etc , is not new and has been available to the public for nearly a decade, most of it has never been presented in an easy-to-understand format using GIS technology and made available to public .

1.2.What is GIS?

Introduction

GIS is a rapidly growing technological field that incorporates graphical features with tabular data in order to assess real-world problems. The GIS field began around 1960, with the discovery that maps could be programmed using simple code and then stored in a computer allowing for future modification when necessary. This was a welcome change from the era of hand *cartography* when maps had to be painstakingly created by hand; even small changes required the creation of a new map. The earliest version of a GIS was known as computer cartography and involved simple line work to represent land features. From that evolved the concept of overlaying different mapped features on top of each other to determine patterns and causes of spatial phenomenon.

Definition of GIS

Like the field of geography, the term Geographic Information System (GIS) is hard to define. It represents the integration of many subject areas. Accordingly there us no absolutely agreed upon definition of a GIS (deMers, 1997). A broadly accepted definition of GIS is the one provided by the National Centre of Geographic Information and Analysis: a GIS is a system of hardware, software and procedures to facilitate the management, manipulation, analysis, modelling, representation and display of georeferenced data to solve complex problems regarding planning and management of resources (NCGIA, 1990). Geographic information systems have emerged in the last decade as an essential tool for urban and resource planning and management. Their capacity to store, retrieve, analyse, model and map large areas with huge volumes of spatial data has led to an extraordinary proliferation of applications.

A Geographic Information System (GIS) is a tool that uses the power of the computer to pose and answer geographic questions. The user guides the program to arrange and display data about places on the planet in a variety of ways – including maps, charts and tables. The hardware and software allows the users to see and interact with data in new ways by blending electronic maps and databases to generate colour-coded displays. Users can zoom in and out of maps freely, add layers of new data, and study detail and relationships.

The key word to this technology is Geography - this usually means that the data (or at least some proportion of the data) is spatial, in other words, data that is in some way referenced to locations on the earth. Coupled with this data is usually data known as attribute data. Attribute data generally defined as additional

information, which can then be tied to spatial data. An example of this would be schools. The actual location of the schools is the spatial data. Additional data such as the school name, level of education taught, school capacity would make up the attribute data. It is the partnership of these two data types that enables GIS to be such an effective problem solving tool.

A Geographical Information System generally is a collection of *spatially referenced* data (i.e. data that have locations attached to them) and the tools required to work with the data. Nowadays we normally associate the term with computers, but a (properly organized) set of file cabinets, a calculator (when available), pens, pencils, drafting table, etc., was the GIS available to people before computers.

The capabilities of GIS are a far cry from the simple beginnings of computer *cartography.* At the simplest level, GIS can be thought of as a high-tech equivalent of a map. However, not only can paper maps be produced far quicker and more efficiently, the storage of data in an easily accessible digital format enables complex analysis and modeling not previously possible. The reach of GIS expands into all disciplines and has been used for such widely ranged problems as prioritizing sensitive species habitat to determining optimal real estate locations for new businesses.

GIS operates on many levels. On the most basic level, GIS is used as computer *cartography*, i.e. mapping. The real power in GIS is through using spatial and statistical methods to analyze attribute and geographic information. The end result of the analysis can be derivative information, interpolated information or prioritized information.

GIS has been defined by the Association for Geographic Information as:

A system for capturing, storing, checking, integrating, manipulating, analyzing, and displaying data which are spatially referenced to the Earth.

Other quotes to answer "What is GIS?" :

"In the strictest sense, a GIS is a computer system capable of assembling, storing, manipulating, and displaying geographically referenced information, i.e. data identified according to their locations. Practitioners also regard the total GIS as including operating personnel and the data that go into the system." **USGS**

"A geographic information system (GIS) is a computer-based tool for mapping and analyzing things that exist and events that happen on earth. GIS technology integrates common database operations such as query and statistical analysis with the unique visualization and geographic analysis benefits offered by maps." **ESRI**

"GIS is an integrated system of computer hardware, software, and trained personnel linking topographic, demographic, utility, facility, image and other resource data that is geographically referenced." **NASA**

GIS has already affected most of us in some way without us even realizing it. If you've ever using an Internet mapping program to find directions, you've personally used GIS. The new supermarket chain on the corner was probably located using GIS to determine the most effective place to meet customer demand.

Components of GIS

Above we have briefly explained what GIS is. The next step in understanding GIS is to look at each component of GIS and how they work together. These components are:

Hardware

Hardware comprises the equipment needed to support the many activities of GIS ranging from data collection to data analysis. The central piece of equipment is the workstation, which runs the GIS software and is the attachment point for ancillary equipment. Data collection efforts can also require the use of a digitizer for conversion of hard copy data to digital data and a GPS data logger to collect data in the field. The use of handheld field technology is also becoming an important data collection tool in GIS. With the advent of web-enabled GIS, web servers have also become an important piece of equipment for GIS.

Software

Different software packages are important for GIS. Central to this is the GIS application package. Such software is essential for creating, editing and analyzing spatial and attribute data, therefore these packages contain a myriad of GIS functions inherent to them. Extensions or add-ons are software that extends the capabilities of the GIS software package. Component GIS software is the opposite of application software. Component GIS seeks to build software applications that meet a specific purpose and thus are limited in their spatial analysis capabilities. Utilities are stand-alone programs that perform a specific function. For example, a file format utility that converts from on type of GIS file to another. There is also web-GIS software that helps serve data through Internet browsers.

Data

Data is the core of any GIS. There are two primary types of data that are used in GIS. A geodatabase is a database that is in some way referenced to locations on the earth. Geodatabases are grouped into two different types: vector and raster. Coupled with this data is usually data known as attribute data. Attribute data generally defined as additional information, which can then be tied to spatial data. Documentation of GIS datasets is known as metadata.

People

Well-trained people knowledgeable in spatial analysis and skilled in using GIS software are essential to the GIS process. There are three factors to the people component: education, career path, and networking. The right education is key; taking the right combination of classes. Selecting the right type of GIS job is important. A person highly skilled in GIS analysis should not seek a job as a GIS developer if they haven't taken the necessary programming classes. Finally, continuous networking with other GIS professionals is essential for the exchange of ideas as well as a support community.

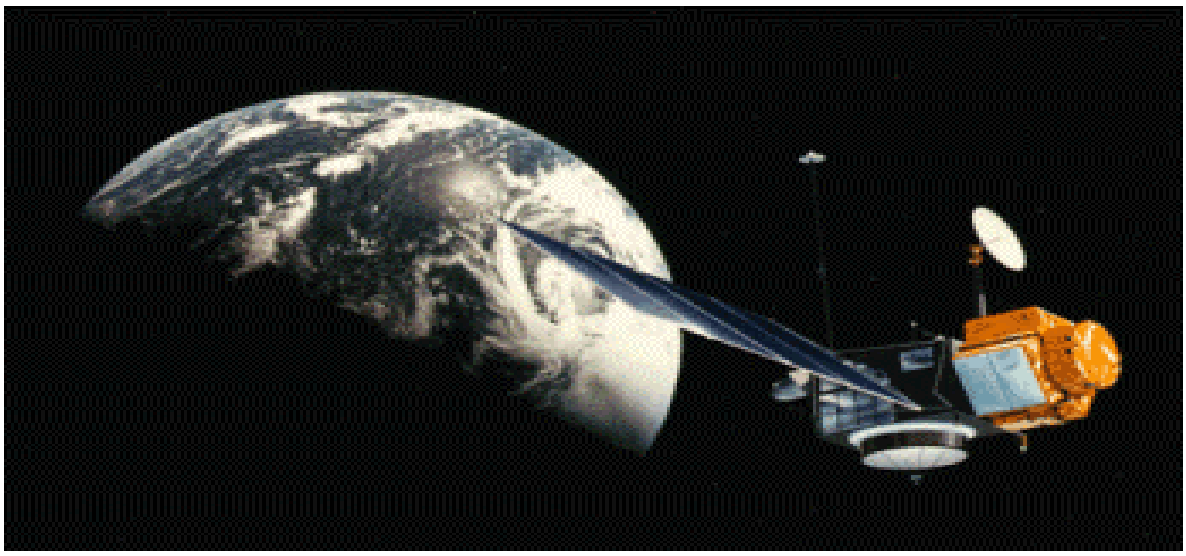

What is satellite remote sensing?

Satellite remote sensing involves gathering information about features on the Earth's surface from orbiting satellites. These satellites carry two types of sensor systems known as "active" and "passive". A "passive" system generally consists of an array of small sensors or detectors which record (as digital numbers) the amount of electro-magnetic radiation reflected and/or emitted from the Earth's surface. A multispectral scanner is an example of a passive system. An "active" system propagates its own electro-magnetic radiation and measures (as digital numbers) the intensity of the return signal. Synthetic Aperture Radar (SAR) is an example of an active system.

The digital data acquired by the satellites is transmitted to ground stations and can be used to reconstitute an image of the Earth's surface not too dissimilar to an aerial photograph.

How is data provided to the end-user?

Data is provided as hard copy photographic data products, or as digital data products which can be viewed and manipulated on a variety of software systems.

1.2.1.Applications

Geography Matters Everywhere

Geography matters in every business and every discipline. Wherever you turn, geography helps people do a better job and make a difference. GIS is helping thousands of organizations around the world.

GIS is utilized in every discipline, everywhere. Beautiful and interesting maps are providing better decisions making tools and analysis and making a difference in

our world. Some of these applications can be found in :

1) Natural Resources

2) Archaeology

3) Meteorology and Climatology

4) Hydrology

5) Forest resource inventory

6) Geology, Lithology and mineral resource inventory

7) Urban and land use

8) Oceanography

9) Natural disaster monitoring (volcano)

10) Global change study and Climatological processes

11) Forest Fire Monitoring

12) Vegetation and Agriculture monitoring

13) Drought Monitoring

14) Landslide and earthquake monitoring

15) Flood monitoring

16) Sand-storm monitoring

17) Water resources and wastewater monitoring

18) Thermal pollution

19) Soil moisture variation

20) Heat and moisture fluxes (exchanges)

21) Evapotranspiration

22) Biomass distribution

23) Transportation and infrastructure planning

1.2.2 Techniques-Method :

Introduction

The availability of remote sensing data that are needed for global, regional and local monitoring has greatly increased over the recent years. New technologies such as global positioning system (GPS), softcopy photogrammetry and multi-source satellite remote sensing are creating data at higher spatial and temporal resolution than have been collected at any other time on earth. Geographic Information Systems (GIS) technologies allow - for the first time- the efficient storage and management of spatial datasets in digital formats. In combination with the appropriate data transfer and interoperability standards that are currently being developed the technology is being put in place that will eventually allow standardized data exchange, processing and dissemination.

GIS and remote sensing techniques :

Global positioning systems (GPS)

A Global Positioning System (GPS) is a set of hardware and software designed to determine accurate locations on the earth using signals received from selected satellites. Location data and associated attribute data can be transferred to mapping and Geographical Information Systems (GIS). GPS will collect individual points, lines and areas in any combination necessary for a mapping or GIS project. More importantly, with GPS you can create complex data dictionaries to accurately and efficiently collect attribute data. This makes GPS is a very effective tool for simultaneously collecting spatial and attribute data for use with GIS. GPS is also an effective tool for collecting control points for use in registering base maps when known points are not available. GPS operate by measuring the distances from multiple satellites orbiting the Earth to compute the x, y and z coordinates of the

location of a GPS receiver.

Uses of GPS

GPS can be used for georeferencing, positioning, navigation, and for time and frequency control. GPS is increasingly used as an input for Geographic Information Systems particularly for precise positioning of geospatial data and the collection of data in the field.

Remote Sensing

Remote sensing includes all information collected from sensors which are physically separate from the object. Remote sensing is concerned with deriving information about the Earth's surface using an elevated platform, to produce such information as satellite data or aerial photography.

Figure 1 : Part of a satellite image

Remote sensing instruments rely upon the detection of energy emitted from, or reflected by, the object under consideration. Remote sensing allows the measurement and monitoring of surface electromagnetic variation, and as such this data provides a unique way of viewing the landscape. Satellite remote sensing is the only source of data with which we can view the entire planet and monitor the change in the nature of the surface of the planet through time, in a consistent, integrated, synoptic and numerical manner.

Satellite remote sensing has the ability to provide complete, cost-effective, repetitive spatial and temporal data coverage, which means that various phenomena can be analysed synoptically, and such tasks as the assessment and monitoring of land condition can be carried out over large regions.

As well as being of use by itself, remote sensing can be also be used as an important data source for the development and refinement of models, and can be used to validate models.

Aerial photographs, air photo interpretation and digital photogrammetric mapping.

Aerial photographic interpretation has been the most widely used form of remote sensing for environmental applications to date, with techniques being well established. This wide use stems from the availability of aerial photographs, and the fact that they can provide very high spatial resolution data, down to metre accuracy, not historically available from other sensors.

Qualitative analysis relies on image interpretation and is basically descriptive. Photo interpretation involves a human analyst viewing an image, and extracting information, and due to its use of the human mind, is unequalled in the possibilities

of pattern recognition and spatial association. The success of this technique is highly dependent on the analyst effectively exploiting the spatial, spectral and temporal elements present in the image. Images, whether aerial photographs or satellite imagery, have a very high descriptive value due to the ability of the human interpreter to interpolate and find patterns.

For both aerial photographs and space-borne remotely sensed data, the scale of the image will determine to a large extent the potential of the interpretation. Photo interpretation, whether of aerial photography or of satellite remote sensing data, is prone to the problems of being non-repeatable and not offering uniformity of analysis. It is highly subjective and depends upon the interpreter's knowledge and understanding of the spatial area under consideration and the process or phenomena involved.

- The combination of aerial photography and air photo interpretation provides information on relatively large areas without inspection of the ground.
- Roads, lakes and water bodies, building, farmland and forests are clearly visible on aerial photographs.
- Other characteristics such as vegetation, soil and geological formations are more difficult to interpret, however skilled and experienced interpreters can extract a great amount of useful information from aerial photography.
- Using air photo interpretation, the aerial photograph is classified by the interpreter, with the data being then input into a database or is used for the updating of previously held information .

Digital photogrammetric mapping uses digital images of a pair of overlapping photographs and operators use special 3D glasses to digitise (x, y, z) coordinates of features.

Hyperspectral imaging :

Multispectral remote sensors such as the Landsat Thematic Mapper and SPOT XS produce images with a few relatively broad wavelength bands. Hyperspectral remote sensors, on the other hand, collect image data simultaneously in dozens or hundreds of narrow, adjacent spectral bands. These measurements make it possible to derive a continuous spectrum for each image cell. After adjustments for sensor, atmospheric, and terrain effects are applied, these image spectral can be compared with field or laboratory reflectance spectra in order to recognize and map surface materials such as particular types of vegetation or diagnostic minerals associated with ore deposits.

Hyperspectral images contain a wealth of data, but interpreting them requires an understanding of exactly what properties of ground materials we are trying to measure, and how they relate to the measurements actually made by the hyperspectral sensor.

Microwave imaging :

Microwave sensing encompasses both active and passive forms of remote sensing. Because of their long wavelengths, compared to the visible and infrared, microwaves have special properties that are important for remote sensing. Passive microwave sensing is similar in concept to thermal remote sensing. All objects emit microwave energy of some magnitude, but the amounts are generally very small. A passive microwave sensor detects the naturally emitted microwave energy within its

field of view. This emitted energy is related to the temperature and moisture properties of the emitting object or surface. Passive microwave sensors are typically radiometers or scanners and operate in much the same manner as systems discussed previously except that an antenna is used to detect and record the microwave energy.

The microwave energy recorded by a passive sensor can be emitted by the atmosphere , reflected from the surface , emitted from the surface , or transmitted from the subsurface. Most passive microwave sensors are therefore characterized by low spatial resolution.

Active microwave sensors provide their own source of microwave radiation to illuminate the target. Active microwave sensors are generally divided into two distinct categories: **imaging and non-imaging**. The most common form of imaging active microwave sensors is RADAR. **RADAR** is an acronym for **RA**dio **D**etection **A**nd **R**anging, which essentially characterizes the function and operation of a radar sensor.

Non-imaging microwave sensors include altimeters and scatterometers**.** In most cases these are profiling devices which take measurements in one linear dimension, as opposed to the two-dimensional representation of imaging sensors.

LIDAR :

LIDAR is a a remote sensing instrument and is an acronym standing for Light Detection and Ranging. It is the direct, optical analog to Radar, which uses radio waves. In a typical LIDAR experiment, laser light is transmitted into the atmosphere. A LIDAR can Measure distance Measure speed Measure chemical composition and concentration.

Infrared imaging :

Infrared imaging (thermography) is a non-contact optical method where an accurate two- dimensional mapping of steady or transient thermal effects is constructed from the measurement of infrared energy emitted by the target. Recent advances in infrared technology, specifically development of high-density imaging sensors have opened a new level of applications unreachable prior to the availability of this technology.

METHOD	EM SPECTRUM	INFORMATION	INTERPRETATION	MISSION
Gamma-Ray Spectroscopy	Gamma rays	Gamma spectrum	K, U, Th Abundances	Apollo 15, 16: Venera
X-ray Fluorescence spectrometry	X-rays	Characteristic Wavelengths	Surface mineral/ chemical comp.	Apollo; Viking Landers
Ultraviolet Spectrometry	UV	Spectrum of Reflected sunlight	Atmospheric Composition: H,He,CO_2	Mariner; Pioneer; voyager
Photometry	UV, Visible	Albedo	Nature of Surface; Composition	Earth Telescopes; Pioneer
Multispectral Imagers	UV, Visible, IR	Spectral & Spatial	Surface Features; Composition	On most missions
Reflectance Spectrometers	Visible, IR	Spectral intensities of reflected solar radiation	Surface Chemistry; mineralogy; processes	Telescopes; Apollo
Laser Altimeter	Visible	Time delay between emitted & reflected pulses	Surface Relief	Apollo 15,16,17
Polarimeter	Visible	Surface Polarization	Surface Texture; Composition	Pioneer; Voyager
Infrared Radiometer (includes scanners)	Infrared	Thermal radiant intensities	Surface & atmospheric temperatures; compos.	Apollo; Mariner; Viking; Voyager

Microwave Radiometer	Microwave	Passive microwave emission	Atmosphere/Surface temperatures; structure	Mariner; Pioneer Venus
Bistatic Radar	Microwave	Surface reflection profiles	Surface Heights; roughness	Apollo 14,15,16; Viking
Imaging Radar	Microwave	Reflections from swath	Topography & roughness	Magellan; Earth systems
Lunar Sounder	Radar	Multifrequency Doppler Shifts	Surface Profiling & imaging; conductivity	Apollo 17
S-Band Transponder	Radio	Doppler shift single frequency	Gravity data	Apollo
Radio Occultation	Radio	Frequency & intensity change	Atmospheric density & pressure	Flybys & Orbiters

1.3 Why use GIS?

Maps have traditionally been used to explore the Earth. GIS technology has enhanced the efficiency and analytical power of traditional cartography. As the scientific community recognizes the environmental consequences of human activity, GIS technology is becoming an essential tool in the effort to understand the process of global change. Map and satellite information sources can be combined in models that simulate the interactions of complex natural systems.

Functions of GIS include: data entry, data display, data management, information retrieval and analysis.

1.3.1. Advantages

Geographic Information Systems (GIS) provide an ideal vehicle for teaching topics in the Earth and environmental sciences . A GIS has a number of advantages over traditional materials when used as an instructional tool. These advantages include the following elements:

Improve Organizational Integration

One of the main benefits of GIS is improved management of your organization and resources. A GIS can link data sets together by common locational data, which helps departments and agencies share their data. By creating a shared database, one department can benefit from the work of another—data can be collected once and used many times.

Make Better Decisions

The old adage "better information leads to better decisions" is true for GIS. A GIS is not just an automated decision making system but a tool to query, analyze, and map data in support of the decision making process. Because GIS products can be produced quickly, multiple scenarios can be evaluated efficiently and effectively.

Make Maps

For simplicity's sake we often call GIS "mapping software." We most often associate maps with physical geography, but the map to the right demonstrates that GIS is flexible enough to map any kind of terrain, even the human body. GIS can map any data you wish.

Making maps with GIS is much more flexible than traditional manual or automated cartography approaches. A GIS creates maps from data pulled from databases. Existing paper maps can be digitized and translated into the GIS as well.The GIS-based cartographic database can be both continuous and scale free. Map products can then be created centred on any location, at any scale, and showing selected information symbolized effectively to highlight specific characteristics. A map can be created anytime to any scale for anyone, as long as you have the data.This is important because often we say "I see" to mean "I

understand." Pattern recognition is something human beings excel at. There is a vast difference between seeing data in a table of rows and columns and seeing it presented in the form of a map. The difference is not simply aesthetic, it is conceptual—it turns out that the way you see your data has a profound effect on the connections you make and the conclusions you draw from it. GIS gives you the layout and drawing tools that help present facts with clear, compelling documents.

Multimedia integration

Other forms of digital information, including animations, video, audio, and digital stills, can be woven into GIS activities, greatly enriching and extending the learning potential.

Technology literacy and transferable skills

The use of GIS promotes technology literacy and provides us with skills transferable to our own research, other course work, and the general marketplace.

GIS-based instructional modules have the potential to impact us learning by reinforcing concepts through discovery and by improving problem solving, visualization and computational skills.

Visualization

Through a process known as visualization, a GIS can be used to produce images not just maps, but also dynamic and customisable maps, drawings, tables, charts, animations, and other cartographic products. These images allow researchers to view their subjects in ways that they never could before and to identify and characterize relationships by manipulating multiple visual representations of data.

The images often are helpful in conveying the technical concepts of a GIS to non scientists.

Thermal infrared (TIR)

TIR images of the Earth's surface can provide accurate distributions of surface spectral emittance and temperature (at local to global scales)

Data output

A critical component of a GIS is its ability to produce graphics on the screen or on paper to convey the results of analyses to the people who make decisions about resources. Wall maps, Internet-ready maps, interactive maps, and other graphics can be generated, allowing the decision makers to visualize and thereby understand the results of analyses or simulations of potential events .

Data analysis

The analytical tools of a GIS enable us to quantify relationships both within and among spatial data sets using database functions, statistical analyses and spatial overlay operations

Mapping and monitoring change

GIS can be used to map the change in an area to anticipate future conditions, decide on a course of action, or to evaluate the results of an action or policy.

Mapping locations

GIS can be used to map locations. GIS allows the creation of maps through automated mapping, data capture, and surveying analysis tools.

Mapping quantities

People map quantities, like where the most and least are, to find places that meet their criteria and take action, or to see the relationships between places. This

gives an additional level of information beyond simply mapping the locations of features.

Mapping densities

While you can see concentrations by simply mapping the locations of features, in areas with many features it may be difficult to see which areas have a higher concentration than others. A density map lets you measure the number of features using a uniform areal unit, such as acres or square miles, so you can clearly see the distribution.

Finding distances

GIS can be used to find out what's occurring within a set distance of a feature.

Other Advantages from the use of Geographic information systems (GIS).

- Visualization of activity-travel patterns on digital map and time grid (temporal components are drawn in another window), showing only appropriate information case by case .
- Capability of zoom in/out of the specific spatial area and time period .
- Easiness of changing input data on not only individual and household characteristics but also level of service of transport network and opportunities on GIS.
- facilitate access to a variety of data and information,
- enhance graphic display of complex phenomena, and thus, our understanding, and
- provide tools for enhancing decision making.

There is an increasing awareness of the importance of the integration of remote

sensing and GIS technologies as shown by the themes of a number of recent workshops and conferences. The trend toward more emphasis on the application of integrated geographic information systems (IGIS, defined here as systems which can process remotely sensed imagery as well as raster and vector data sets in a consistent fashion) stems in part from:

- improvements in the quality and quantity of remotely sensed data available,
- improvements in computer hardware and software,
- increasing population and competition for natural resources,
- decreasing resource availability and environmental quality
- recognition of the global nature of problems,
- an increase in the number of public and private organizations working on local, national, regional and international problems,
- continuous acquisition of data and creation of larger and larger data bases to provide information in various scales.
- good spectral resolution (including infra-red bands)
- good spatial resolution
- ability to combine satellite digital data with other digital data
- cost effective data
- map-accurate data
- large archive of historical data

2° CAPITAL

2.1.SATELLITE TIR MONITORING OF SEISMICALLY ACTIVE AREAS

2.1.1 Introduction

The satellite techniques, of the Earth observation , find always more wide application in various disciplines , mainly in the environment, that they demand the continuous monitoring and to the world scale, of the atmosphere, of the oceans surface and of the land surface .The remote sensing of the land surface, in particular, knows already important applications for the realization of thematic cartographies (topography, geology, idrology , vegetation etc.), is for the monitoring of the main environment emergencies and natural as fires, floodings, pollution of water and air , earthquakes etc.

The use of satellitare platforms offers, regarding the traditional techniques, numerous advantages as the possibility of being able to observe phenomena to large-scale, the access to difficultly reached remote areas, the quickness with which the informations are obtained , the possibility of having given data with continuous temporary , to relatively low costs, thanking also the possibility of being able to use the same data for various applications. The sensors of remote sensing can be subdivided in active sensors (Radar, scatterometers, laser altimeters etc.), that emit and receive the reflected energy from the land surface, and in passive (radiometers , interferometers etc.), that measure the reflected solar radiation or the thermally emitting from the land surface.

Based on the parameters that we want to investigated, is possible to take advantage of the observations in various spectral bands.In the thermal one, the

measured largeness is the radiation, which comes normally measured in temperatures of brightness.

In the eighties, satellite techniques have been proposed for the observation of pre and co-seismic events, just as for the estimation of the following years over the seismic of events .

Between these , those that today are considered to be more promising for the study of pre and co-seismic phenomena are :

- The analyse of crystal deformations, with the use of interferometria SAR differential (DInSAR) (Ganas and others, 1995);
- The analyse of motion, the ionosferic heating and the instability of the plasma, causes the emission of the electromagnetic potentially correlated with the pre-seismic events (Molchanov , 1994, 1999 of heating; Frase Smith , 1994; Parrot, 1999);
- Analyse of the radiation emissions from the Earth of the infrared thermal , potentially correlabile with the preparation phases of the seismic events .

In this job of thesis we occupying the third phenomenologia , that is the study of possible pre and co-seismic events, on the base of measures of the infrared thermal , of the radiation emitted from the land surface .

2.1.2.Thermal Infra Red (TIR)

Thermal infra red is the sensing of emissive energy or "temperature" energy
It is governed by various laws and concepts including; Blackbody concept, Stefan-Boltzmann Law, Wiens Law, and Kirchoff's Law
For satellite remote sensing purposes Thermal IR applications are typically limited to two distinct portions due to atmospheric interference, the two portions include;

3 to 5 um range and 8 to 13 um range .

With the use of the passive sensors, in the infrared, it is possible, to measure the temperature of one radiating surface by means of the analysis of the intensity of the elettromagnitic emission from the same surface to several wavelengths, in fact the temperatures of the issuing emissions and the maximum emission of the wavelength, are obvious from the law of the movement of Wien :

$$\lambda max = A/T$$, where

A= constant(2900μm/K)

T= temperature (kelvin)

λmax = wavelength(μm)

the surface emission, is behaved like a black body, in the interval of the considered wavelength.

The electromagnetic radiations, ordered in increasing wavelength, they form the electromagnetic phantom, that in the taxonomy, it seems to ends the cosmic rays (short wavelength and high frequence), and in radiowave(large length and low frequence) .

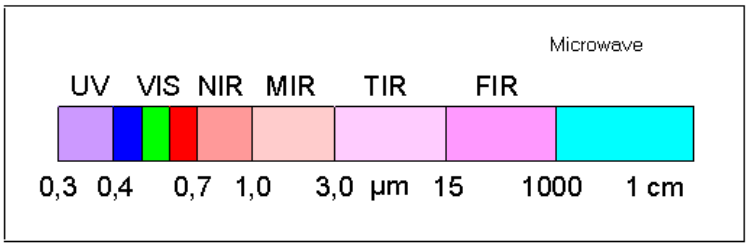

Figure 1: electromagnetic phantom

The regions of the infrared are subdivided in :

- Near-infrared (NIR), 0.7-2.5 μm

- Middle-infrared (MIR), 2.5-4 μm

- Thermal-infrared (TIR), 4-20 μm

- Far-infrared (FIR), 20-350 μm

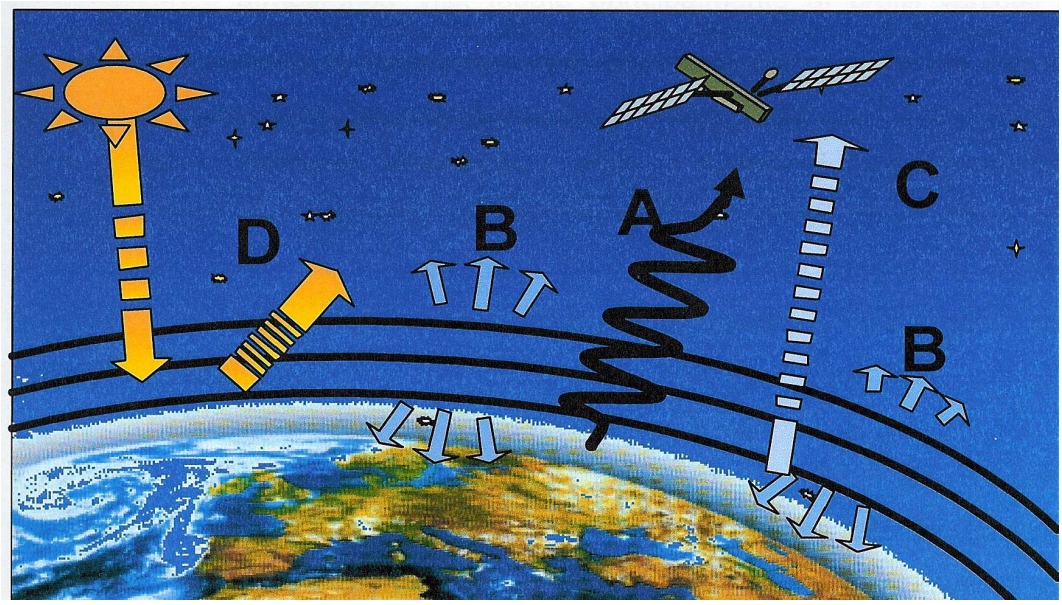

Figure 2: The signal measured from satellite: Electromagnetic emitted radiation e/o,reflected in the various wavelength of the electromagnetic phantom.
A, Thermal radiation emission from the earth(MIR-TIR)- B, Thermal radiation emission from the atmosphere(TIR)- C, Reflected atmospheric radiation(VIS-TIR)- D, Reflected solar radiation(VIS-MIR) .

Thermal Energy Detectors

There is a wide range of thermal detectors available The simplest systems are video based and have been used successfully in low cost remote sensing systems

Typically low temperature systems require cooling (usually liquid nitrogen)

Common Satellite Sensors in Thermal IR include:

Landsat Band 6 (10.4-12.5um)

NOAA AVHRR Band 4 (3.55-3.93 um) (TIR)

Large number of meteorological and ocean monitoring satellites with resolutions around 2km-5km -10km including GOES, GMS, MOS 1, SeaWiFs, Nimbus CZCS (1 thermal), SeaSat, HCMM

2.2. REMOTE SENSING OF THERMAL ANOMALIES IN SEISMOACTIVE AREAS

2.2.1.Introduction

The analysis of the correlation between space-temporal and TIR measured from satellite and the occurrence of seismic events, was being object of studies already from eighties.(Wang L. and Zhu,1984,Gorny,1988,etc..) .

The scientific community has always considered such studies with much precaution, because of a not clear definition of the thermal anomalies signal and of insufficient analysis of the data, that gave insufficient importance to those factors that, independently from seismic phenomena, influences the measured signal from satellite (meteorological effects, season , preseason effects of area, etc).

Although ,the great amount of reserved observations, has determined an increased interest in the comparisons of searches of this kind ,part of some of the most great international spaces organizations, which:

- CEOS-DMSG,(Committee on Earth Observation Satellite, reports 2001 and 2002 of Disaster Management Support Group).
- NASDA , Space Agency of Japan, which have introduced one 5-year project (Earthquake Remote Sensing Frontier Research , Final Report 2001).
- IGOS (Integrated Global Observation Strategy) ,which in 2001 have approved the start of a new subject in Geo-Hazard.
- NASA-JPL, which have started the study of the feasibility of

GESS(Global Earthquake Satellite System), one 20-year programme for satellite mission applied in the monitoring of seismic risk .

- DEMETER(experiment to study the disturbances of the ionosphere due to the seismo-electromagnetic effects, and due to anthropogenic activities (Power Line Harmonic Radiation, VLF transmitters, HF broadcasting stations))
- L'ASI (Space Agency of Italy), which in 2002 have started one specific project(SEISMASS) in order to study the possible correlation between the thermal anomalies space-thunderstorms and seismic events.

2.2.2.Previous studies

Many studies have been based on observations TIR that support the existence of possible relations between thermal signal measured from satellite and seismic events. Already in 1984 by using data's of AVHRR(Advanced Very High Resolution Radiometer on board NOAA satellites),Wang and Zhu , had the ability to evidence the presence of thermal anomalies (TIR observations corresponding to soil surface temperature anomalies) in the zone of preparation of the seismic event of Tangshan in 1976 (China). Gorny in 1988 leads the first studies on the seismic active areas of central Asia (South Kazakhstan), taking advantage the data of sensor AVHRR inside of polar satellite NOAA. Quiang Zu-ji (1990), using the given thermal infrared acquired with Meteosat, observes thermal anomalies, associated with anomalous values (up to 1000-1500 ppm) of emitted greenhouse gases(mainly CO_2 ,H_2,H_2 O), few days before the seismic event of Datong (China) in 1989 with a period of quiescence just one day before the event. Also he analysed the seismic event of Ghangsu (1990) and few days before the event, Meteosat TIR anomalies

were observed in combination with anomalous air temperature increase from the earth surface up to the altitude of 5.5km(with a maximum increase around 1.5km). Always this one ,with the use of AVHRR images, in order to preview, applying method Q&D (Quiang Zu-Ji, 1990), data , epicentre and magnitude of numerous seismic events.

Tronin (1994), studied the seismic event of Gazli, 1976, and on the base of night vision AVHRR images, characterizes one positive anomaly in correspondence of the fault scarps(rupture) of Kopetdag, with linear extension of 25-30 km and width of 500 km. He notes also that TIR anomalies increase their spatial extension(but not intensity) in significant temporal relation to the seismic activation of the Tien Shan and Turan plates in the point of intersection of major crust faults (Karatau and Tamdy-Tokraus),in Central Asian seismoactive zones. Analogous studies have been executed from Emilio Careeno in 1996, in one financed plan from European community (SEISMOSAT).

The results of such studies, agree in describing anomalous TIR like the increase of temperature of brightness of some Kelvin degrees, over distant areas until 1000km from the epicentral area, that appear in advance some days until some weeks before the seismic event (for events of magnitude greater of 6).

Such studies have all showed an insufficient importance attributed to highly variable contributions (that influence heavy signals measured in thermal), natural (atmospheric transmittance, surface emissivity and morphology ,etc), and observational (time, season, solar and satellite zenithal angles), and which below we will call it "noise naturale/observable", can be hidden, and is independently

determined to the appearance of the anomalies from the occurrence of a seismic event (wrong alarm).

The phase of counterfeiting turns out, in such studies, is particularly overlooked. In fact in many cases, the presence of anomalous signals, apparently in no correlation with seismic events or with active tectonic structures, is not commented. As an example (fig3), Tronin (1995), evidences the existence of one positive anomaly along the fault scarps(rupture) of Kopetdag some days before the earthquake of Gazli of 1976, without justifying the presence of other also anomalies in the image, and in distance from the epicentral area.

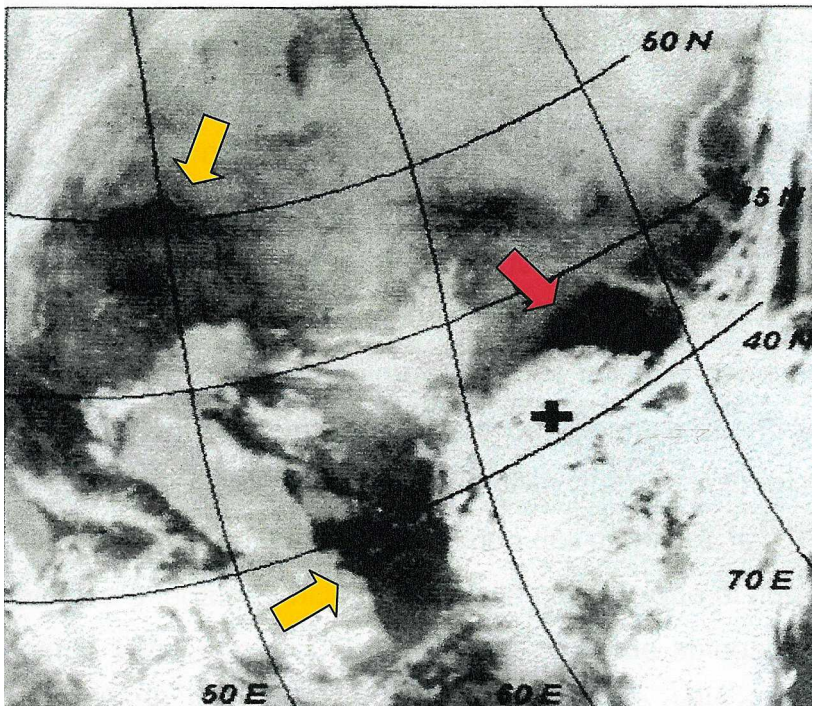

Figure 3:Earthquake of Gazli, 8 April 1976. With the red arrow is indicated the anomaly evidenced by Tronin , in correspondence to the rupture of Kopetdag , with the yellow arrows are indicated the anomalies of comparable intensity, but in an zone in distant from the epicentral area(+) , of which Tronin have mentioned .

2.2.3.Explanations proposed for the observed thermal anomalies .

Also the referred studies do not give one agreeing explanation, of the origin of the observed anomalies TIR .

Tronin(2000), supposed that the main causes of their formation are in hydrogeologic factors, in the optically active gases emissions and in the convettive transport of heat, speeds up from pre-seismic processes.

Analyzing the composition of the thermal equation balance to the land surface, there is noticed only some of the considered possible causes of the origin of one pre-seismic thermal anomaly.

The turbulent exchange of heat between the land surface and the atmosphere, conjucted mainly to the winds, could justify the variation of observed signals TIR, but Tronin (1999), noticed that the presence of such anomalies have been observed also independently from the presence of strong winds. Also the evaporation, which comes mainly from the content of water in the ground, is a parameter that, during the day, could sufficiently increase the surface temperature ,but during the nightly hours on influence is much weaker and it would not be enough to justify the thermal anomalies observed at night. The geothermal flow includes two terms, one conductive term and one convettive.

The first one is conjucted to the conductive property of rocks, and the rapidly development of observed thermal anomalies (few days), excludes such composition, in how much the formation of an increase of temperature generates thermal anomalies, with intensity comparable to those found from satellite, through conduction exchange of heat , which would demand an interval time of 10^7 –10^8 years.

The thermal convettive is conjucted mainly to the warm and rich fluid circulation of optically active gases, like CO_2 and CH_4 , and could explain the formation of the thermal anomalies. In fact a quick release of heat from the land surface could be explained with one quick ascent of flow fluids (water and gas) for convention, from deep zones, in previous period to the seismic event. At the same process that a gas release would be combinable optically active(CO_2,CH_4,H_2, etc..) could generate a sufficient heating of the land surface for the greenhouse effect.

Many studies have been lead on the nature of the local variation of the physical phenomena, which variation of the field of tectonic deformation , of the relationship of waves V_p / V_S, of the electrical resistivity of rocks, of gas emissions, of electrotelluric currents etc, related to pre-seismic phases, and between the theories most of them mentioned in the "dilatanza", introduced from Osborne to the end of '800, and retaken in first years of '70 from Nur (1972), Anderson and Whitcomb (1975), which have proposed a model of preparation and origin of the called earthquake "Dilatanza-Diffusione" and Myachkin ET al.(1972), Mogi (1974) and Stuart (1974) , which have proposed a analogous model called " Dilatanza-Instabilità ".

The model of the “dilatanza” can be outlined in three phases:

1)after the phase of storing up energy, that lasts from some years until to some hundreds, begins the preparation phase of an earthquake, with primary microcracks of the areas subordinates to stress;

2) with the increase of the energy there is an expansion of a amount of rocks volume with a following consequent closing to the microcracks that had previously been formed;

3)when the maximum of energy has been caught up, this is released, and this is the phase that an earthquake occurs.

Such theory seems not to contrast the hypothesis of a possible relation between the evolution temporal space of the observed thermal signals from satellite and the release of temperature (for convection) e/o of greenhouse gases, described previously. During the phase of microcracks, the release of greenhouse gases (as also the ascent for convention of flow fluids), can carry out an increase of the surface temperature and the atmosphere temperature; with the closing of the microcracks, decreases also the concentration of gases, and would observe a reduction of the surface temperature, for which the thermal anomalies reducing immediately a reduction of the time of occurrence of the earthquake, in order to return immediately after the occurrence of the earthquake (with further rupture and consequently ascent of the warm fluids and gases to the surface).

2.2.4.Factors that affect Thermal imagery

- The high level of spectral sensitivity required
- The optimum times for thermal sensing are at night
- cloud shadowing - temperature in cloud shadow is often slightly lower than
- ambient, can result in false interpretation.
- slope aspect - orientation and facing direction of slope
- sun angle and diurnal temperature due to local weather conditions and seasonal
- variation

2.3. ROBUST APPROACH FOR SATELLITE THERMAL ANOMALIES OF SEISMOACTIVE AREAS .

2.3.1.INTRODUCTION

Many satellite techniques have been proposed to remotely map seismically active zones and monitor geophysical phenomena possibly associated with earthquakes. In particular, several studies suggest that space-time anomalies in the satellite Thermal Infrared (TIR) radiance field, can be related to seismogenic areas distribution as well as to their activation before earthquakes . TIR signal measured from satellite, depends on observational (time of the day, day of the year, satellite zenithal angle, etc.) and physical conditions of Earth surface (mainly temperature and spectral emissivity) and atmosphere (mainly spectral transmittance). Corresponding contributions to space-time variability of the observed TIR signal should be preliminarily evaluated (as a *natural/observational noise*) in order to properly define space/time TIR anomalies in the context of seismogenic areas monitoring by satellites. Actually this noise can be as large as (sometimes greater than) the TIR signal variations reported in literature as thermal anomalies and attributed to seismogenic activity. A robust approach (RAT) to space-time anomalies detection in satellite observational fields, in the presence of highly variable natural and observational conditions, has been recently proposed [6] and successfully applied to the major natural and environmental hazards. Results achieved by applying the same approach to the problem of seismogenic area monitoring by satellite TIR surveys are presented with reference to some devastating earthquakes occurred in Europe during past 20 years.

Space-time TIR anomalies, observed from weeks to months before earthquakes occurrence, have been, by several authors suggested as pre-seismic signals. A robust satellite data analysis approach, allowing a statistically based definition of TIR anomaly (even in the presence of highly variable natural/observational contributions) has been proposed as a suitable tool to investigate possible correlations with seismic activity. In this work its potential is particularly evaluated in the case of 12 relatively low magnitude (M˜4-5) earthquakes occurred in Greece and Turkey since 1995. The analysis was performed exploiting about 10 years of METEOSAT TIR observations in order to characterize TIR signal behaviour in seismically unperturbed conditions. The possible relationships between intensity (and space-time distribution) of TIR anomalies and the low-magnitude earthquakes occurrence is critically evaluated also by comparison with the space distribution of seismogenic sources and other tectonic lineaments as reported in the literature. The robustness of the proposed approach against the possibility of false events detection (particularly important for this kind of application), its intrinsic exportability not only on different geographic areas but also on different satellite instrumental packages will be discussed in detail.

2.3.2. Thermal anomaly definition

A sequence of satellite imagery can be represented by a (spectral) space-time process giving the radiance $R_{\Delta\lambda}(r, t)$, collected in correspondence of a location centered on the ground coordinates $r \equiv (x, y)$ at time t, in the spectral band $\Delta\lambda$. For each fixed location $r = r'$ the quantity $R_{\Delta\lambda}(r', t)$ represents a time-series. A satellite image collected, at a fixed time $t = t'$, in the spectral band $\Delta\lambda$, can be then represented by a purely spatial process $R_{\Delta\lambda}(r', t')$. A single satellite sounding

referred to a fixed location r' and time t' is a punctual process $R_{\Delta\lambda}$ (r', t') in the space-time domain.

Thermal infrared radiance, R_{TIR} (r, t), measured from satellite (usually given in terms of Brightness Temperatures, BT) at the time t, within the TIR, 8-14 μm, atmospheric window, depends on observational (time t of the day and of the year, satellite zenithal angle θ_{SAT}) and physical conditions of Earth surface (mainly temperature T_S and spectral emissivity ε_{TIR}) and atmosphere (mainly spectral transmittance $\Im_{TIR}$)

R_{TIR} (r, t) = f [ε_{TIR} (r, t), $\Im_{TIR}$ (r, t), T_S(r, t), θ_{SAT} (r, t)]. (2.1)

By separately considering each contribution it

must be noted that:

a) Spectral emissivity, which strongly influences TIR signal (variations in the estimate of land surface temperature from 1 to 3 °C are expected as a consequence of uncertainty on the emissivity of only $\Delta\varepsilon_{TIR} \approx 0.01$, [e.g., Becker, 1987]) , is quite constant (~0.98) on oceans. Over land mainly depending on soil cover (from bare up to highly vegetated) and humidity it is highly variable taking values within 0.90 and 0.98 .

b) Spectral transmittance depends mainly on atmospheric temperature and humidity vertical profiles and can be assumed weakly variable in the spatial domain only in very stable meteorological conditions.

c) Temporal variations of surface temperature are obviously related to the regular daily and yearly solar cycles but sensitive also to meteorological (and climatological) factors leading considerable local variations within one day (one

year) and another.

d) Surface temperature spatially depends on local geographical (altitude above sea level, solar exposition, geographic latitude) and physical factors (thermal inertia, albedo, emissivity, etc...).

e) Variations in observational conditions, related mainly to differences in satellite zenithal angles (with consequent reduction of both spatial resolution and measured TIR signal in off - nadir views), introduce spatial variations of the registered signal which are systematic and not related to real near surface thermal discontinuities.

As far as instrumental packages on board polar satellites like NOAA (and differently from geo-stationary platforms) are concerned:

f) the same location is observed, at each revisiting time, at a different satellite zenithal angle introducing, even assuming a perfect image-to-image co-location, a spurious temporal variation of the measured signal due simply to the change in observational conditions (e.g. air-mass).

g) A perfect image-to-image co-location is impossible due to the change in the size of the ground resolution cell consequent to the change in the satellite angle of view. Then a spurious temporal variation of the measured signal have to be expected, not only as a consequence not only of a residual co-location error, but also because of the change in the size of the ground resolution cell.

h) also considering the same type of satellite pass (e.g. descending/ ascending) which, in case of polar platforms is assumed to cover the same area around the same local time (e.g. noon, midnight), this happens each day at different times falling in a time-slot up to 3 hours around the nominal time of pass. Spurious variations of the measured signal have to be then expected as a consequence of

such (time) variability of observational conditions which, depending on the place (geographic location, land cover etc.) and on the season, can reach values greater than 10^0 C for each hour of time-delay [see for example Peck,1966] .

These aspects should at least be considered, and their individual contributions to space-time variability of the observed TIR signal evaluated, as a natural/observational noise, in order to define space-time TIR anomalies correctly in the context of seismogenic areas monitoring by satellites.

As an example, variations of brightness temperature greater than 5 K can be easily measured in the NOAA-AVHRR TIR channel 4 (10.3-11.3 μm) , as a consequence of the change of only one of the above mentioned natural/observational factors.

This noise can then be as large as (in some cases greater than) the TIR signal variations reported in literature as thermal anomalies and related to impending earthquakes.

In this context, it is quite obvious that only those signal variations not related to the normal (i.e. independent from any variation in seismogenic areas distribution and/or activation) space-time variability of the signal itself , could be assumed as anomalous.

Particularly important becomes then the preliminary definition of this *normal* behaviour of the TIR signal . In fact as both experience and common sense teach, *no signal can be interpreted as anomalous «in se» but only by comparison* with a normality which must be preliminarily defined. On the other hand, it is obvious that *the same signal, which is normally observable at a specific time and place, could appear to be anomalous when observed in a different time and place.*

Therefore suitable criteria for space/time anomaly-detection should take into account the *normal* space/time variability of the observable with reference to the specific time *t* and place *r* of the observation.

2.4. A ROBUST APPROACH : RAT

A various approach is proposed for the identification of space time thermal anomalies, that holds R-on account multiple variable natural and the observable ones, that increase the measured signals.

Comparing measures carried out on the same one pixel, in the same period of the year (month) and in the same hour of the day attending, the variations of the signal, due to the variation of the natural conditions, (vegetation cover, daily solar cycle and yearly variations of the temperature, etc) or observable (hour of observation, sight angle), they come drastically reduced.

In this approach, in fact, the excess $\otimes_T$ (x, y, t) of the measured signal T(x, y, t), come estimated not only in relation to generally a "a normal" $< T_{RIF}(x,y) >$ definition on the base of a set data extension (of many years) of observations executed on the same site (x, y), but also regarding the variations of the signals σ_T (x,y), historically observed, in relation to factors observed at night (vegetation, daily and yearly temperature, hour t of observation, variation of the satellite sight angle , etc) and few nights (ascent of temperature depending from local factors of variable nature, like fires, eruptions of volcanoes, rain) (Tramutoli , 1998)

$$\otimes_T (x, y, t) = \frac{T(x, y, t) - \langle T_{RIF}(x,y) \rangle}{\sigma_T (x,y)}$$

Can give afterwards (with different degrees of intensity), an estimation of how the measured signal is anomalous regarding the previous history.

An other aspect that was considered between the factors that influence the variability of the signal (attributes greater value of σ_T (x,y)), is conjucted in processing errors (navigation e/o Co-location imprecise). In fact, georeferenced errors, make the attributed radiation on the same the site, corresponding nevertheless, in some sites situated, or enough(a little second of the precision of the technique of used navigation), different between them.

This is particularly important for satellites to polar orbit, as much as, between a passage and the following , that the polar orbit satellites are moved a little towards to the west, because of the earth moving, for which the sight of the field with the sensor which observes the same site is not similar to the previous one.

In order to reduce such variability (contributing the increasion of the sensibility of the index $\otimes_T$ (x, y, t) technique RAT which have been applied with success to the geostazionari satellites .The arrangement of geostazionario , in fact, beyond eliminating the origin of the effects of variation of the sight angle (the same site is observed under the same angle) and the errors which had to inaccurate a georeferenced, guarantees the acquisition of the temporal slot data in precise(<30 minutes) against 3-4 hours of the polar , guaranteeing a homogeneity still more pushed of the set date which is used for concerning the hour of observation.

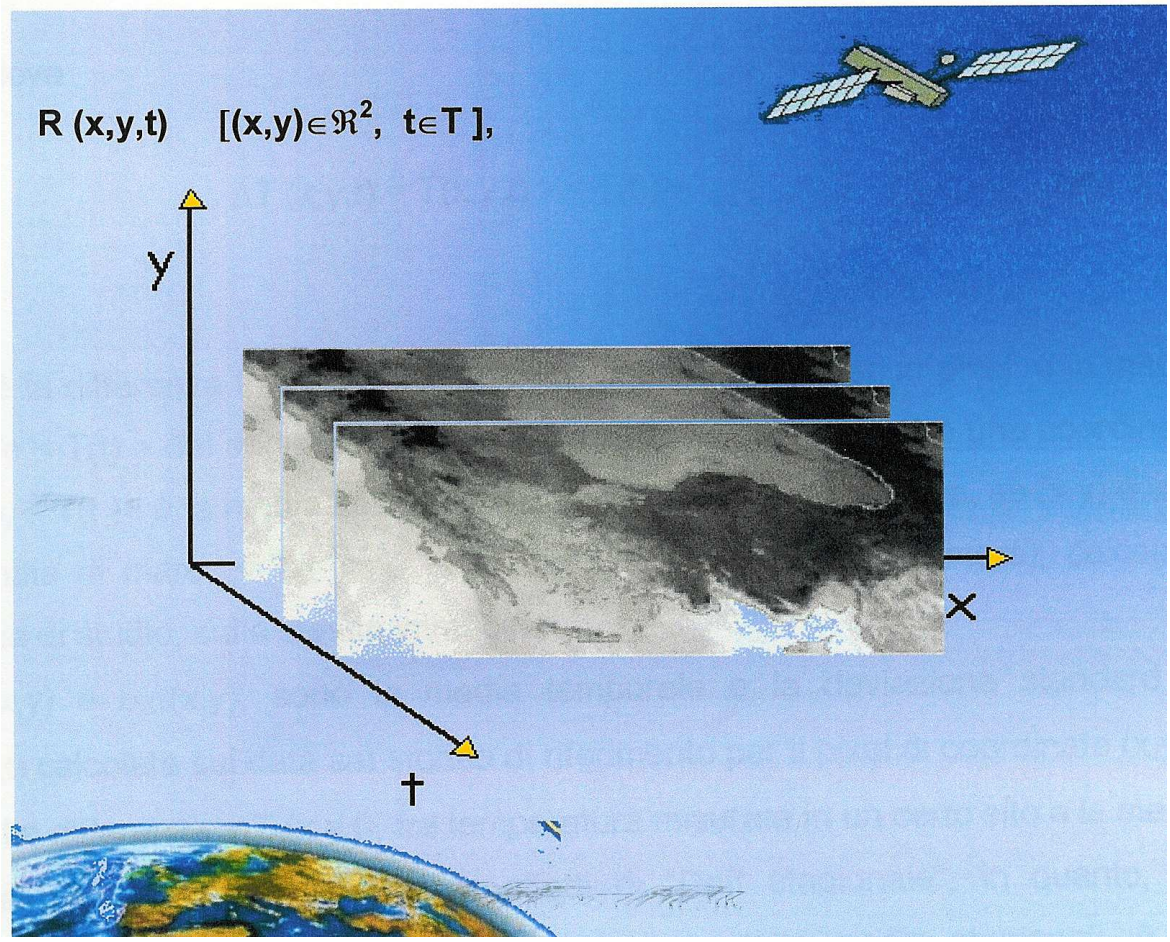

Figure 4: Construction of one serie of temporal reflections

A last element of the variability of the measured signal TIR, is that the ascent increases the variations of the medium season temperatures , between a year and following . It can succeed, in fact, that the temperatures that are recorded in a determined month, can turn out higher results (or lower), regarding the evolution of medium temperatures recorded in previous years, for the same month, in the determined site, for reasons independent from the seismic activity.

Such problem has been confronted (Tramutoli, 2001) by not considering anymore the thermal signals T(x, y, t) , but its difference regarding the average of the measured signals at the same time t, in the area of study.

In the case of the signal T(x, y) measured in the thermal infrared in the point (x, y)

and at the time t, the proposed index, has been : (Tramutoli ET al., 2001).

$$\otimes_T (x, y, t) = \frac{\Delta T(x, y, t) - < \mu_{\Delta T} (x,y) >}{\sigma (x,y)}$$

where

$\Delta T(x, y, t) = T(x, y, t) - < T (t) >$

is the difference between the signal T(x, y, t), measured in every pixel ,and the average space <T(t)> of the signal on the pixel of the same type, (if (x , y) is one coordinate of earth, <T(t) > is the average space executed only on pixels of earth, if (x, y) is one coordinate of sea, <T(t) > is the average space on the pixel of sea), calculated in the study area, on the same image.

$\mu_{\Delta T}$ (x , y) and $\sigma_{\Delta T}$ (x , y), are the time average and the average inclination of $\Delta T(x, y, t)$ calculated on the set historical data of reference for the pixel of coordinate(x, y).

The difference ΔT (x, y, t), between the measured temperature in one specific site and a medium space, reduces remarkable the effects of the "Drift ages ", as much as, a temperature increase of the variation of medium seasons, is a phenomenon not limited to a single pixel, but is one phenomenon typically observable at least to regional scale.

2.5. Data collection and analysis:

a) historical METEOSAT and NOAA/AVHRR records, and, as soon as possible, MSG-SEVIRI TIR observations, are being used as instrumental test beds in order to evaluate the trade-off between different observational strategies and instrumental attributes. The possible correlation, in the space-time domain, between TIR anomalies and pre/co-seismic phenomena are being checked by using different methodologies in different geographic scenarios (Italy, Greece, Turkey, Spain and Asian mainland). Algorithms falsification are being attempted considering also seismically unperturbed periods/areas in the past.

b) independent measurements based on GPS (TEC and deformation transients), seismometric (seismic and micro-seismic analyses), multi-parametric (geo-chemical, geothermal and geo-electrical) networks, as well as systematic campaigns of magnetotelluric and electromagnetic tomographic survey are being analysed in order to verify (and/or proposing new) explanatory physical models which can justify satellite observations. All significant changes in the measured parameters (and particularly, deformation fields, TEC and geo-electrical signals) are being compared with both satellite TIR anomaly fields and/or earthquakes occurrences, in order to confirm or reject, by a validation/falsification approach, the proposed models for thermal anomaly occurrence explanation.

2.6. THE IMLEMENTATION OF AN INTERGRATED GIS TO SEISMIC AREA MONITORING

2.6.1. Introduction

In this job of thesis, the analysis of space temporal thermal anomalies, observable in seismic active areas, it has been carried out by applying method RAT (Robust AVHRR Technique, Tramutoli 1998), to images acquired in the thermal infrared (10.5-12.5μm) of the Meteosat, NOA satellite. On the area of study,which contains the region of Irpinia-Basilicata, was possible to study seismic events by using the RAT method .

2.6.2. The investigated area and the Irpinia-Basilicata earthquake (23 November 1980, M_s = 6.9)

Southern Italy is one of the most active areas of the Mediterranean region. It is commonly accepted that the largest historical and recent earthquakes which occurred in this area, are typically generated by main normal faults running parallel to the Apennines, while moderate earthquakes are produced by secondary trans- verse strike-slip faults. Figure 1 a shows the locations of the main seismogenic faults, together with the thermically anomalous (T > 17 °C) source springs, recognised all over the considered area (e.g., Valensise et al., 1993; Boschi et al., 1995, http://faust.ingv.it; Albarello and Martinelli, 1997);/-
In particular, concerning the Irpinia-Basilicata area, three events with Ms ~ 7.0 (1694, 1930 and 1980) occurred in the last four centuries. The November 23, 1980 normal-faulting earthquake (Ms = 6.9; seismic moment M_o = 26 x 10^8 Nm) was one of the largest events observed in the Southern Apennines in this century

(Westaway and Jackson, 1987; Bernard and Zollo, 1989; Pantosti and Valensise, 1990; Amato and Selvaggi, 1993). It was the first well- documented example of surface faulting in the Italian peninsula. The seismological analysis revealed that the event was characterised by at least three different rupture episodes occurring at 0 s, ~20 s and ~40 s. The aftershocks were concentrated within 15 kill depth (similarly to the other well-determined focal depths in Central and Southern Apennines) outlining a fault extending approximately 40 km (see for instance Amato and Selvaggi, 1993). For this area, Pantosti and Valensise (1990) hypothesise the existence of a «characteristic earthquake» with Ms ~ 7.0 that releases completely the deformation energy of the area, without producing a consistent energy release through significant aftershock sequences.

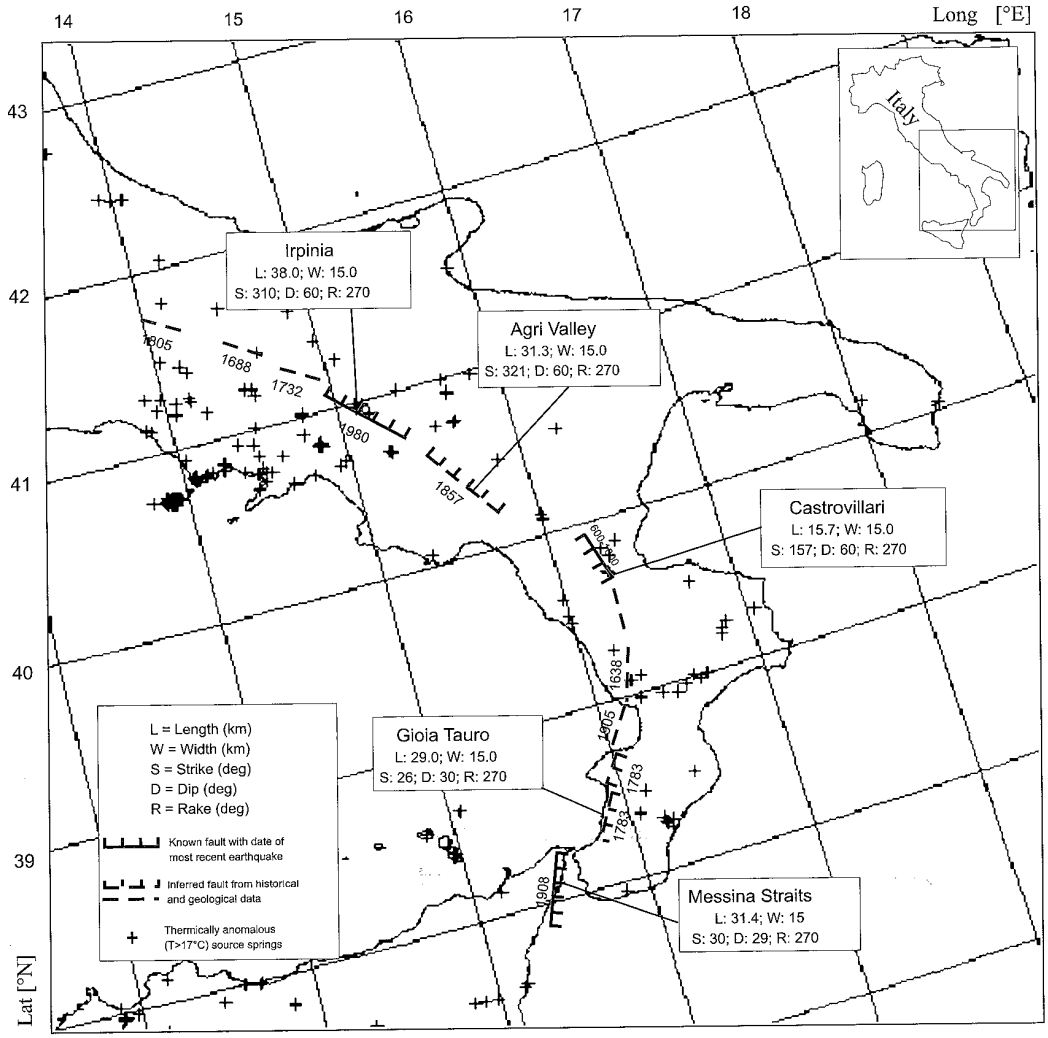

Fig.1a. Study area : the main seismogenic faults (from Valensise et al.,1993) and thermically anomalous (T>17 C) source springs as selected by Albarello and Martinelli (1997).

Another historically relevant event, the December 16, 1857 normal-faulting earthquake (Mallet, 1862), occurred in Val d' Agri. The seismic activity, which occurred in the study area after the 1980 event, consists of medium intensity earthquakes ($M_d \leq 5.0$, duration magnitude, as estimated by the seismometric network of National Institute of Geophysics) located close to the border between the Campania and Basilicata regions (Alessio et at., 1995). The May 5, 1990 (M_d = 5.0) and May 26, 1991 (M_d = 4.5) earthquakes were the strongest events (Tertulliani et at., 1992) to occur after the 1980 event. The seismological analysis of these events shows that they were generated by a strike-slip fault in the WE direction, perpendicular to the Apennine chain (Ekstrom, 1994; Boschi et at. , 1995). This fault lies north of the town of Potenza and is located between the two great seismogenic faults that caused the 1857 Val d' Agri earthquake to the south and the 1980 Irpinia earthquake to the north, respectively.

This area was chosen as test-area, and the Irpinia-Basilicata 1980 event as test case, mainly for the following reasons:

a) Together with one of the largest and well- documented events in the Italian peninsula, this area offers a seismic quiescence period long enough to permit the characterisation of the TIR signal in unperturbed conditions.

b) The area is also characterised by strong CO_2-dominated gas emissions (Doglioni et at. , 1996).

c) As part of an area of relatively recent orogenesis (lower Miocene -upper

Pliocene- Pleistocene) characterised by a complex morphology and geology, it permits to better appreciate the performances of the proposed technique also in the less favourable conditions in terms of spatial homogeneity of ground elevation and spectral properties.

With reference to this test-area/event this study was carried out considering a quite extended area for which the following additional information was available:

1) Seismogenic faults as reported in the most recent studies (e.g ., Pantosti and Valensise, 1990; Valensise et at., 1993; Boschi et at., 1995, http://faust.ingv.it).

2) Locations of thermically anomalous (T > 17 °C) source springs (fig. Ia) as possible vehicle of greenhouse gases like CO2 and CH4 (here- after simply source springs) selected by Albarello and Martinelli (1997).

3) Epicentres of earthquakes of magnitude M_s > 3 from 1963 to date (fig. Ib) as reported in the Catalogue of the U.S. Council of the National Seismic System .

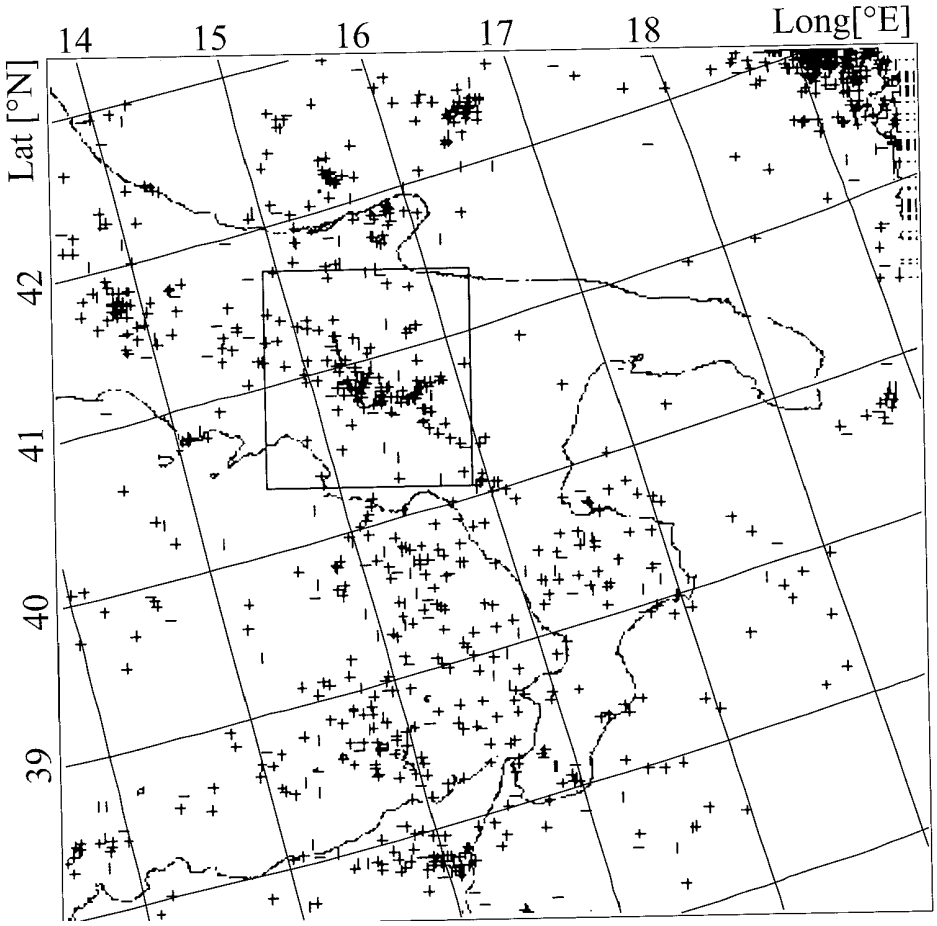

Fig.1b. Study area : crosses indicate epicentre locations of earthquakes with magnitude M_s >3 from 1963 to date as reported in the catalogue of the U.S. Council of the National Seismic System (CNSS). The box represents the area reported in figs 4 and 5 .

2.7. TIR ANOMALIES MAPS :

Below we can view a variety of maps with observed anomalies that occured in different alices for different periods of the November of 1980,during the Irpinia-Basilicata earthquake (23 November,Ms=6,9).

Alice 111180

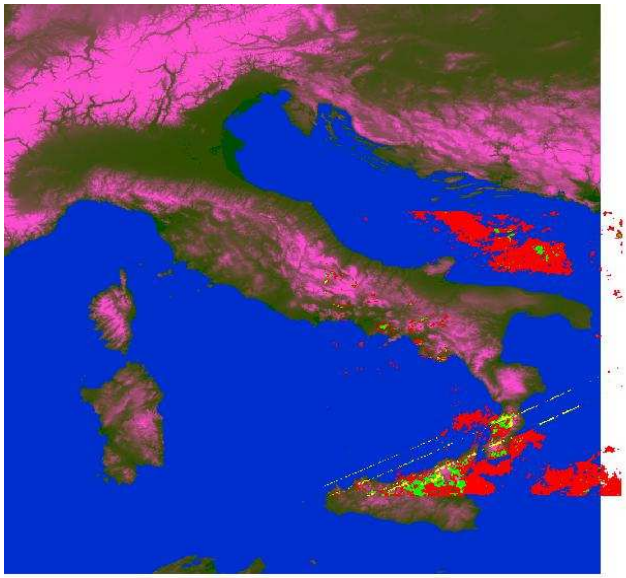

Alice 111180 > 1

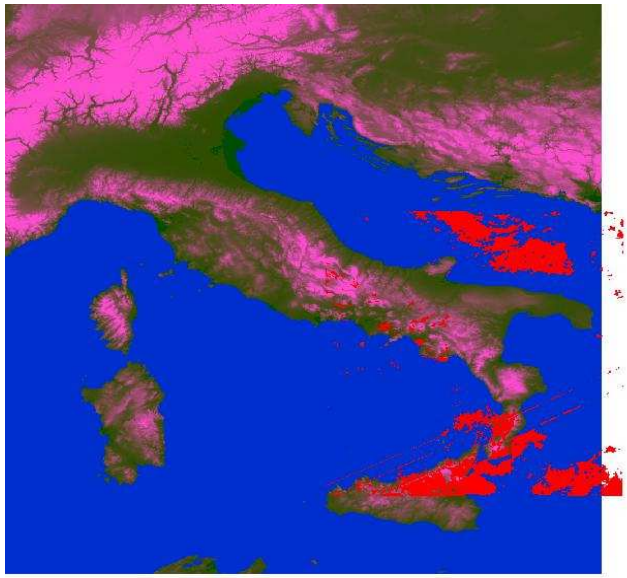

Alice 111180 > 1.5

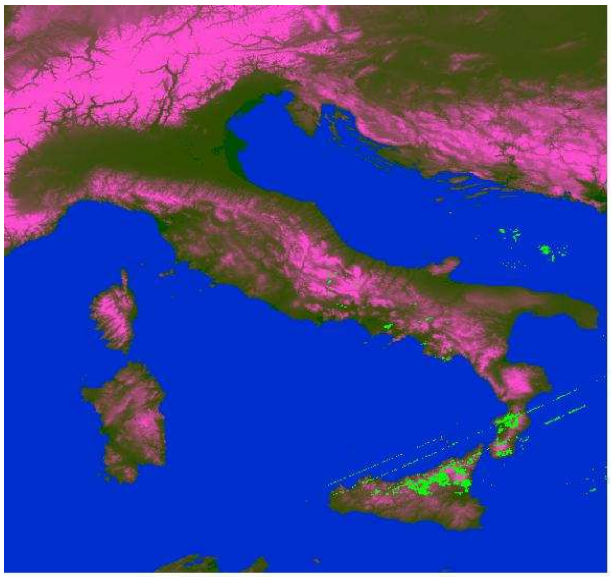

Alice 111180 > 2

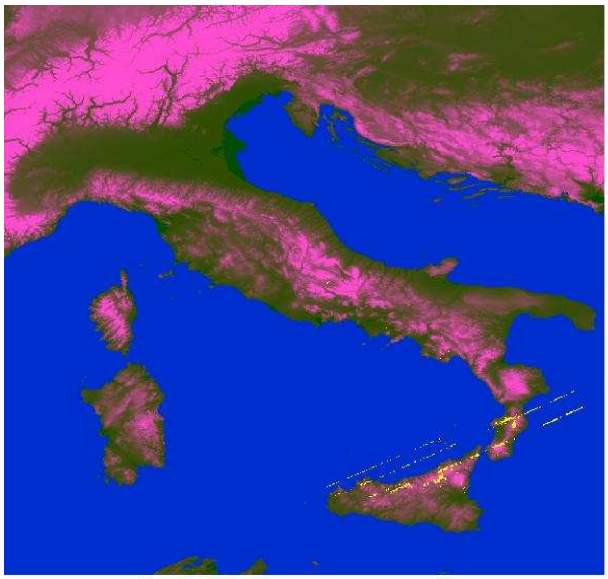

Alice 151180

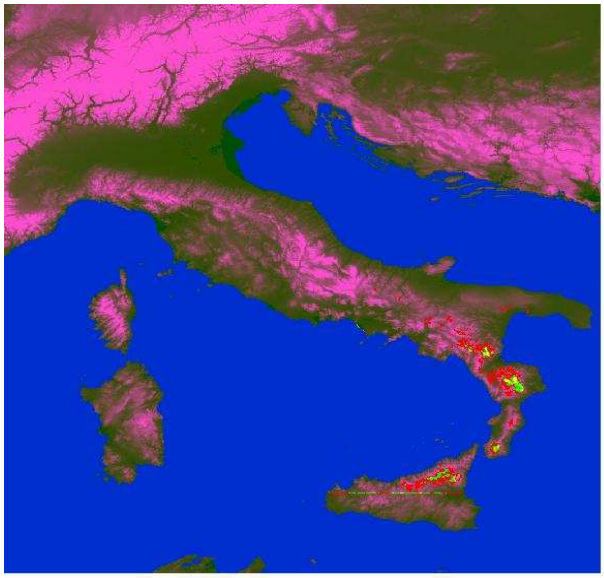

Alice 151180 > 1

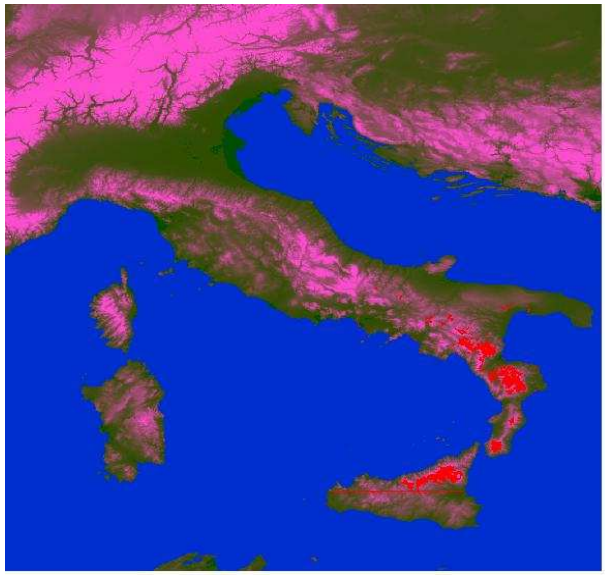

Alice 151180 > 1.5

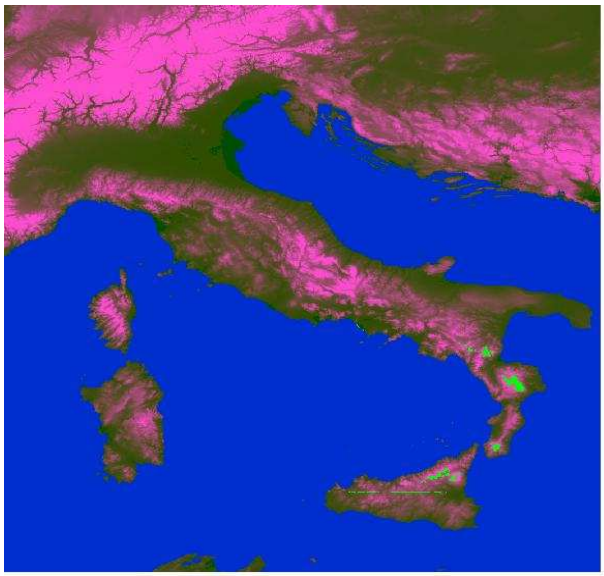

Alice 151180 > 2

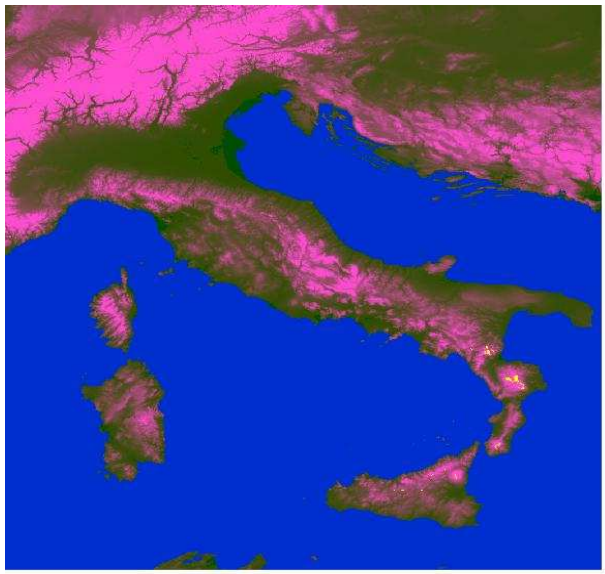

Alice 161180

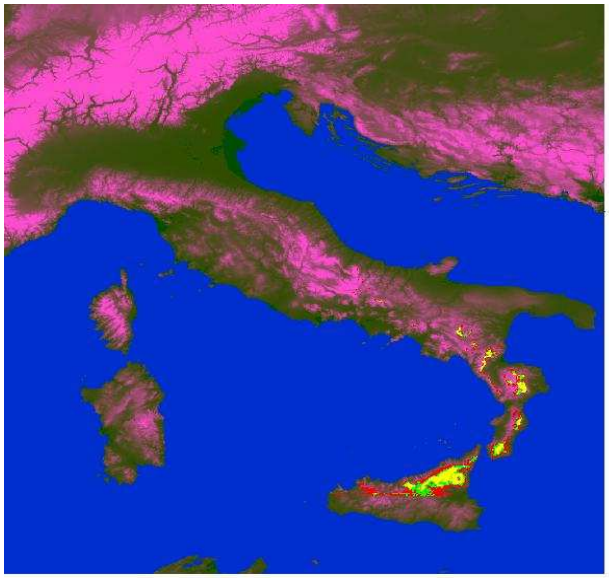

Alice 161180 > 1

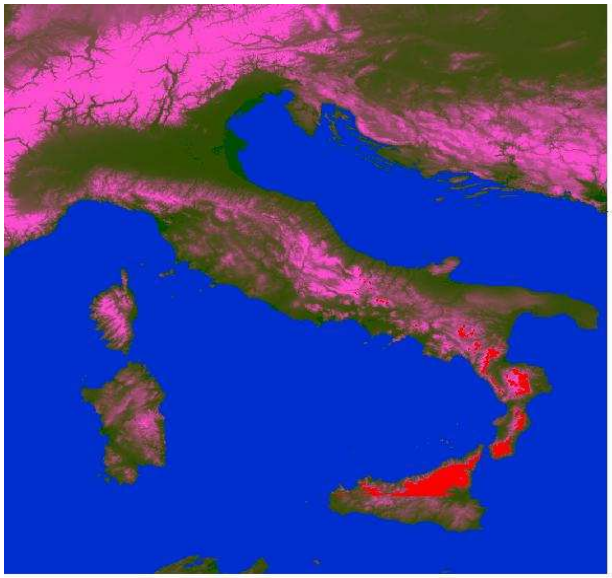

Alice 161180 > 1.5

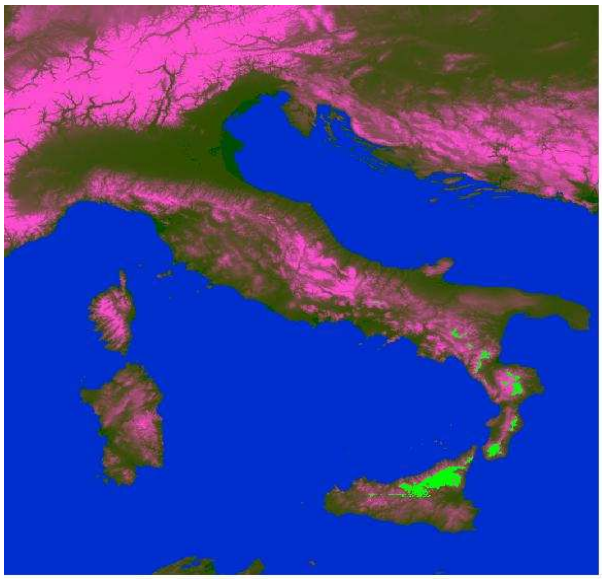

Alice 161180 > 2

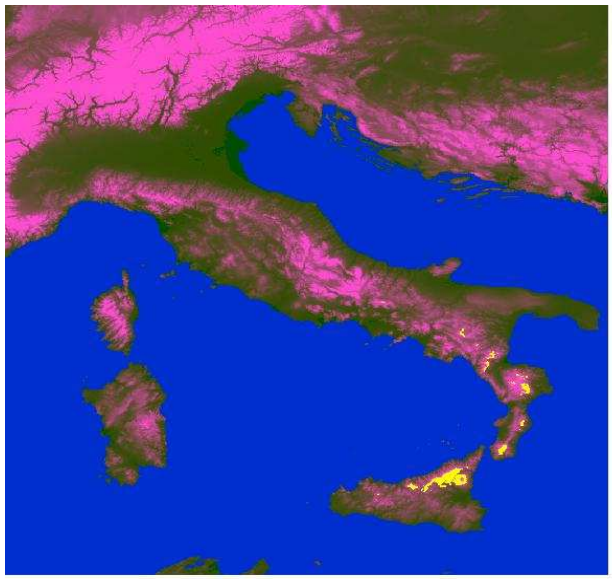

Alice 201180

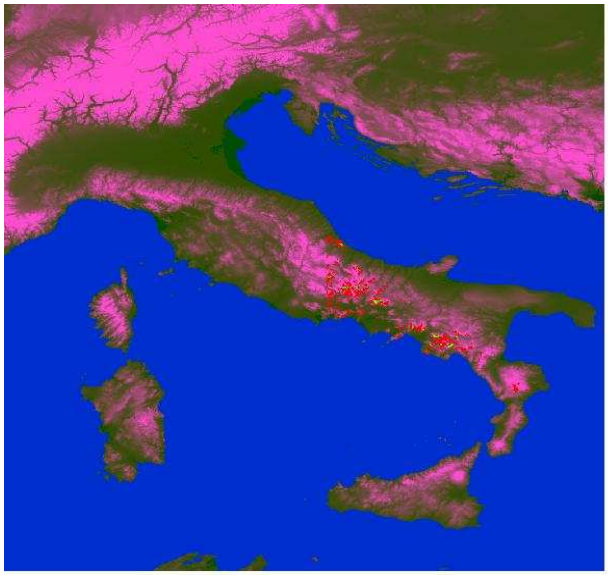

Alice 201180 > 1

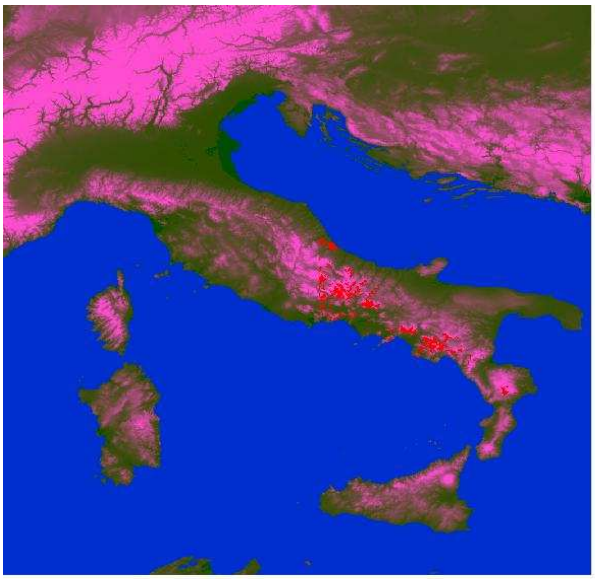

Alice 201180 > 1.5

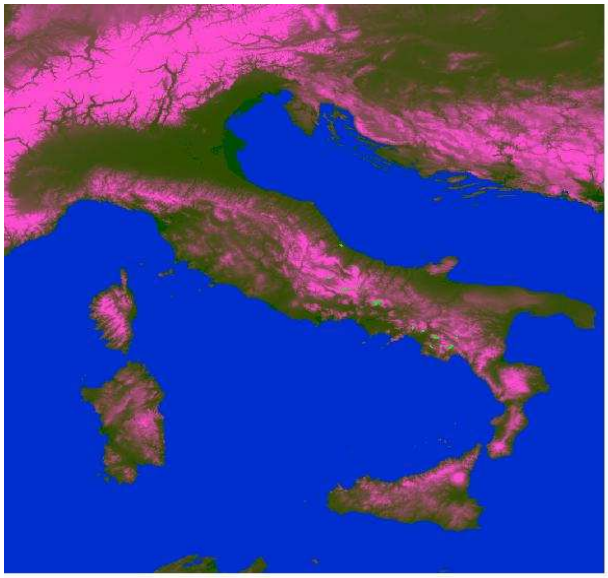

Alice 201180 > 2

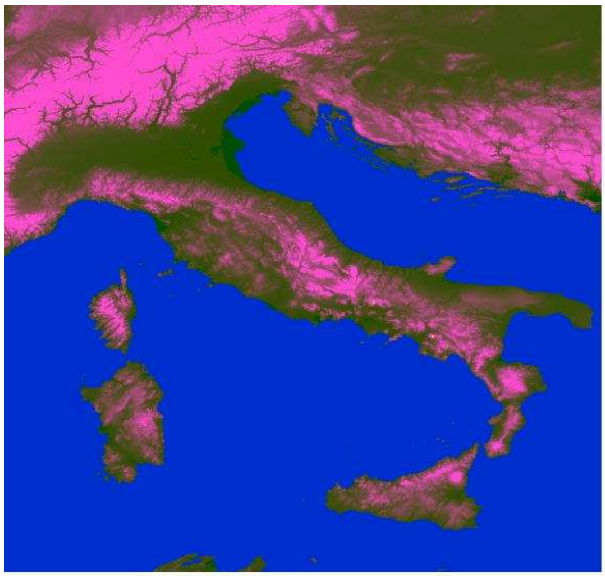

Alice 231180

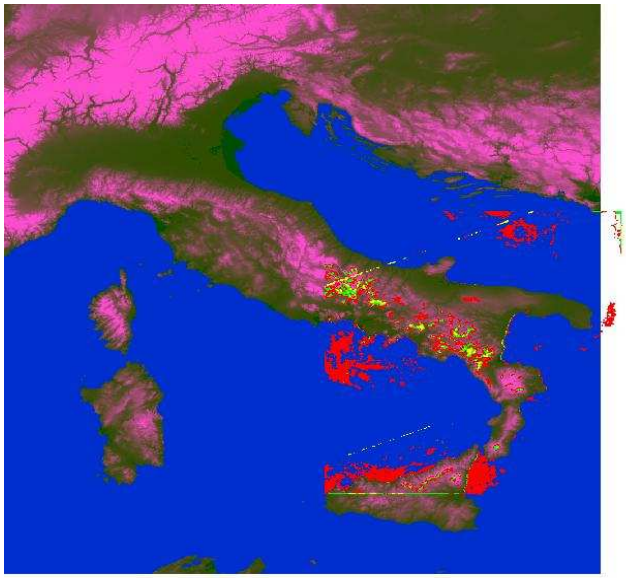

Alice 231180 > 1

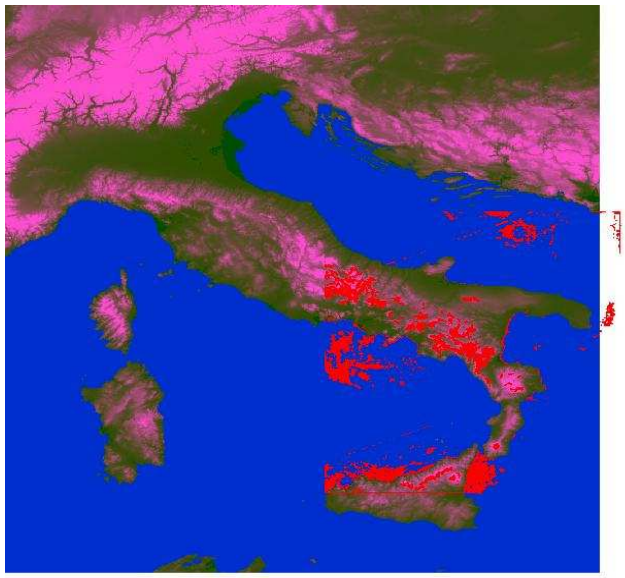

Alice 231180 > 1.5

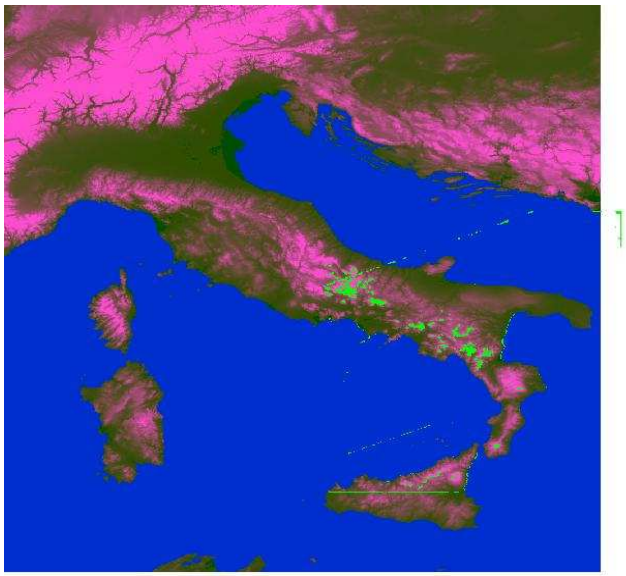

Alice 231180 > 2

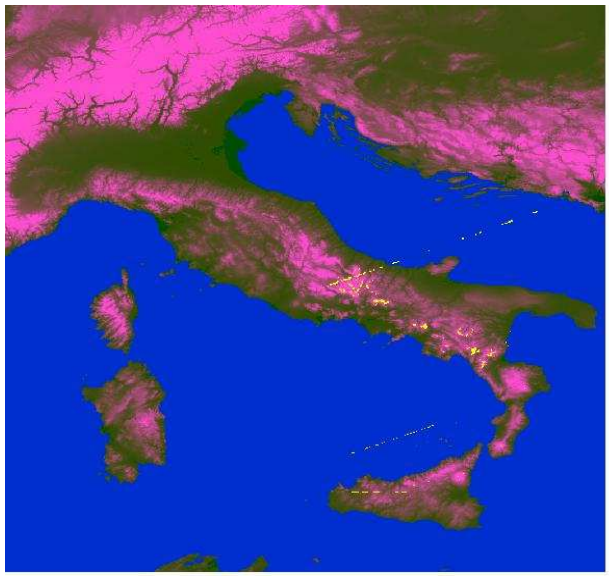

Alice 241180

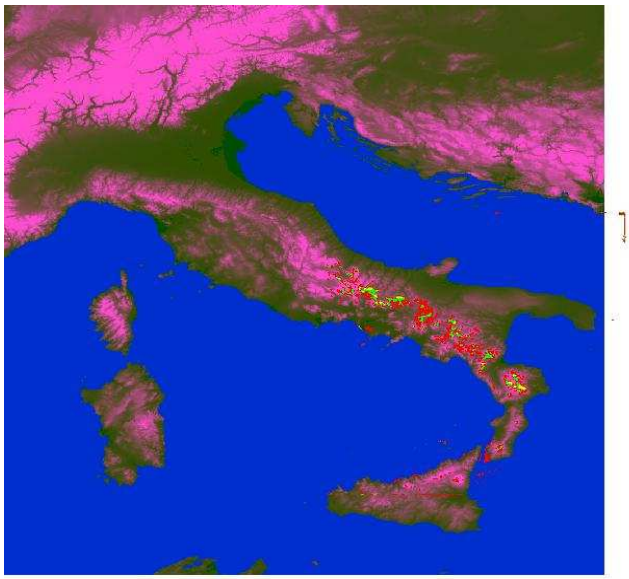

Alice 241180 > 1

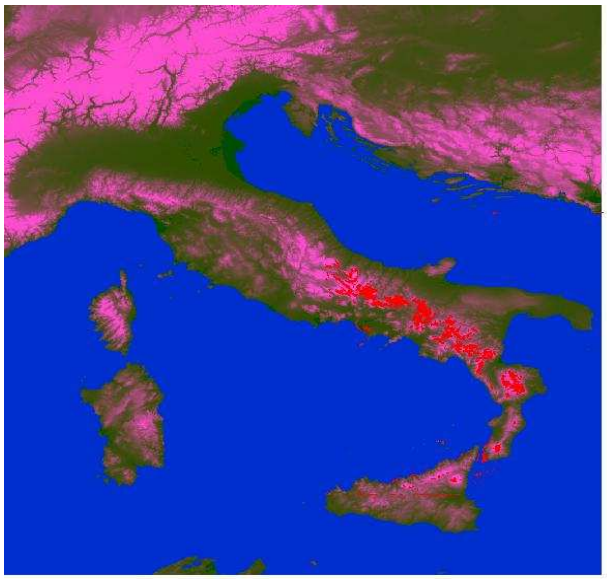

Alice 241180 > 1.5 **Alice 241180 > 2**

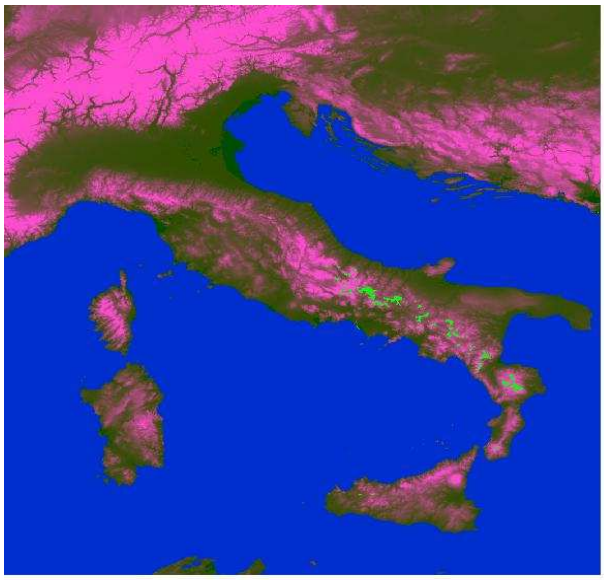

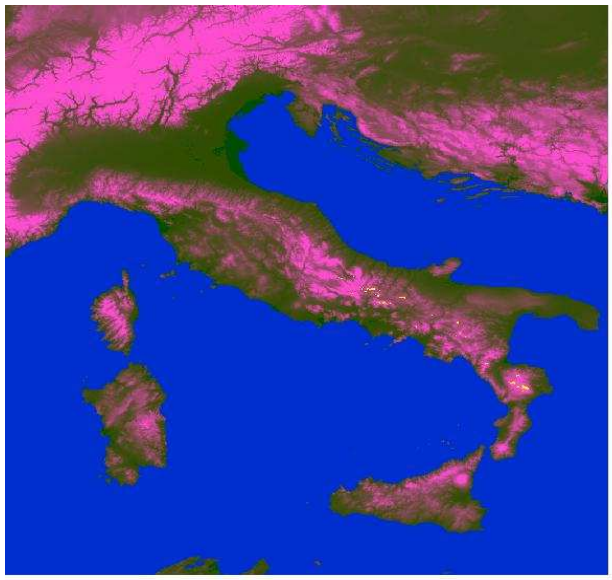

2.7.1 Calculation of index ALICE

According to RAT [6] prescriptions a long term (at least five years long) time-series of satellite imagery (homogeneous for observational time-slot and month of the year), precisely navigated (following SANA navigation and co-located have been used . Once it gains the reference fields , is proceeded the calculation of index ALICE, $\otimes$ (x, y, t) (Absolutely Llocal Index of Change of the Environment, Tramutoli, 1998). This specific application was :

$$\otimes_{\Delta T}(x, y, t) = \frac{\Delta T(x, y, t) - \langle \Delta T(x, y) \rangle}{\sigma_{\Delta T}(x, y)}$$

x , y pixel coordinates on satellite image

t time of image acquisition with $t \in T$ where τ define the homogeneous domain of satellite imagery collected in the same time- slot (hours of the day) and period of the year (month, in this case)

ΔT (x,y,t) temperature difference between the pixel value T(x,y,t) and the (spatial) average value <T(t)> computed *in place* on the study area (to reduce possible contribution (e.g. occasional warming) due to year-to-year climatological changes and/or season time-drift)

< ΔT (x,y) > time average value of ΔT(x,y,t) for the pixel (x,y) computed on the selected data set ($t \in \tau$)

$\boldsymbol{\sigma_{\Delta T}(x,y)}$ standard deviation of T(x,y,t) for the pixel (x,y) computed on the selected data set ($t \in \tau$)

It gives the *excess* of the actual ΔT *(x,y,t)* signal compared with an *unperturbed* reference value < ΔT *(x,y)* **>** and weighted by its *normal* variability $\sigma_{\Delta T}(x,y)$. Both, < ΔT *(x,y)* **>** and $\sigma_{\Delta T}(x,y)$ are computed, once and for all, for each location (x,y) processing homogeneous historical satellite records.

The signal ΔT(x,y,t) is measured in every pixel, it is confronted with the average time ,< ΔT(x,y,t) > calculated on the same one pixel, and weighed with the average inclination , $\sigma_{\Delta T}$(x,y), also calculated it for those pixel, on the base of the set data of Meteosat images from 1992 to 1999. The average inclination represents the variability of the signals, characteristic of the site, but includes in also the variabilities tied to the variations of the observation conditions (for example atmospheric effects).

2.7.2. A different ALICE index :

In fact water vapour is one of the most variable components of the atmosphere , partly absorbing the outgoing, Earth emitted TIR radiation. Variations of atmospheric water vapour content contribute to further increase *llocal* variability of measured ΔT_4 (x,y,t) signal. Moreover, even if AVHRR images are precisely navigated and co-located (in order to permit the computation of reference images $<\Delta T_4$ (x,y,t) > and $\sigma_{\Delta T4}$ (x,y) by multi-temporal analysis), at each revisiting time *t* the same location (x,y) is observe at different satellite zenithal angles (which means also different ground-resolution cells). This circumstance may produce a further spurious temporal variation of the measured signal. It should be noted however that, all the residual "noisy" contributions to the TIR signal (included the above mentioned ones related to the variability of atmospheric conditions and view angles) are intrinsically taken into account by the RAT approach, as they generally increase the *llocal* value of $\sigma_{\Delta T4}$ (x,y) reducing corresponding $\otimes_{\Delta T4}$ (x, y, t) values and ,consequently, false anomaly appearance probability. In order to take into account the effects related to atmospheric water vapour variability, we applied a different ALICE index , to the same event (Irpinia-Basilicata earthquake) and using the same AVHHR data-set (November 1994-1998, 18:00 GMT) :

$$\otimes_{\Delta LST}(x,y,t) = \frac{\Delta LST\ (x,y,t) - <\Delta LST\ (x,y)>}{\sigma_{\Delta LST}\ (x,y)}$$

It differs from the one defined in expression for the use , instead of the simple TIR signal T_4 (x,y,t) , of the LST (Land Surface Temperature) AVHHR product, obtained

following Becker and Li (1990) split-window technique :

$$Lst = 1.274 + \frac{T_4+T_5}{2}\left[1+\left(0.15616^* \frac{1-\varepsilon}{\varepsilon}\right)\right] + \frac{T_4 - T_5}{2}\left[6.26+\left(3.98^* \frac{1-\varepsilon}{\varepsilon}\right)\right. + \left(38{,}33 * \Delta\varepsilon / \varepsilon^2\right) \quad (1)$$

Here, ε_4 and ε_5 are , respectively, the emissivity in the AVHHR channel 4 and 5, $\Delta\varepsilon = (\varepsilon_4 - \varepsilon_5)$ and $\varepsilon = (\varepsilon_4 + \varepsilon_5)/2$, T_4 and T_5 the radiances (expressed in brightness temperatures)measured in AVHHR TIR channel 4 (around 11μm) and 5 (around 12μm). The algorithm mainly exploits the direct proportionality expected between atmospheric total water vapour content (TWVC) and the measured difference $T_4 - T_5$ (due to the higher extinction operated by atmospheric water vapour in the AVHHR channel 5 than in channel 4) to correct land surface temperature estimates for the effect of atmospheric water vapour content. Using the values $\varepsilon_4 = 0.95$ and $\varepsilon_5 = 0.96$) suggested by Becker and Li for the month of November, expression (1) reduces to :

$$Lst(x,y,t) = 1.274 + 1.01264^*[T_4(x,y,t)+ T_5(x,y,t)] / 2 + 6.027^* [T_4(x,y,t)+ T_5(x,y,t)] /2$$

that well emphasizes as, such algorithm; basically exploits only T_4 and T_5 AVHRR radiances. Even if the comparison with ground based observations ascribes, to such LST estimates, quite high biases (>3 ^{0} C r.m.s., Pozo Vasquez *et al*., 1995), the correlation with near-surface thermal conditions has been demonstrated to be quite high (more than 95%, Cuomo, *et al*., 2002) in the temporal domain. Such biases on LST estimates, as well as the parametric choice of surface emissivity values (based only on the season and not on local surface

properties) are both expected not to affect $\otimes_{\Delta LST}$ index that is, in fact, based on LST variations (both in space and time domains) and not on its absolute values. Figure 1 summarizes the result of the analysis performed in the case of the strong earthquake (M= 6.9) occurred in Southern Italy (Irpinia-Basilicata) on November,23th,1980 at 7:32pm local time. This is the same event already analysed in a previous study(Tramutoli *et al.*,2001b) by using $\otimes_{\Delta T}$ index instead of $\otimes_{\Delta LST}$. As in that study, also in this case all NOAA / AVHRR satellite passes, collected in November, from 1994 to 1998, around 18:00 GMT over Southern Italian peninsula have been processed in order to build average, $\{\Delta LST(x,y)\}$ and standard deviation $\sigma_{\Delta LST}(x,y)$, reference images. In the same way, monthly averages $\otimes_{\Delta LST}(x,y)$ of $\otimes_{\Delta LST}(x,y,t)$ have been computed for the month of November 1980 (the year of the earthquake for validation purposes) and for the relatively unperturbed (no earthquakes with M_S >4)years 1994 and 1998 (for falsification purposes). The results of this analysis are reported in Figure 1 , where pixels $\otimes_{\Delta LST}(x,y)>1$ are depicted in red and aftershock locations in green. By comparison with results previously achieved by using $\otimes_{\Delta T}$ index it is possible to note that :

a) for the November 1980 (validation), the spatial distribution of pixels with $\otimes_{\Delta LST}(x,y)>1$ is quite similar to the one of pixel with $\otimes_{\Delta T4}>0.6$.

b) as far as unperturbed years (November 1994 and 1998) are concerned (falsification), pixels with $\otimes_{\Delta LST}(x,y)>1$ almost disappear with respect to the already rare presence of pixels with $\otimes_{\Delta T4}>0.6$.

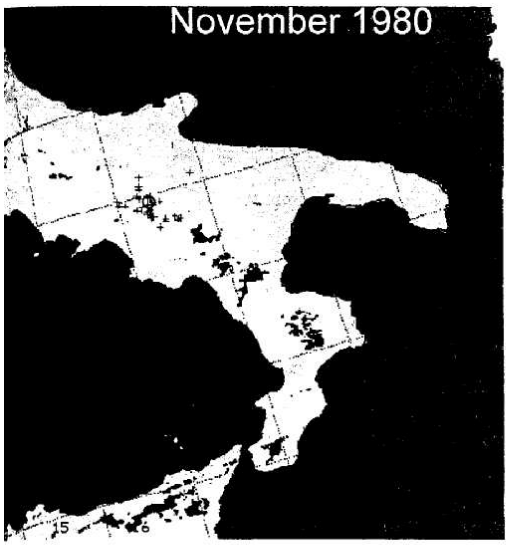
November 1980
15
16

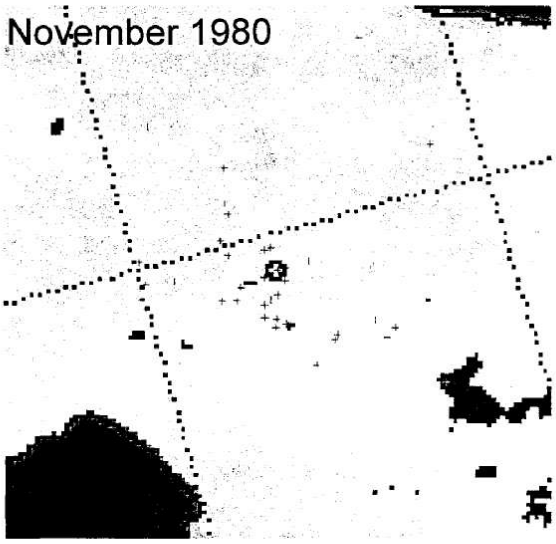
November 1980


November 1994
15
16

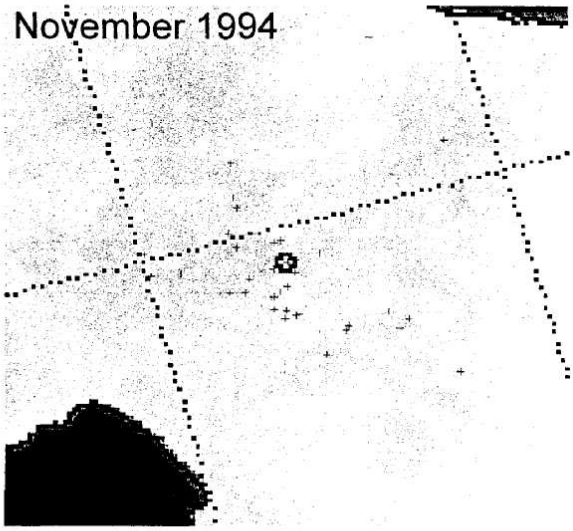
November 1994


November 1998
15
16

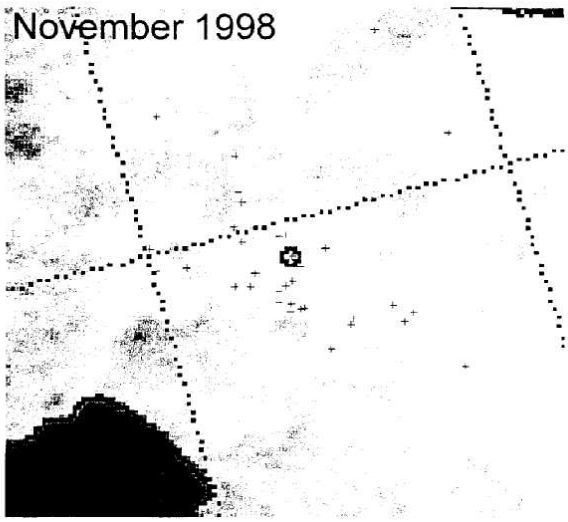
November 1998

Figure 1 :Results of the analysis on monthly $\otimes_{\Delta LST}$ (x,y) of $\otimes_{\Delta LST}$ (x,y) index (computed on the basis of NOAA-AVHHR images collected around 18:00GMT during the months of November from 1994 and 1998) for the month of November 1980,1994,1998. The aftershocks of the Irpinia-Basilicata earthquake and the main epicentral area(circled)are depicted in green. Pixels with $\otimes_{\Delta LST}$ (x,y)>1 are depicted in red. The zooms,on the epicentral area, of images shown on the left are shown on the right side.Note the absence of high $\otimes_{\Delta LST}$ (x,y) values in the unperturbed(no earthquakes with M>4) month of November 1994 and 1998 .

It seems that the use of $\otimes_{\Delta LST}$ instead of $\otimes_{\Delta T4}$ (taking into account the contribution to TIR signal variability due to variations of the atmospheric water vapour content) mainly produces a reduction of the *llocal* value of $\sigma_{\Delta LST}$ (x,y),(compared to $\sigma_{\Delta T4}$ (x,y)), permitting a substantial increase of the signal-to-noise(S/N) ratio (inherent in the definition of ALICE indexes) from 0.6 to 1.

Also the indications (e.g. on the possible relations between occurrence of higher $\otimes_{\Delta T4}$ values and seismogenic area distribution and activation) coming from the previous study of Tramutoli *et al* .(2001b) appear reinforced by the increased S/N ratio associated to the observed $\otimes_{\Delta LST}$ space-time patterns. Their confirmed extension, far away(up to several hundred kilometres) from the epicentral zone is no minor importance, reinforcing the idea that spatial resolution is not the main constraint for satellite packages devoted to such studies.

Further reductions of the observational noise can then be expected by the extension of the proposed technique to geo-stationary satellites, like Meteosat. In particular, significant improvements are to be expected by the extension of the proposed approach to MSG-SEVIRI (Meteosat Second Generation-Spinning Enhanced Visible and Infra-Red Imager) offering a time resolution of 15 minutes

and a channel selection that saves (and extends) present AVHRR capabilities. Even at a lower spatial resolution (3km compared with 1.1km of AVHRR in the TIR channels) and thanks to the MSG geo-stationary attitude, SEVIRI will offer :

a) a precise navigation and image-to-image co-location, as well as constant (for each location) view-angles that permit a significant reduction of the observational noise and an increasing of the sensitivity of the proposed method, which strongly relies on the multi-temporal analysis of the satellite radiance at pixel level.

b) an improved time-resolution that will reduce both the natural (lower image-to-image variability of the *llocal* signal) and observational (greater homogeneity of time-series elements) noise increasing, once more, the sensitivity of ALICE indices toward relatively lower signal variations.

3° CAPITAL

3.1 PRE-PROCESSING

23rd November 1980 IRPINIA (Southern Italy) earthquake (M_s=6.9)

In this case (prescriptions on t) only AVHRR imagery collected during the month of November (in the period 1980-1999) around 18:00 GMT (afternoon passes) were considered for the computation of reference fields $< \Delta T(x, y) >$ and $\sigma_{\Delta T}(x, y)$.

3.2 GEOLOGIC AND TECTONIC EVALUATION OF THE INVESTIGATED AREA

Fault Background

The Irpinia fault is a major NW-striking normal fault located in the southern Apennines (Italy) (Figure1) The Apennines form the NW-trending backbone of the Italian peninsula and formed as a result of NE-shortening that produced a pile of thrust sheets on which extensional activity has been superimposed since Middle-Upper Pliocene. The most recent large earthquake on this fault was a Ms6.9 event on November 23, 1980. The 1980 fault rupture was mapped in detail by Westaway and Jackson (1984) and Pantosti and Valensise (1990) (Figure2). The 1980 rupture extent was up to 38 km long , NE side down, with average coseismic vertical displacement of 0.6 m (Figure3). The fault terminations and internal complexity of the rupture appear to be controlled by pre-existing structures, transverse to the Apennine chain. Fault location, slip distribution, and fault complexity deduced from the 1980 surface rupture have been found to be in good agreement with the seismological observations. The peculiarity of the Irpinia fault is that it does not show the geomorphic evidence of repeated long-term tectonic activity, typical of normal faults. In fact, it occurs mainly within a mountain range, cuts across linear

valleys, basins, mountain crests and slopes, and produces subsidence of the highest elevations (Figure2). This suggests that the Irpinia fault is a relatively young structure which has not yet developed mature geomorphic features.

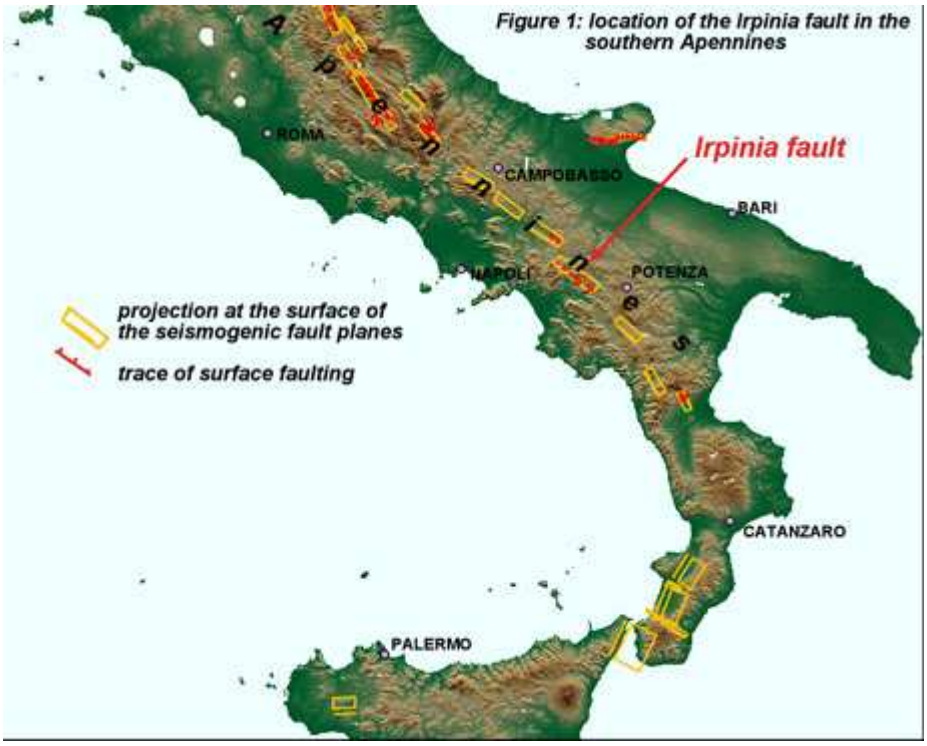

Figure 1 The Irpinia fault is a major NW-striking normal fault located in the southern Apennines (Italy)

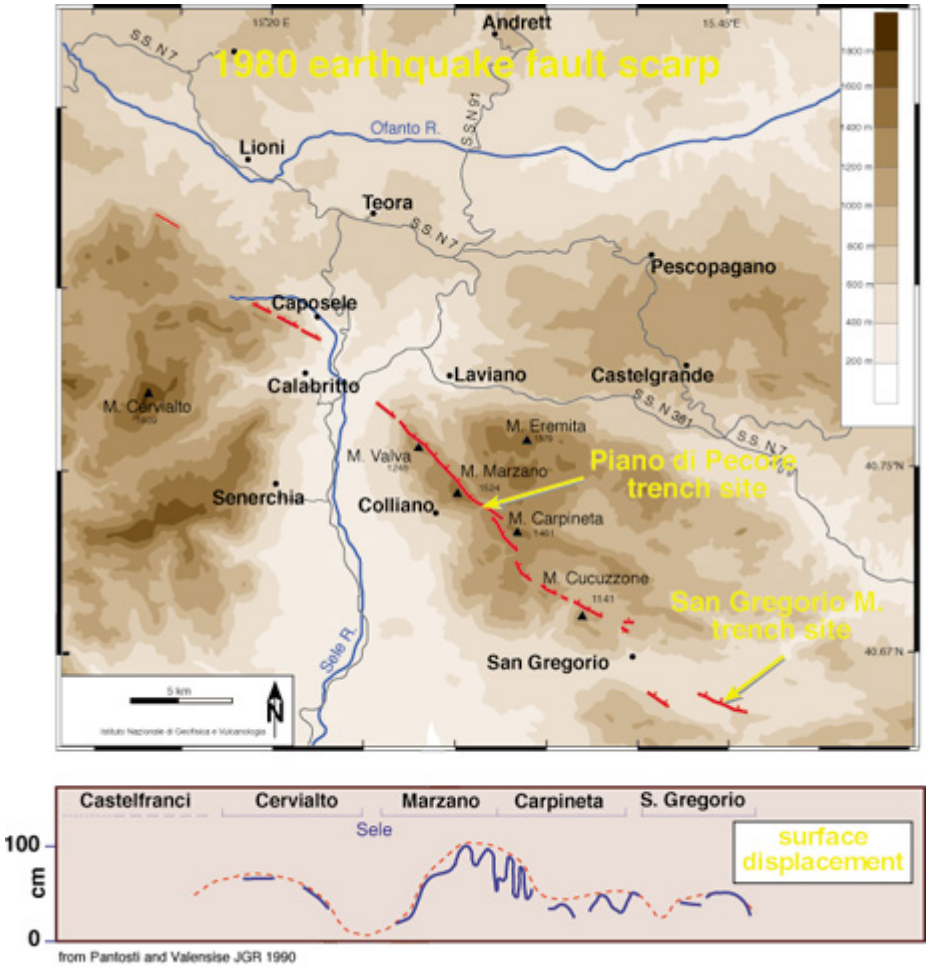

Figure 2 - Map of surface faulting produced by the 1980 earthquake and location of trench sites. Notice that the rupture cut mainly across a mountain range and produced a reversal in the present topography, causing subsidence where the highest peaks are located. Lower inset shows the distribution of the coseismic slip (from NW to SE), blue lines join measured points, dashed red lines shows the general trend of the highest slip in the central part of the rupture.

Figure 3 - View of the 1980 surface rupture at Monte Carpineta. The fault back-dips with respect to the slope producing subsidence of the top of the range (to the left).

Site Background

The Piano di Pecore trench site is within a circular, 250 m-wide intermontane basin, itself located high on a calcareous ridge, along which the Irpinia fault extends (Figure2). The 1980 rupture formed a well-defined NE-facing flexure in the middle of the basin, but changing to a clear free-face scarp toward its edges. Measured vertical throws are between 0.4 and 0.8 m. Because the fault displacement opposes the slope, this results in the damming of drainage and consequent flooding of the basin and ponding against the scarp (Figure4). This was observed after the 1980 earthquake. Filling of the basin by ponding may eventually bury the fault scarp. Piano di Pecore is considered a favorable site for trenching because: (1) previous 1980-type earthquakes may have caused similar damming depositional cycles, providing a good geologic record of paleoearthquakes, (2) the fault runs along the highest part of the range and thus it is one of the few locations where

some sediment deposition occurs, (3) there is high likelihood of finding datable horizons because of the low stream energies in a prevalently ponding area. Two trenches were excavated at Piano di Pecore, trench 1 was in the middle of the basin, and trench 2 was on its west side.

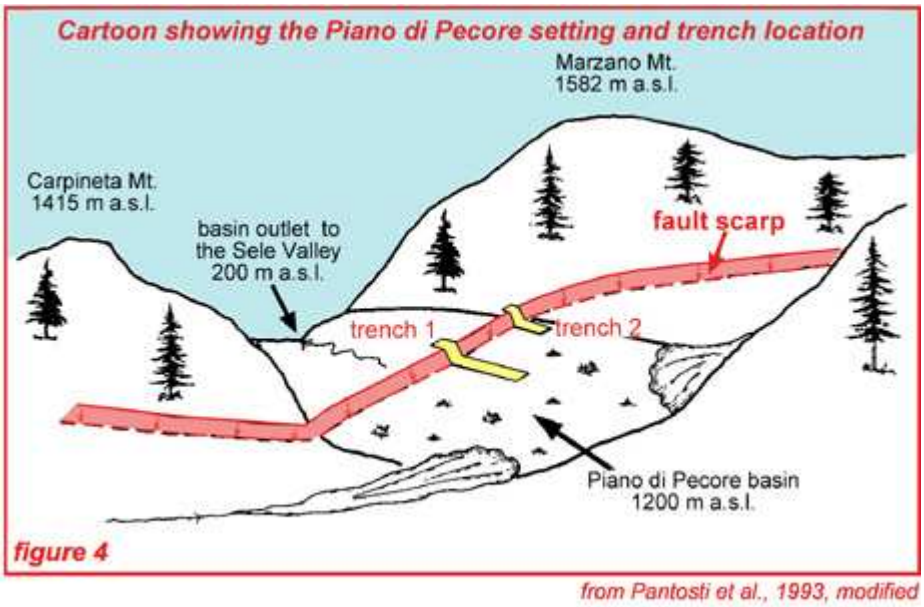

Figure 4 - Sketch of the Piano di Pecore trench site showing trench locations and the trace of the 1980 scarp damming the basin.

The trench

Trench 1 is 33 m-long and up to 4 m-wide. It exposes a 4 m-thick sequence of lacustrine and colluvial deposits containing a large component of volcanic pumice, sand, and ash (Figure5) .This volcanic component presumably originated from explosive activity of the Mt. Vesuvius and Phlegrean Fields located 80 to 100 km to the west. The stratigraphic sequence was divided into nine main units several of which were radiocarbon dated (Figure6). The flexure that formed during the 1980 earthquake appears to faithfully reproduce the style of deformation at depth, produced by previous events. In fact, a buried flexure of the lacustrine and colluvial

deposits sits exactly below the 1980 scarp and is associated with minor faulting and fracturing. A minor zone of antithetic warping occurs in the hangingwall ca. 15 m from the main zone. A total net vertical throw of 3.0-3.1 m is measured across the main zone of deformation

Figure 5 - View of trench 1 east wall. The 1980 scarp apears as a clear warp of the ground (below the van) that coincides with the cummulative scarp at depth where all the layers are warped. Notice that the old layers (pink or orange flags) show a warp of larger amplitude than the ground surface, indicating the occurrence of surface faulting events prior to the 1980 earthquake.

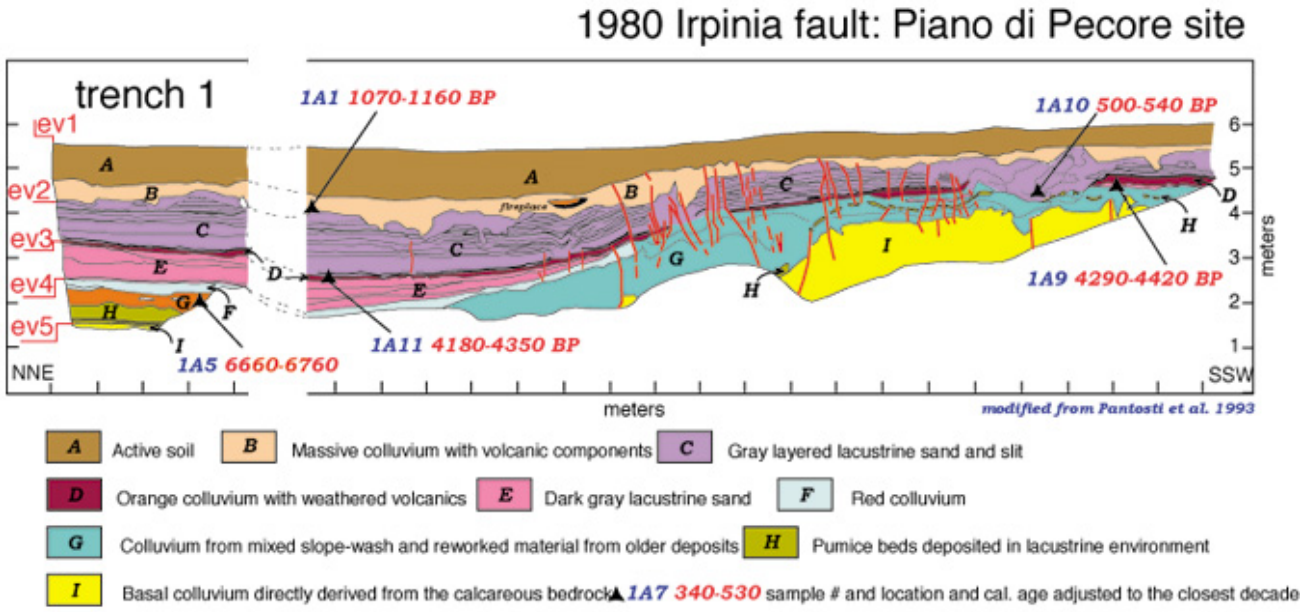

Figure 6 - Log of trench 1 simplified from a 1:10 field survey. Sets of layers show increasing amount of warping with age, indicating distinct increments of deformation. A small antithetic warp exists about 10 m NNE of the main warp (step in the blank zone

Paleoearthquake recognition

Recognition of paleoearthquakes in trench 1 is based on a combination of stratigraphic relations and reconstruction of the amount of displacement recorded by sedimentary units that extend across the fault zone. Event horizons (i.e., ground surface at the time of an earthquake) were recognized based on unconformities and onlap geometry of sediments that develop as result of warping and subsequent deposition (Figure7). Vertical displacements of layers measured across the fault zone, assuming an original sub-horizontal deposition (suggested by uniform thickness of each layer), show that the net vertical displacement of the buried layers is larger than the displacement of the ground surface in 1980 earthquake and that the displacement increases systematically with depth

(Figure6). Moreover, distinct sets of layers show similar amount of displacement, but each set shows a discrete increase of displacement with respect to the upper one. Based on these observations we recognized four event horizons (i.e., paleoearthquakes) predating the 1980 earthquake. A graphic reconstruction of the tectonic and sedimentary history recorded in trench 1 was performed by subtracting the displacement of progressively older earthquakes from the cumulative deformation recorded in the sequence (Figure8) .The reconstruction shows the stratigraphic and tectonic relations before and after each event and helps to estimate the amount of vertical coseismic displacement produced by each paleoearthquake.

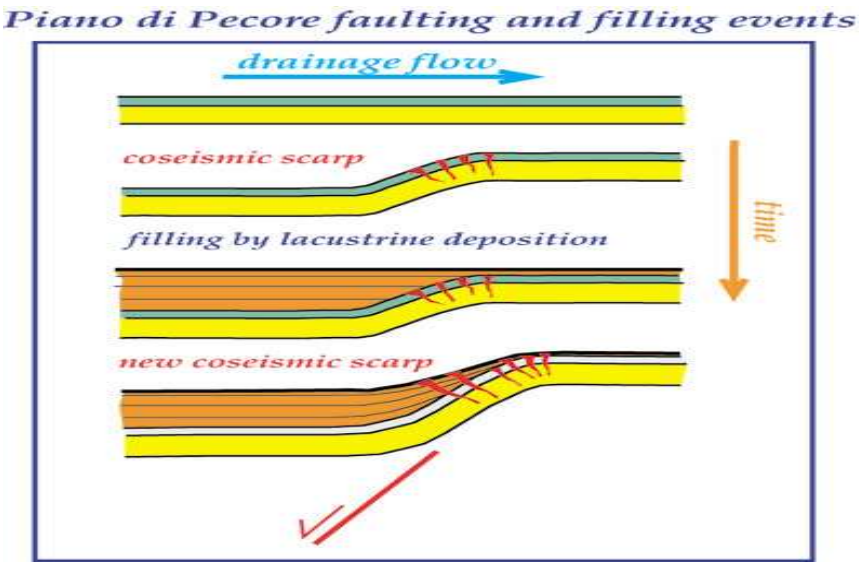

Figure 7 - Each time a coseismic warp occurs at the Piano di Pecore site it prevents the natural drainage from flowing through the outlet and sediments start to fill the subsided area, onlapping the scarp. When the basin is filled, the drainage may recommence through the outlet and sedimentation/erosion occurs over the whole area. If a new earthquake occurs the sedimentary sequence is warped again and the older deposits record greater warping than the younger deposits.

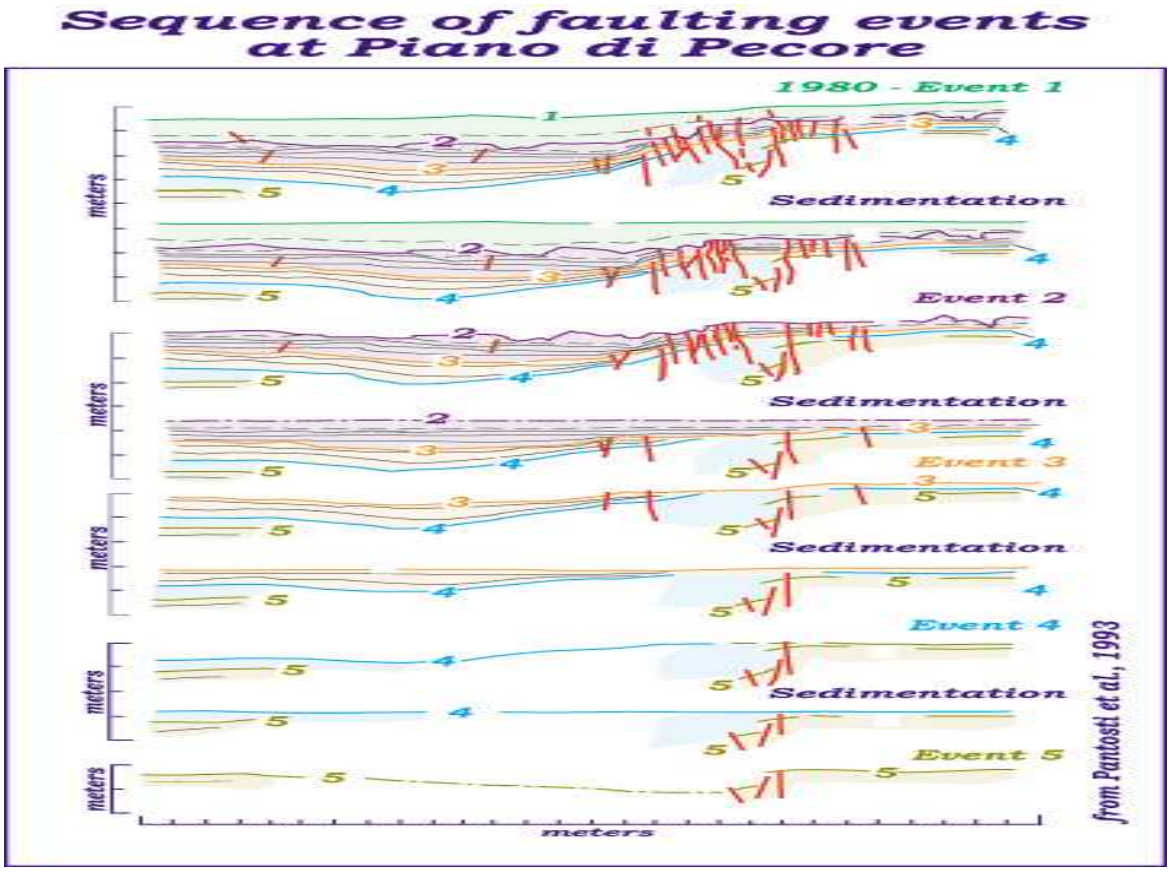

Figure 8 - Reconstruction of the stratigraphic and structural relations of the sediments exposed in trench 1. These were obtained by subtracting the displacement produced by each individual event.

Dating of paleoearthquakes

Because of the limited amount of datable material available in trench 1, and the good stratigraphic correlation with trench 2, we also used data from trench 2 to constrain the age of the paleoearthquakes (Figure9). Dating of events is based on 10 radiocarbon ages obtained on detrital charcoal, lignite or humus-enriched sediment samples, and on the correlation of a pumice deposit with one of the major eruption of Mt. Vesuvius: the Mercato eruption of 7910±100 B.P. (Table1). These ages have been corrected for isotopic fractionation (d13C), and for secular atmospheric 14C fluctuations, and have been converted to calendar years using the program Radiocarbon by Stuiver et al. (1993) (see table). On the basis of the

stratigraphic position of the dated samples with respect to the event horizons we can constrain the interval within which each paleoearthquake occurred. For example, event 4 occurred before unit D (sample 1A11) was deposited and after unit G (sample 1A5) was deposited. That is, between 4180-4350 B.P. and 6660-6760 B.P., respectively, so event 4 occurred between 4180 and 6760 B.P. Ages of paleoearthquakes are summarized in the following table. Because of the limited number of dated samples, age ranges of events are quite large. Dating more horizons could help to refine the age of each of the paleoearthquakes.

Age of the paleoearthquakes recognized at Piano di Pecore trench 1

	min yr BP	**max yr BP**	**vertical throw (cm)**
event 1	1980 A.D.	1980 A.D.	45-53
event 2	1410	2780	47-55
event 3	3470	4350	47
event 4	4290	6760	73-81
event 5	6660	8980	74-98

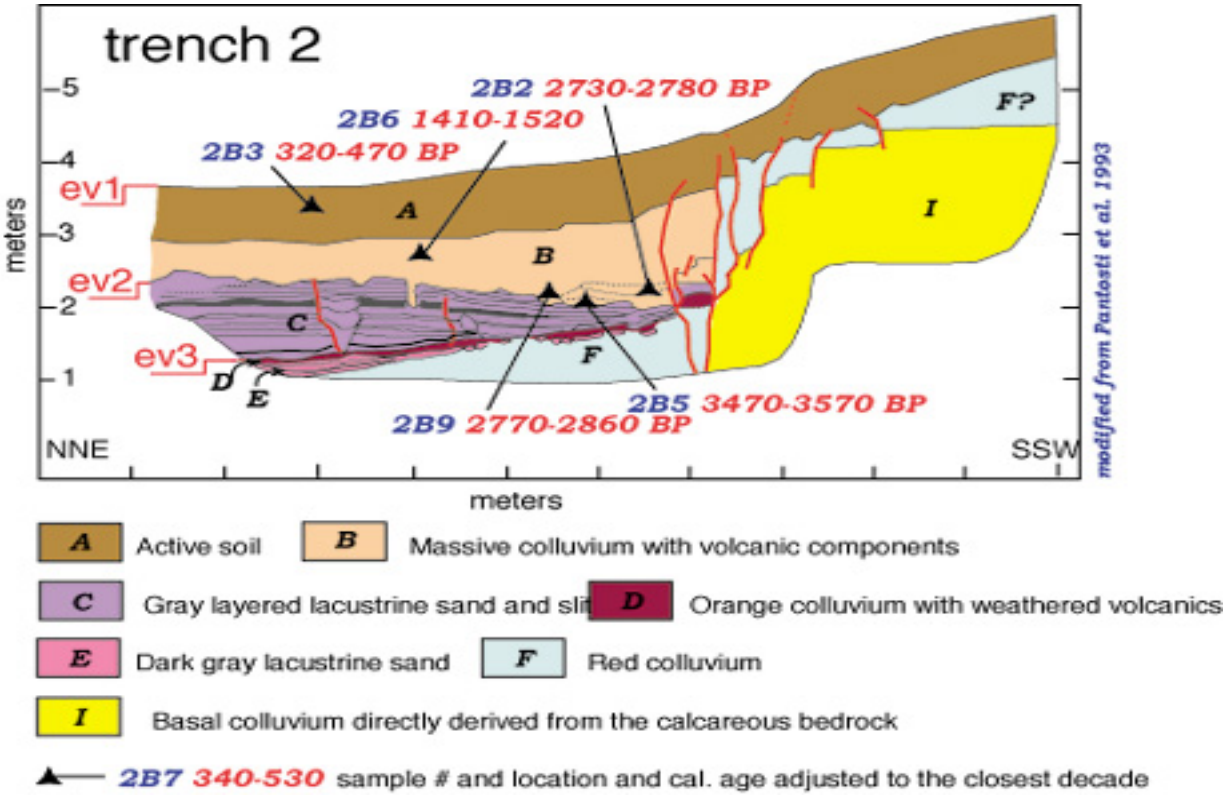

Figure 9 - Log of trench 2 simplified from a 1:10 field survey. Notice the different style of deformation respect to trench 1.

Radiocarbon ages from Irpinia trench 1

SAMPLE	Radiocarbon Age 14C yr B.P.	calibrated age 1s range cal. yr B.P. (*)
1A1	1220?40	1160-1070
1A10	480?45	540-500
2B3	345?50	470-320
2B6	1550?50	1520-1410
1A5	5900?50	6760-6660
1A9	3920?50	4420-4290
1A11	3850?55	4350-4180
2B2	2620?45	2780-2730
2B5	3295?45	3570-3470
2B9	2730?45	2860-2770
Mercato	7910?100(**)	8980-8600
(*) ages are adjusted to the nearest decade; B.P.: before present where pesent is yr 1950 A.D.		
(**) by *Arnò et al.* (1987)		

3.3 Investigating possible origin of observed TIR anomalies.

Toward a Better Understanding of Non-Seismic Pre-Earthquake Phenomena

Large earthquakes release enormous amounts of energy in the form of seismic waves. Some of the energy, which builds up in the Earth's crust, however, is expected to "leak" into non-seismic channels prior to catastrophic failure. The most basic process at seismogenic depth is stress-induced deformation of rocks. Stress and deformation increase rapidly as the time of rupture approaches. The question arises: What are the consequences of stress-induced deformation of rocks? Igneous and high-grade metamorphic rocks contain dormant electric charge carriers that are activated by deformation [*Freund*, 2002]. The activation generates highly mobile charge carriers. These are defect electrons in the O 2p-dominated valence band, also known as positive holes or p-holes for short. In spite of intense studies of rock mechanics [*Dmowska*, 1977; *Lockner*, 1995], the generation of p-holes in rocks undergoing deformation has been overlooked for decades. We now have learned how to identify p-holes and how to study their effects. A prominent attribute is that, as defect electrons in the valence band of silicate minerals, p-holes can flow out of a highly stressed "source volume" and propagate into unstressed rocks. As the p-holes move through the crust, they represent an electric current. Such currents set up polarization fields that counteract the outflow of p-holes and induce a counter flow of other charges. Two currents, which are coupled through their electric fields, represent a system that can go into oscillations [*Freund et al.*, 2002b]. A predictable consequence of the waxing and waning of currents in the Earth's crust is the emission of low to very low frequency electromagnetic radiation,

possibly in a pulsating mode. When p-hole clouds reach the Earth's surface, they lead to a plethora of phenomena. Being carriers of positive charge, p-holes are expected to change the ground potential. A need for high positive ground potentials has been inferred from studies of pre-earthquake ionospheric perturbations [*Liu et al.*, 2000]. Another predictable effect is the build-up of high electric fields at the rock-to-air interface – so high that we need to consider the possibility (i) of field-ionization of air molecules and emission of positive ions into the atmosphere close to ground, and (ii) of dielectric breakdown of the air and corona discharges. Small air ions will act as nucleation centres for fog and haze, providing a possible explanation for the reported occurrences of pre-earthquake "ground-hugging fog". Air-borne positive ions could provide a explanation for strange pre-earthquake animal behaviour, reported for centuries [*Tributsch*, 1983]. Corona discharges could be the cause of luminous phenomena, so-called "earthquake lights" [*Derr*, 1986; *St-Laurent*, 2000]. In addition, corona discharges could be the cause of static at KHz frequencies reported by radio operators [*Warwick et al.*, 1982]. Yet another effect derives from the prediction that, while the generation of p-holes at depth costs energy, the recombination of p-holes at the Earth's surface regains energy. Depending on the recombination energy, the outermost skin of the rocks, only a few atomic layers thick, could become very "hot" and radiate excess energy in the thermal infrared. This may be relevant to the reported pre-earthquake "thermal anomalies" seen in mid-IR satellite images [*Tronin*, 2002]. This effect has recently been studied in the laboratory by measuring the mid-IR emission from granite undergoing deformation [*Freund et al.*, 2002a]. Though we are only at the beginning of this work, the discovery of p-holes, which can be activated in rocks,

may hold the key to a better understanding of pre-earthquake phenomena.

Generally physical processes that govern earthquakes mechanisms are extremely complex and not easily identifiable. In recent years major efforts of the scientific community have focused on understanding seismic-tectonics phenomena in relation to earthquakes prediction.

Ground deformations, stress field and velocity at which energy accumulates are parameters useful to earthquakes prediction, yet, at the moment, it is not known which level of deformation they need to reach in order to be considered precursory phenomena. Actually, the status of the art does not allow to forecast on a statistical basis the time, place and magnitude of an earthquake. By such considerations it is meant to underline the need of the scientific community to get to accurate seismic-tectonics modelling to interpret earth surface motions correctly.

The models that have been developed so far are based on historical seismicity data and on the analysis of the tectonic configuration, without taking into account the current data on seismic-tectonics activity, which should be acquired by monitoring active areas accurately and systematically.

Lack of these data is due to the characteristics of traditional monitoring systems of seismic activity (seismic stations) and of ground deformations of the earth surface (tiltmeters and leveling), as they can only provide occasional and partial covering of the area of interest.

3.4. LAYERS OF ITALY AREA

3.4.1. How we take these layers?

The layers above were taken from one programme and they were transferred in order to be used by another programme. In the programme which we were using and where we wanted to import these layers as vectors and rasters we had the ability to view all these layers simultaneously. Also we were given the chance to view more than one vectors together and make remarks and affairs over the vectors that interests us. By following this process it was good by the remarks which we were able to make , to have an overview of the seismicity of an area and be able to take the appropriate decisions over the specific area. Also we are able to make a compare between all these layers and have the capability to reach in more optimistic conclusions and decisions of the main source and the conditions below which one earthquake occurs .It is a useful and helpful tool which help us in many conditions in order to have a general idea of a specific area and its behaviour.

3.4.2.What are they?

Spatial data places the features on the map. The coordinates of a point are the most obvious example of this, but it also incorporates projection systems, line and polygon attributes, and other information. There are two main classes of spatial data: vector and raster.

VECTOR

Vector is a data structure, used to store spatial data. Vector data is comprised of lines or arcs, defined by beginning and end points, which meet at nodes. The locations of these nodes and the topological structure are usually stored explicitly. Features are defined by their boundaries only and curved lines are represented as a series of connecting arcs.

Vector storage involves the storage of explicit topology, which raises overheads, however it only stores those points which define a feature and all space outside these features is 'non-existent'.

A vector based GIS is defined by the vectorial representation of its geographic data. According with the characteristics of this data model, geographic objects are explicitly represented and, within the spatial characteristics, the thematic aspects are associated. There are different ways of organising this double data base (spatial and thematic). Usually, vectorial systems are composed of two components: the one that manages spatial data and the one that manages thematic data.

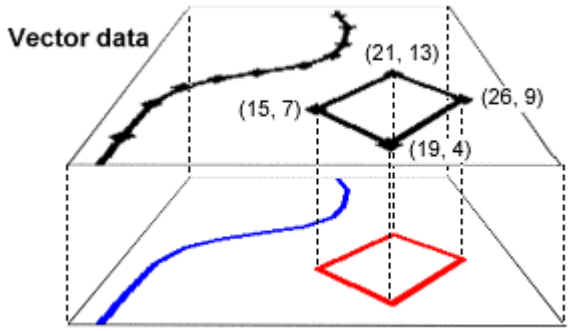

In vector data the features are recorded one by one, with shape being defined by the numerical values of the pairs of **xy** coordinates.

- A **point** is defined by a single pair of coordinate values.
- A **line** is defined by a sequence of coordinate pairs defining the points through which the line is drawn.
- An **area** is defined in a similar way, only with the first and last points joined to make a complete enclosure.

RASTER

Raster is a method for the storage, processing and display of spatial data. Each area is divided into rows and columns, which form a regular grid structure. Each cell must be rectangular in shape, but not necessarily square. Each cell within this matrix contains location co-ordinates as well as an attribute value. The spatial location of each cell is implicitly contained within the ordering of the matrix, unlike a vector structure which stores topology explicitly. Areas containing the same attribute value are recognised as such, however, raster structures cannot identify the boundaries of such areas as polygons.

Raster data is an abstraction of the real world where spatial data is expressed as a matrix of cells or pixels , with spatial position implicit in the ordering of the pixels.

With the raster data model, spatial data is not continuous but divided into discrete units. This makes raster data particularly suitable for certain types of spatial operation, for example overlays or area calculations.

Raster structures may lead to increased storage in certain situations, since they store each cell in the matrix regardless of whether it is a feature or simply 'empty' space.

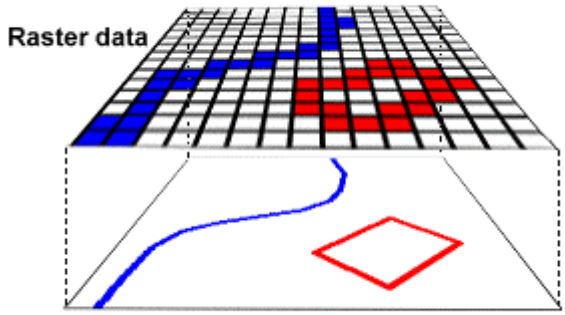

advantages/disadvantages of raster and vector data models

	raster	vector
precision in graphics	X	✔
traditional cartography	X	✔
data volume	X	✔
topology	X	✔
computation	✔	X
update	✔	X
continuous space	✔	X
integration	✔	X
discontinuous	X	✔

3.4.3.Contents of layers in Italy area :

Seismogenic Sources

The seismogenic sources are divided into six main categories (*From Geologic/Geophysical Data*, *Historical-Well Constrained with Geological Background*, *Historical-Well Constrained with no Geological Background*, *Historical-Poorly Constrained with Geological Background*, *Historical-Poorly Constrained with no Geological Background*, *Deep*) and can be displayed separately or simultaneously.

Seismogenic Sources from Geologic/Geophysical Data

This category stores data on seismogenic sources, belonging to the *Geologic/Geophysical* category, for which either geological or geophysical evidence is available. For all sources of this group the compiler has brought together geological, seismological and other geophysical information .The name of the associated physical table is **SourceGeol.tab**.

Notice that the *minimum depth of the fault plane from topographic surface* must be intended as the depth of the seismogenic portion of the source. To avoid ambiguities and potential modelling problems, the minimum value for this parameter was conventionally set at 1 km. The underlying assumption is that the shallowest 1 km of crust above a seismogenic source may only react passively to slip on the underlying fault even if sizeable surface faulting may occur.

Each seismogenic source will be displayed as a yellow rectangle and a yellow

line parallel to one side of it. The first represents the surface projection of the fault plane with its size and orientation, the second represents its cut-off. Coseismic fault scarps are represented as red barbed lines (with barbs on the down-thrown block).

Seismogenic Sources - Historical-Well Constrained

Sources of this category are divided into two sub-sets that can be displayed separately or at the same time. Since sources of this type derive exclusively from good quality intensity data using the method of *Gasperini et al.* [1999], their orientation is calculated but their plunge and dip are unknown. They are represented as oriented and scaled rectangular boxes.

Seismogenic Sources - Historical - Well Constrained with Geological Background

Includes all seismogenic sources, belonging to the *Historical-Well Constrained with Geological Background* category, derived exclusively from intensity data following the method proposed by *Gasperini et al.* [1999] and for which the quality of the solution obtained was enough to allow the representation by an oriented rectangular box

The name of the associated physical table is **SourceHistARev.tab**, where

- ***Hist*** indicates that the source was derived from intensity data exclusively.
- ***A*** indicates that sources of this type are of better quality among all those obtained from intensity data.
- ***Rev*** indicates that there has been a revision by the compiler.

Notice that the structure of this table differs from that of **SourceGeol.tab** for the following reasons:

- lack of fields Dip, Rake, Min_Depth and Max_Depth, all of which cannot be assessed using the procedure of analysis of intensity data proposed by *Gasperini et al.* [1999].
- lack of fields describing the location of the surface expression of the source.
- more quantitative definition of Quality (two distinct parameters).
- uncertainty in the definition of Strike.

Sources of this category are shown in blue to highlight them with respect to the remaining intensity-based sources.

Seismogenic Sources - Historical - Well Constrained, no Geological Background

Includes all seismogenic sources, belonging to the *Historical-Well Constrained, no Geological Background* category, derived exclusively from intensity data following the method proposed by *Gasperini et al.* [1999] and for which the quality of the solution obtained was enough to allow the representation by an oriented rectangular box. The name of the associated physical table is **SourceHistA.tab**. The structure of the table is the same as for **SourceHistARev.tab**.

Sources of this category are shown in black.

Seismogenic Sources - Historical-Poorly Constrained

Sources of this category are divided into two sub-sets that can be displayed separately or at the same time. Sources of this type derive exclusively from intensity data using the method of *Gasperini et al.* [1999], but in this case the quality of the solution was not good enough to allow their representation as oriented rectangular boxes. For this reason they are shown as scaled circles.

Seismogenic Sources - Historical - Poorly Constrained with Geological Background

Includes all seismogenic sources, belonging to the *Historical-Poorly Constrained with Geological Background* category, derived exclusively from intensity data following the method proposed by *Gasperini et al.* [1999] and for which the quality of the solution obtained was not enough to allow the representation by an oriented rectangular box . The source was then represented as a circle having the diameter equal to the estimated source length.

The name of the associated physical table is **SourceHistBRev.tab**, where

- ***Hist*** indicates that the source was derived from intensity data exclusively.
- ***B*** indicates that sources of this type are of lesser quality among all those obtained from intensity data.
- ***Rev*** indicates that there has been a revision by the compiler.

Notice that the structure of this table differs from that of **SourceHistARev.tab**/ **SourceHistA.tab** for the following reasons:

- lack of fields Strike, Length, Width due to lesser quality of solution.
- use of Radius to characterise the size of the source.

Sources of this category are shown in blue to highlight them with respect to the remaining intensity-based sources.

Seismogenic Sources - Historical - Poorly Constrained, no Geological Background

Includes all seismogenic sources, belonging to the *Historical-Poorly Constrained, no Geological Background* category, derived exclusively from intensity data following the method proposed by *Gasperini et al.* [1999] and for which the quality of the solution obtained was not enough to allow the representation by an oriented rectangular box. The name of the associated physical table is **SourceHistB.tab**. The structure of the table is the same as for **SourceHistBRev.tab**.

Sources of this category are shown in black.

Seismogenic Sources - Deep

This category contains seismogenic sources, belonging to the *Deep* category, derived exclusively from intensity data following the method proposed by *Gasperini et al.* [1999] and for which the compiler hypothesised a depth larger than ordinary (usually below 10 km). They are represented as an hexagon.

Sources of this category are shown as open purple scaled hexagons.

Seismogenic Sources Integrated Source Dataset

The structure of the *Database* allows for multiple solutions for the same physical seismogenic source. For example, a source of the category *Historical - Well Constrained* will always have also the corresponding solution in the category *Historical - Poorly Constrained* and possibly also in the *Geologic/Geophysical*. The *Integrated Source Dataset* (**SourcePreferred.tab)** displays the "preferred" set of sources, that is to say, in case of multiple solutions the compiler has made a decision concerning which source should be used for further elaborations. The

decision is made by setting the field *Preferred* to "*T*" or "*F*" depending on whether the compiler wants the specific source to be included or not included in the *Integrated Source Dataset*.

Seismic Behaviour

The table **Seismic_Behaviour.tab** stores parameters used to characterise the behaviour of each seismogenic source for all source categories.

Fault Scarps

The table **FaultScarps.tab** lists genuinely tectonic surface ruptures that are thought to slip in conjunction with one or more sources of the *Geologic/Geophysical* category. The ruptures are usually more than one and include primary ruptures located along the fault projection onto the surface and secondary ruptures located within the surface projection (e.g., in the hanging-wall compartment of a normal fault). Each rupture is identified by an IDScarp code and is logically linked to one or more individual sources through the IDSource code. However, this does not preclude that it may move as a result of the activation of other sources.

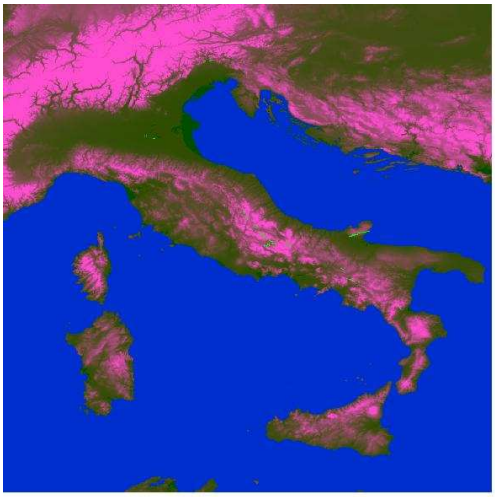

Tectonic Lineaments

The tables **TransverseTectLineaments.tab** and **GenericTectLineaments.tab** contain linear tectonic features taken from published literature. The first table contains lineaments that lie nearly perpendicular to the general trend of the main seismogenic sources, while all the remaining lineaments are included in the second table. These two subsets are able to be viewed together in **Tectonic_Lineaments.tab** . Each lineament may be mapped as a single line or as a segmented element.

These are the linear tectonic features taken from published literature , they are shown as yellow dashed lines.

Tectonic Lineaments - Transverse Tectonic Lineaments

Shows only the linear tectonic features that lie perpendicular to the general trend of the main seismogenic sources.

Tectonic Lineaments - Generic Tectonic Lineaments

Shows all the other lineaments.

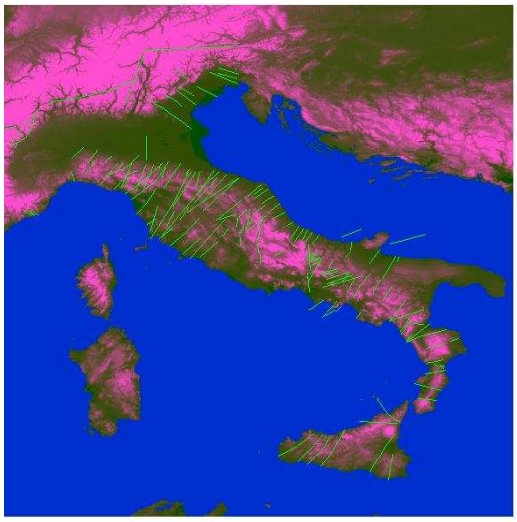

Seismological data: Historical seismicity

Historical Earthquakes

This command allows the user to display one of the catalogues of Italy's historical seismicity available at the end of the year 2000. The three catalogues can be displayed either separately or together, and the earthquakes are shown with squares of different colour according to the catalogue to which they belong (blue for the CFTI, purple for the NT, and red for the CPTI).

Historical Earthquakes > CFTI

Displays the earthquakes contained in the CFTI 3 Catalogue [*Boschi et al.*, 2000].

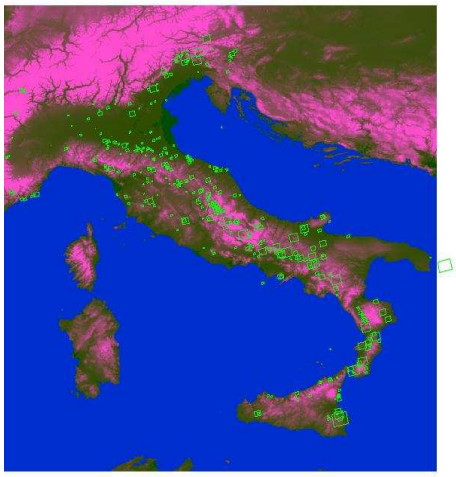

Historical Earthquakes > NT

Displays the earthquakes contained in the NT 4.1.1 Catalogue [*Camassi and Stucchi*, 1997].

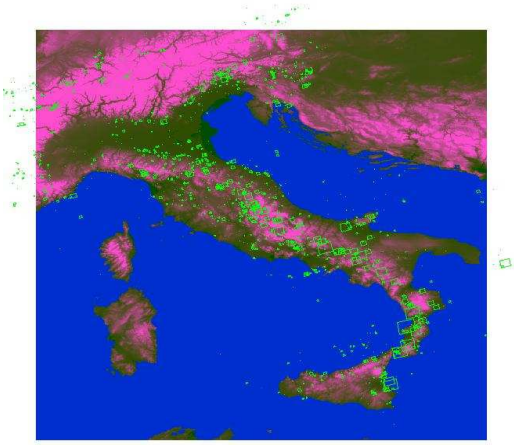

Historical Earthquakes > CPTI

Displays the earthquakes contained in the *Catalogo Parametrico dei Terremoti Italiani* [*CPTI Working Group*, 1

Historical seismicity is taken from the three largest compilations that were available at the end of 2000:

- NT 4.1.1 [*Camassi and Stucchi*, 1997], a parametric catalogue containing 2,488 earthquakes that is largely based on the DOM 4.1 database of macroseismic observations [*Monachesi and Stucchi*, 1997];
- Catalogue of Strong Italian Earthquakes, 461 b.C to 1997, or CFTI 3 [*Boschi et al.*, 2000], the third version of a "new generation" catalogue containing parameters and basic data for 605 large Italian earthquakes;
- Catalogo Parametrico dei Terremoti Italiani [*CPTI Working Group*, 1999], a purely parametric catalogue derived from the two previous catalogues and containing 2,480 earthquakes.

The three catalogues can be displayed separately or simultaneously. Each earthquake is plotted as a coloured empty square. The size of the square (in km) corresponds to the expected source length obtained from magnitude (Ms for NT 4.1.1, Me for CFTI 3, Ma for CPTI) using *Wells and Coppersmith's* [1994] empirical relations.

The special function "Felt Reports" allows the basic intensity data contained in the NT 4.1.1/DOM 4.1. and CFTI 3 catalogues to be displayed as dynamic layers of the cartographic interface.

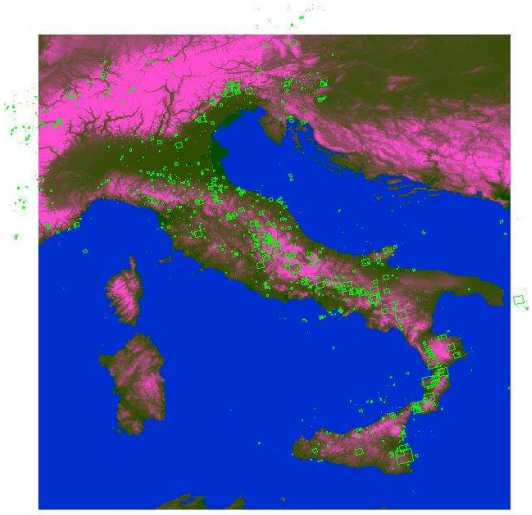

Previous Fault Compilations

The *Previous Fault Compilations* are figures from articles or from the web or printed maps containing active faults, seismogenic faults and lineaments. The figures are representative of a wide selection of investigators and areas and the only requisite for their inclusion in the *Database* was the correctness of the figure's (map's) geographic layout.

Additional Geophysical/Seismological Data

The *Database* may be complemented by other geophysical and seismological data that are pertinent to the general problem of identifying seismogenic sources, characterising their behaviour, or simply placing them in their tectonic context for further elaboration or representation purposes.

Thermal_Springs.tab

Distribution and characteristics of thermally anomalous springs.

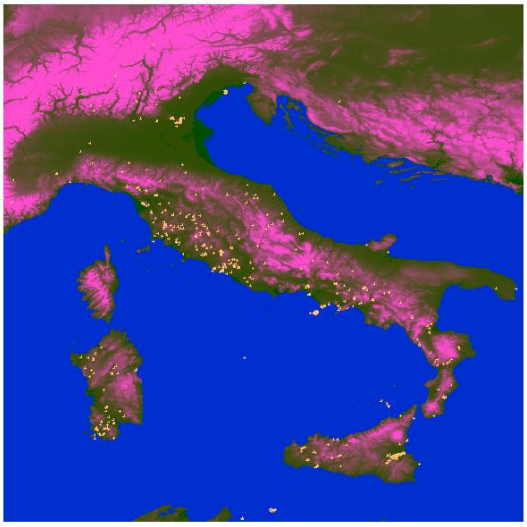

External_Thrusts.tab

External limit of outermost thrusts of Southern Alps, Apennines, Calabrian Arc and Iblean Plateau.

SourceGeol_noHistActivity.tab

Geologic/Geophysical Sources without documented historical activity.

Shmin_breakouts.tab

Orientation of minimum horizontal stress axis from borehole breakout data.

Shmin_breakouts_quakes.tab

Orientation of minimum horizontal stress axis from both borehole breakout and earthquake data.

Shmin_earthquakes.tab

Orientation of minimum horizontal stress axis from earthquake data.

Regional_Divide.tab

Regional drainage divide.

Beach_Balls.tab

Schmidt stereonet representation of focal mechanisms of all Geologic/Geophysical Sources.

ZS4_Scandone.tab

ZS4, seismogenic zonation scheme by Gruppo Nazionale Difesa dai Terremoti (GNDT).

RSN.tab

RSN, Italian seismometric network managed by INGV .

Geographic/Drainage

Three different options for the drainage network coverage can be displayed using this command. All drainage is represented by thin blue lines (rivers) or solid blue regions (lakes).

Geographic/Drainage - Main rivers only

Follow this path to display the main Italian rivers and the main Italian lakes.

Geographic/Drainage - Main and intermediate rivers

Follow this path to display the main and intermediate Italian rivers and the main Italian lakes.

Geographic/Drainage - Full drainage

Follow this path to display the full hydrographic network and the main Italian lakes.

Administrative data

Most of these data are provided by I.S.T.A.T. (Italian national agency in charge of countrywide statistics on economic and demographic data) and reflect the results of

the 1991 national census. The layers *Large Cities* and *Intermediate Cities* include "capoluoghi di regione" and "capoluoghi di provincia", respectively. The *SmallTowns* layer includes 8,100 "comuni", the smallest territorial unit in the Italian public administration. The *All Localities* layer is supplied courtesy of E.N.E.L./Hydro (former I.S.M.E.S.) and includes 61,595 "frazioni", small settlements that are under the jurisdiction of a "comune".

Cities

This command allows the user to display Italian cities selected from four classes based on their administrative relevance.

Cities - Large Cities

Displays only large cities (capital cities of the administrative *Regions*). The symbol used is a solid violet circle.

Cities - Intermediate Cities

Displays only intermediate cities (capital cities of the administrative *Provinces*). The symbol used is a solid orange circle.

Cities - Small Towns ("Comuni")

Displays only small towns (capital cities of the Italian municipalities or *"Comuni"*). The symbol used is a solid yellow circle.

Cities - All Localities ("Frazioni")

Displays even the smallest localities ("*Frazioni*"). The symbol used is a solid light blue circle.

Administrative boundaries

This command prompts the application to display one out of three classes of

administrative boundaries. All administrative boundaries are shown as thin black lines.

Administrative - Regions

Show the boundaries of the 20 main administrative *Regions* into which the Italian territory is currently subdivided.

Administrative - Provinces

Shows the boundaries of the 103 administrative *Provinces* into which the 20 *Regions* are currently subdivided.

Administrative - "Comuni"

Shows the boundaries of the 8,100 Italian *Comuni* (municipalities).

Geographic grid

This command allows the user to display a regular geographic grid. The grid spacing varies in the range 0.1° to 2.0° and is automatically selected by the application as a function of the current zoom range.

Networks

Network-Seismic stations

View all the seismic stations that exists in Italian area.

Bathymetry

View all the depths in Mediterranean sea area.

3.5. RESULTS OF INVESTIGATION

3.5.1.Introduction

Below we will see the results that achieved by using, as temperature estimator simply brightness temperatures measured (around 11mm) with TIR AVHRR channel 4. This preliminary study permitted to have a first estimate of the S/N ratio associated to possible thermal anomalies. The study demonstrated that, even though with a S/N as low as 0.6, the areas with higher TIR excesses appeared in some spatial relation with the seismogenic areas distribution and their activation in the considered cases-study . Also we will see the results achieved by using, as temperature estimator, the Land Surface Temperature (LST) computed, according to Becker & Li [1], on the base of AVHRR TIR channels 4 and 5. By comparison with previous results (achieved by using the same data processing scheme on the same satellite data set) the main difference is an evident improvement (from 0.6 up to 1.0) in the S/N ratio associated to thermal anomalies. That mainly depends on the reduction (operated by the LST estimator by means of the split-window term T_4 - T_5) of the natural noise related to variable atmospheric water vapour content which, instead, affects BT in the AVHRR channel 4.

3.5.2. Imagery :

1) Imagery selection: only AVHRR imagery from 1978 up to 1998 collected in the same month of the year (November) around the same (local) time of day (6:00 PM) was considered as a potential reference data set. Effects related to yearly and daily cycles are therefore reduced. Moreover, late afternoon imagery is less influenced by effects related to soil-air temperature differences, normally higher during other hours of the day, and less sensitive to local solar exposition. This step corresponds to the prescriptions on the *temporal support* (Tramutoli, 1998) *T* which defines satellite passes to be included in the following processing steps, on the basis of their acquisition time *t* E *T* .

2) Imagery pre-processing: for each AVHRR scene radiometric calibration was performed, following Lauritson *et al.* (1979) and brightness temperature *T4* in the TIR AVHRR channel 4 (10.3-11.3 *,urn,* the last influenced by space-time variation in atmospheric water vapour content) saved for the following steps with the exclusion of all cloudy soundings (detected by using standard threshold tests on AVHRR IR channels).

3) Imagery co-location: all images were accurately geo-referenced (using the automated procedure proposed by Pergola and Tramutoli, 2000), co-located and re-mapped in the same geographic projection (Lambert Azimuthal Equal Area with Nearest Neighbour resampling) in order to build the *T4(r,4Jeference* data set. All soundings over sea were excluded at this stage from the following steps.

4)Reducing climatological effects: for each scene the (spatial) average *T4(t')* of *T4(r, t')* and its standard deviation *aT4(t')* were computed and the quantity *LIT4(r,t') = T4(r, t') -T4(t')* saved for the following steps. The use of spatial averages, to take into account the year-to-year variation in the temperature field, will increase in efficiency the larger the area considered with respect to the

expected extension of thermal anomalies and the more representative of different temperature regimes (mainly related to altitude) and soil emissivities (depending on soil cover properties and particularly on vegetation). In this way, the observable to be used will no longer be the *llocal* (using hereafter the double *l* introduced by Tramutoli, 1998, to indicate a punctual value in the space and time domain) value of the absolute brightness temperature *T4(r', t')* measured at the time *t'* and place *r',* but its *llocal* excess with respect to the value *T4(t')* assumed as representative of the normal trend of the temperature field on the area at the observation time *t'* .This, in principle, ~ill permit us to compare values assumed by the observable *LIT4(r, t')* (which completely preserves, as *a LIT4(t')* = *(JT4(t'),* the spatial dynamics *ofT4(r', t')* across the scene) in different years having different climatological temperature trends.

In our case, only land locations within an area *(D)* of about 600 x 600 km around the main epicentral zone of the Irpinia-Basilicata earthquake (23 November 1980, *Ms* = 6.9) were considered to which we will refer, hereafter, simply by the word «scene» *(r* E *D,* are then the prescriptions on the *spatial support,* requested in Tramutoli (1998), which defines the spatial domain and arrangement of sites to be processed).

The following aspects were evaluated by applying the above procedure to the Irpinia-Basilicata earthquake (23 November 1980, *Ms* = 6.9) using only NOAA-AVHRR observations collected in November from 1980 up to 1999.

a) No ancillary data *(e.g.,* ground observations) are required, so that their computation can be completely automated for operational real-time monitoring purposes. For the same reason, they are intrinsically exportable to different satellite packages and different geographic areas.

b) They strongly reduce (as explained previously) the effects of known sources

of natural/ observational noise, but take into account (by means of the denominator term) the effects of the residual noise due to non-predictable signal variability related to *llocal* atmospheric and earth surface conditions *(e.g.,* change in soil and atmospheric moisture).

c) By including the maximum of possible residual noise they are intrinsically resistant to false alarms proliferation (which means, on the other hand, that the signal to be detected must be strong enough to stand out with respect to the remaining natural and observational noise).

3.5.3. Results

Performances of the proposed approach were tested with reference to the strong earthquake *(M_S* = 6.9) which occurred in Southern Italy (Irpinia-Basilicata) on November 23, 1980 at 7.32 PM local time.

All NOAA/AVHRR satellite passes, collected in November, from 1994 to 1998, around 6.00 PM GMT (RAT prescriptions on the *temporal support T*), over the Southern Italian peninsula (RAT prescriptions on the *spatial support D),* were processed to build reference fields, (following steps from 1 to 5 described in Section 3). The mean < $\Delta T_4(r)$ > and standard deviation $\sigma_{\Delta T4}(r)$ fields were computed for each lo- cation *r,* and time-series $\Delta T_4(r, t)$, (with $t \in T$ and $r \in D$) deriving, for every year considered, the ALICE indexes, defined in (3.1) and (3.2).

In order to investigate a possible residual dependence on surface elevation and emissivity, indices (3.1) and (3.2) were co-located with the USGS GTOPO30 Digital Elevation Model (DEM) produced by the EROS Data Centre (with a ground resolution cell of about 1 km) and with a vegetation map

(Normalized Difference Vegetation Index, NDVI) computed by means of the visible and near-infrared AVHRR channels 1 and 2. Results of the correlation analyses performed on the investigated area, shown in figs. 2 and 3 for November 1980, reveal a null dependence of the ALICE index $\otimes^{t}$ *'(r, t')* on both the elevation and the vegetation cover. The correlation coefficients, in both cases near to zero, assure, for such an index, a good protection by these natural noise sources. Residual observational noise, for example, from considering TIR radiances acquired from the same ground location under very different view- angles, as well as from errors in image-to-image co-location, are intrinsically taken into account in the standard deviation $\sigma_{\Delta T4}$. In this way, every residual «noisy» contribution to the TIR signal will contribute to increase the *llocal* value of *a* $\sigma_{\Delta T4}$ reducing the corresponding ALICE values and probability of false anomalies.

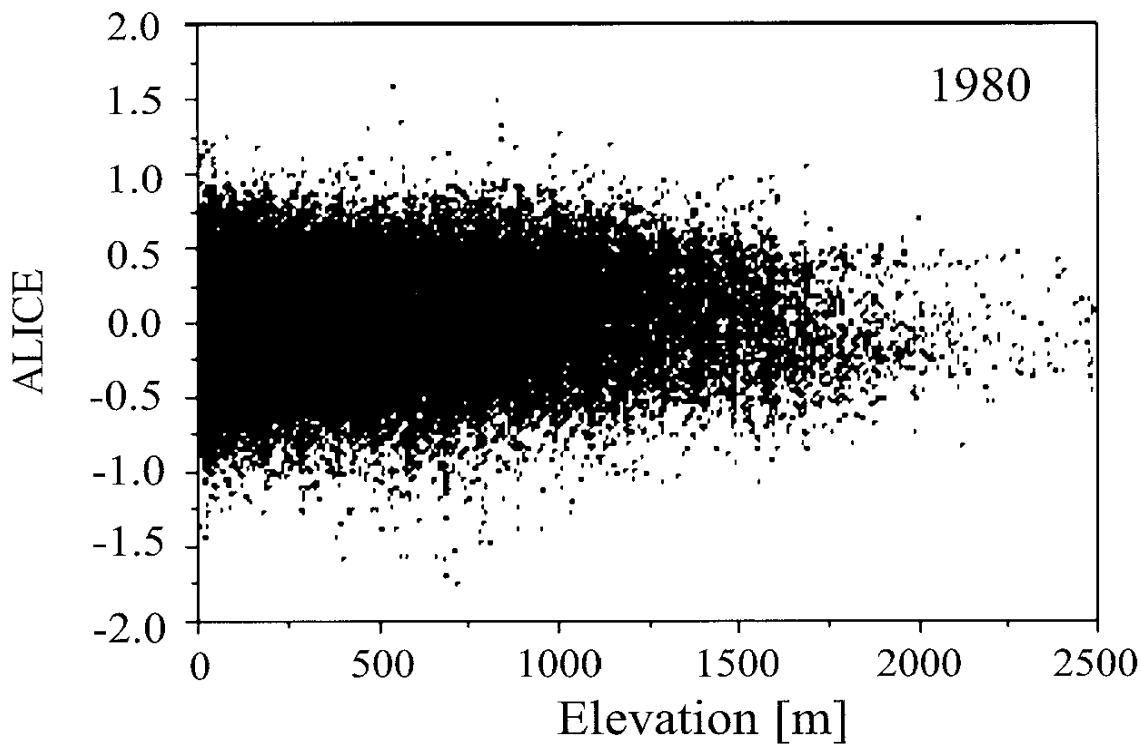

Fig.2.Correlation analysis between the average ALICE index $\otimes^{t}$ (r , t) and the elevation for the study area in November 1980.

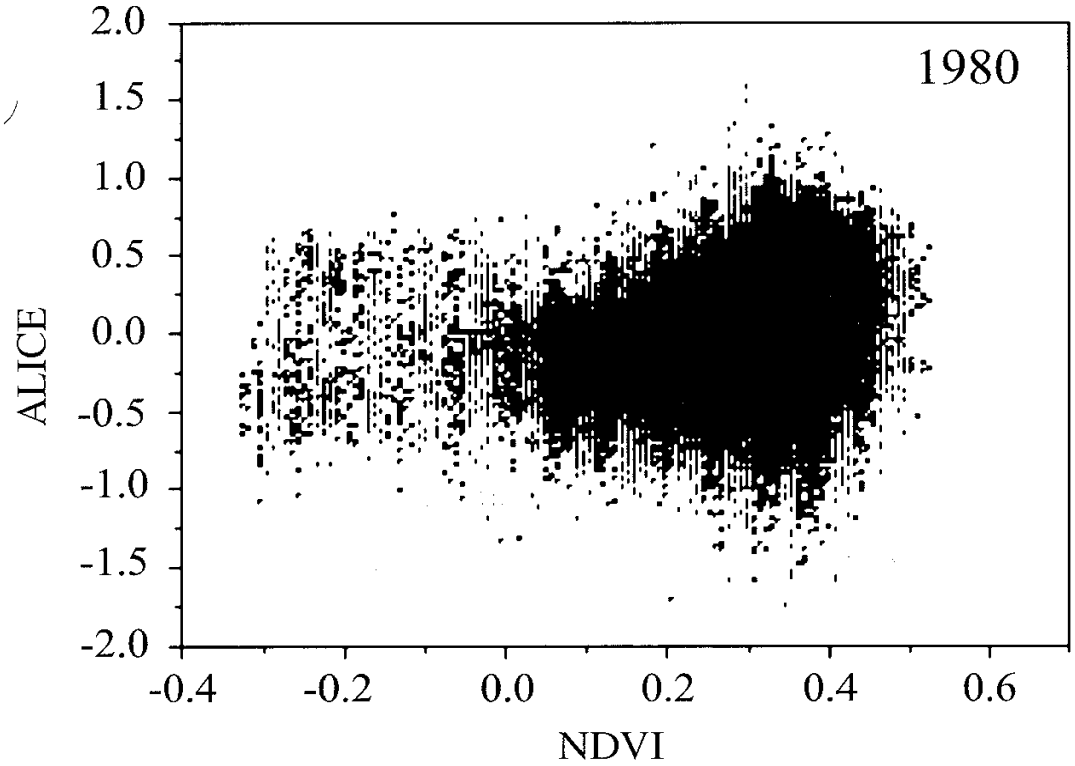

Fig3.Correlation analysis between the average ALICE index $\otimes^{t}$ (r , t) and the vegetation index (NDVI) for the study area in November 1980.

By limiting our analysis only to the epicentral zone, the achieved results can be summarised as follows:

a) Figure 4 shows for the area around the epicentre (plotted together with\its aftershocks) the average values of $\otimes^{S}(r, t)$ computed for November 1980. Only pixels with $\otimes^{S}$ greater than 1.5 are depicted together with aftershock epicentres and source spring sites. From the picture it is easy to note how the epicentral zone and aftershocks alignments are well marked by higher values of $\otimes^{S}$.
High values of $\otimes^{S}$ can also be observed in several zones away from the epicentral zone. By comparison with figs. 1a and 1b it is easy to see how they are well related to seismically active areas and/or source spring sites.

b) The average values of $\otimes^{t}(r, t)$ were computed for November 1980. They are generally lower and well within the present natural/observational noise level. In fig. 5 only pixels with $\otimes^{t}$, values higher than 0.6 are depicted together with aftershock epicentres and source spring sites. They still result in good correlation with the epicentral zone and aftershock alignments and, as in the previous case, when observed away from the epicentral zone, they are well related to seismically active areas and/or source spring sites (see figs. 1a and 1b by comparison).

Fig4.Irpinia-Basilicata earthquake(Ms=6.9,November 23,1980,7:32PM) : spatial distribution of the average ALICE index $\otimes^{s}(r, t')$ over the area around the epicentre (circled) for November 1980.Yellow crosses indicate aftershocks position; green symbols localise spring sources. Pixels with $\otimes^{s}>1.5$ are depicted in red. In the background the reference field $<\Delta T_4(r')>$ is depicted in grey tones (from dark to bright).

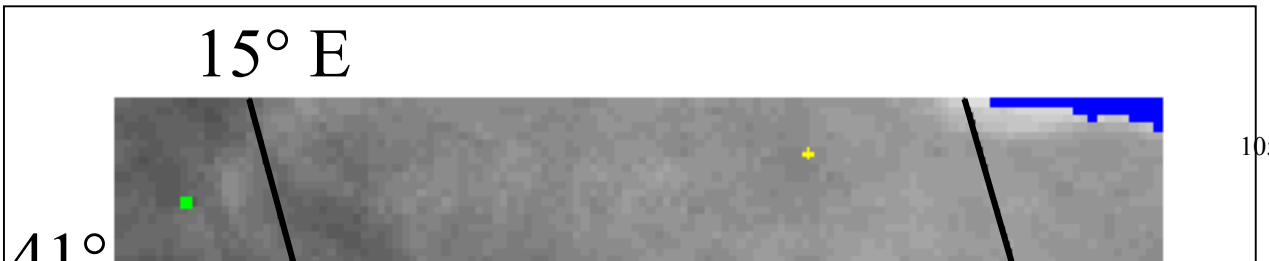

Fig.5. As fig.4. spatial distribution of pixels with monthly average for the ALICE index $\otimes^{t}$ (r ,t).Pixels with $\otimes^{t}$ >0.6 are depicted in red. *By comparison epicentres of the main shock and aftershocks are plotted together with (in green) the location of the main thermal spring sources in the area.*

c) Figure 6 shows the temporal evolution of the area (measured in AVHRR pixels) with $\otimes^t$ values greater than 0.6 in a circle of 100 km of radius around the epicentre, a few days before and after the earthquake. Even though temporal gaps are present (only AVHRR imagery free of clouds on the area have been used), it is nevertheless possible to appreciate the doubling of the extension of the over-threshold area from November 16 and 20 with a further outstanding increase during the following three days preceding the earthquake.

By extending our analysis all over the investigated area (depicted in fig. 1a,b), we achieved the following results:

d) Figure 7 represents an extended view of fig. 5, showing the average values of $\otimes^t (r, t)$ computed for November 1980 (only pixels with values higher than 0.6 are depicted). It is possible to note how over-threshold pixels can also be observed far away (up to several hundred kilometres) from the epicentral zone. Figures 8 and 9 refer, respectively, to the relatively *un- perturbed* cases of November 1994 and November 1998 for which only a few events with *Ms* > 3 (no one with *Ms* > 4) can be found in published catalogues; By comparison, it is easy to recognise how the extension of over-thresh- old areas is incomparably higher during November 1980.

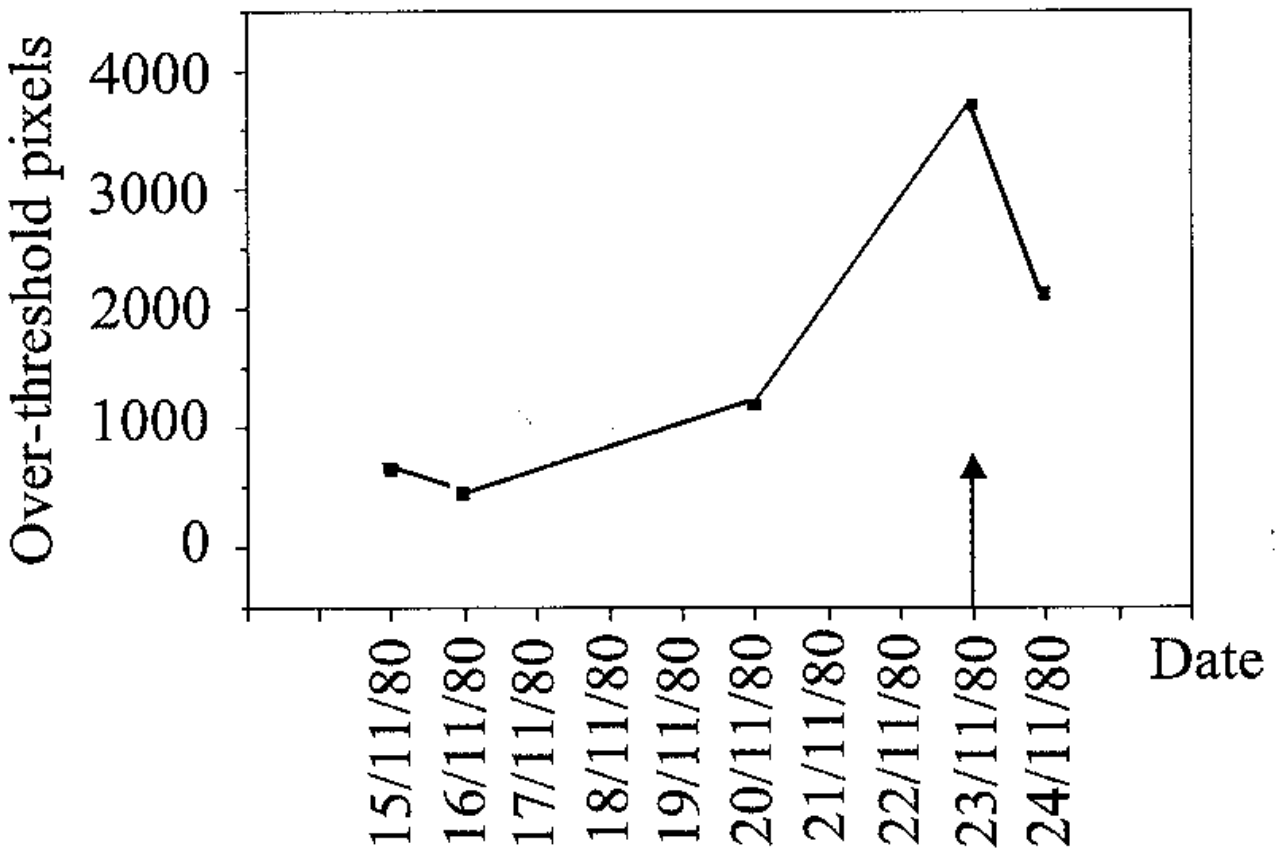

Fig.6.Irpinia-Basilicata earthquake(M_S = 6.9,November 23,1980, 7:32 PM) : temporal evolution of the extension of the over-threshold area around the epicentre. The number of pixels with $\otimes^t$ >0.6, in a circle of 100km of radius around the epicentre, is plotted a few days before and after the earthquake occurrence (black arrow)

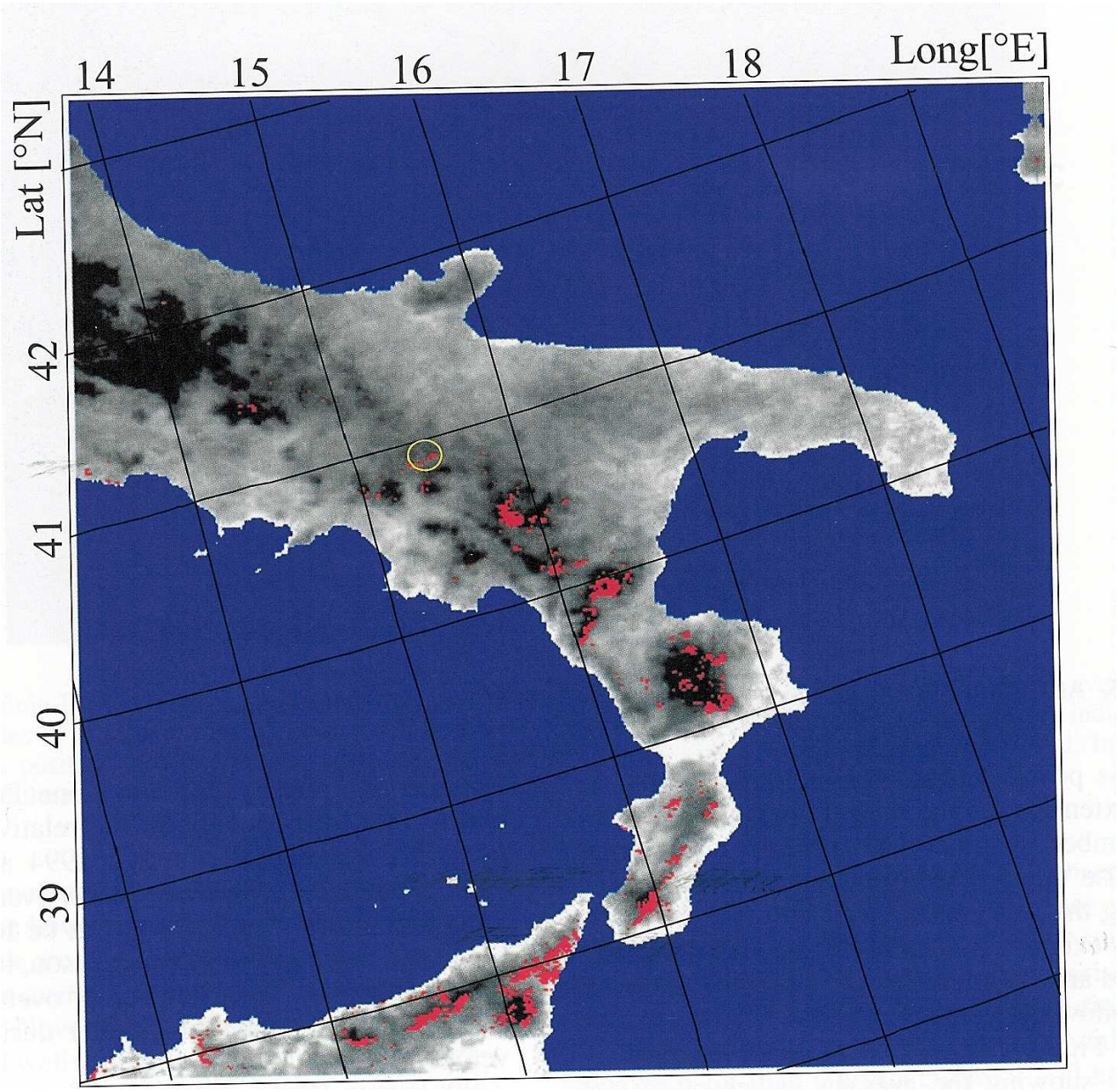

Fig.7.Irpinia-Basilicata earthquake(M_S = 6.9,November 23,1980, 7:32 PM) :spatial distribution of the average ALICE index $\otimes^t$ (r ,t) over the whole study area for November 1980.Pixels with $\otimes^t$ >0.6 are depicted in red .the yellow circle represents the epicentral zone. In the background the reference field < ΔT_4 (r′) > is depicted in grey tones (from dark to bright)

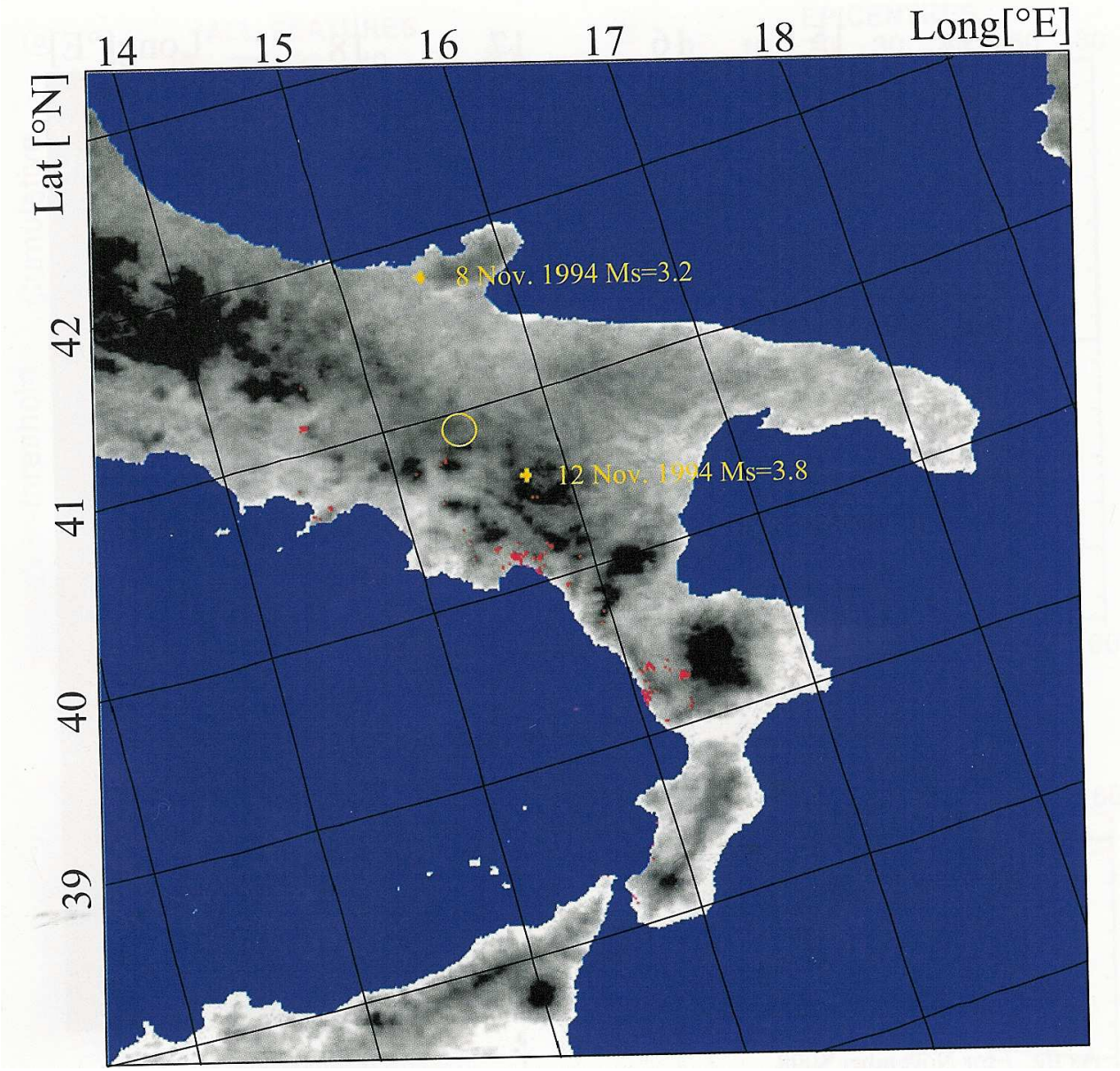

Fig 8.As fig.7 for November 1994.The yellow crosses indicate the location of the two events with $M_S > 3$ in the area during November 1994.

e) Figure 10 shows the temporal evolution of the percentage, with respect to their number all over the investigated area, of the over-thresh- old pixels within a circle of 100 km of radius around the epicentre a few days before and after the 23 November 1980 Irpinia-Basilicata earthquake. It is remarkable that the number of over- threshold pixels in the epicentral area, representing no more than 1O% of the total on November 16, passes suddenly to a value higher than 40% on November 20, maintaining such high values also on the following days. This suggests that the process of extension of the over-threshold area was particularly intense in the epicentral zone a few days before the earthquake.

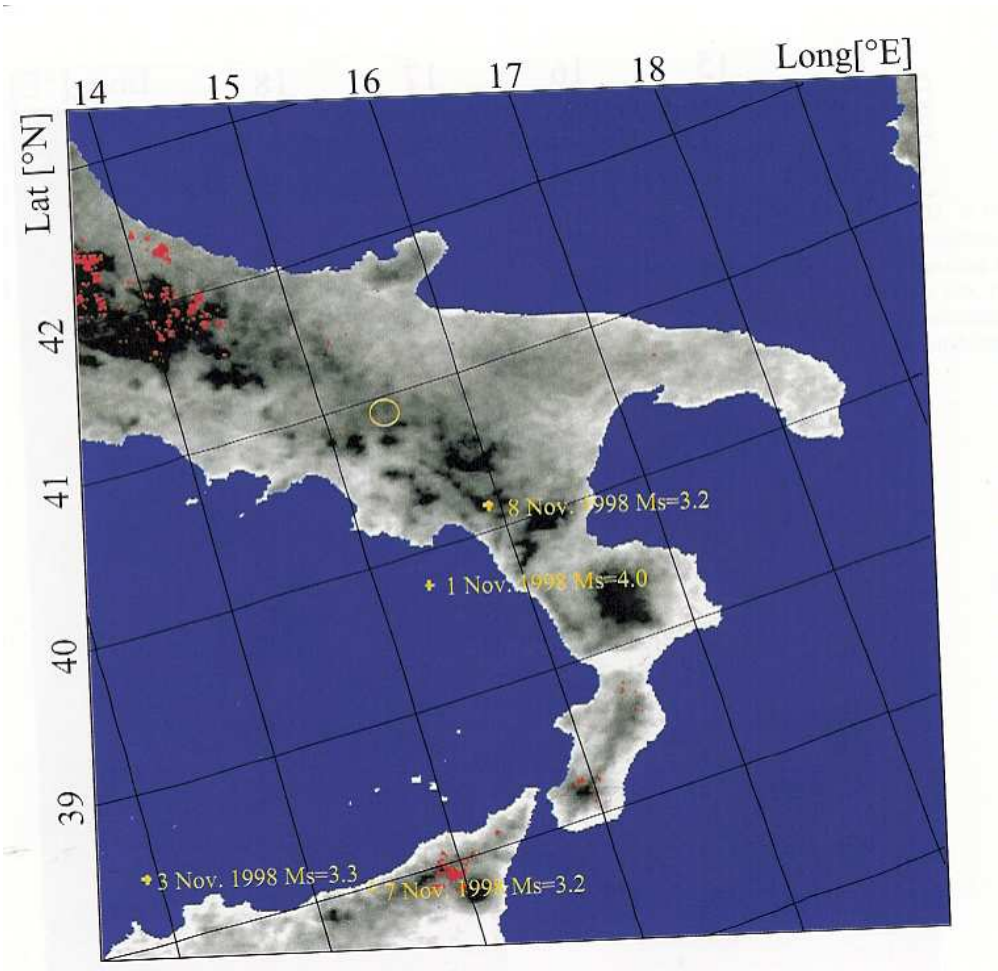

Fig 9. As fig.7 for November 1998

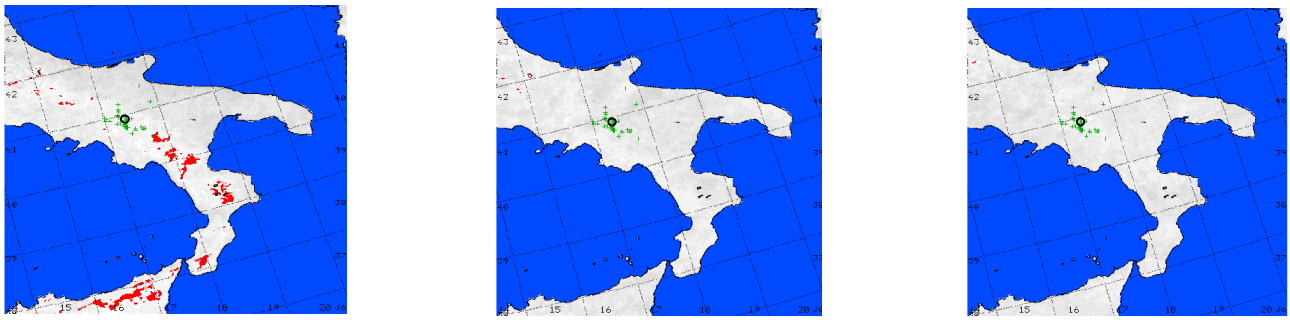

Top: spatial distribution of the monthly averaged ALICE indices over the whole study area for November 1980, 1994, 1998.

Bottom : a zoom of the images shown above over the epicentral area of Irpinia earthquake. Note as no anomalies were detected during unperturbed (no events with M_s>4) years and, by comparison, how big is , during November 1980, the extension of over-threshold pixels even faraway the epicentral area.

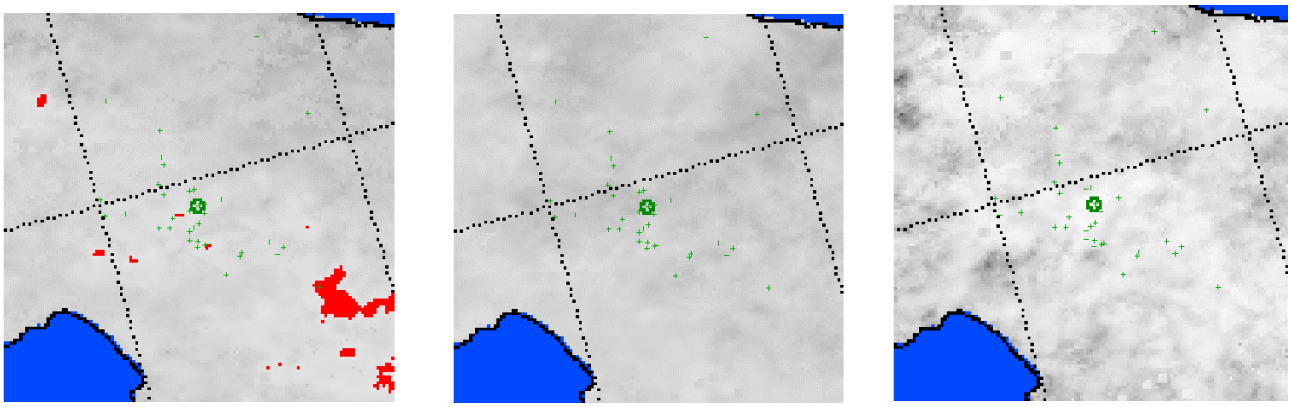

Pixels with ALICE index > 1

Aftershocks position of Irpinia earthquake

Main shock of Irpinia earthquake

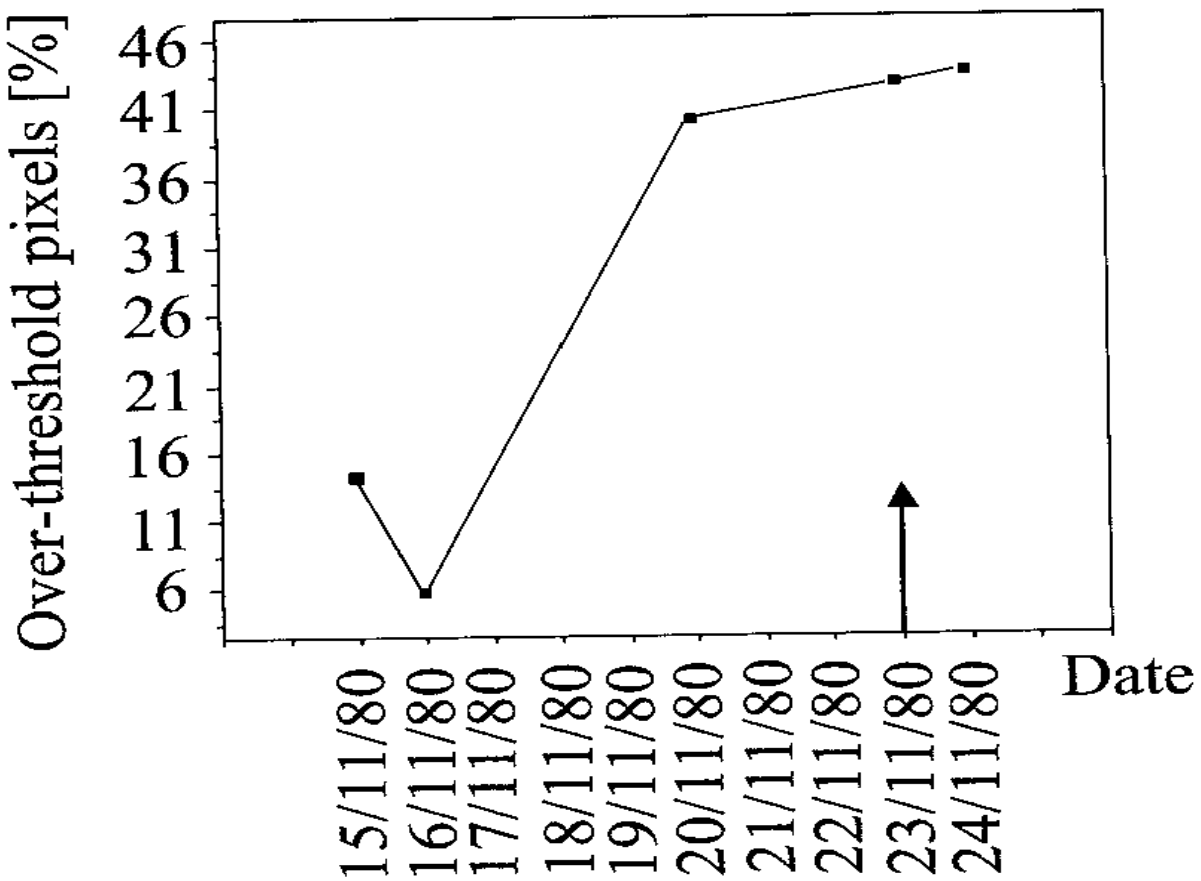

Fig.10. Irpinia-Basilicata earthquake(M_S = 6.9,November 23,1980, 7:32 PM) : comparative analysis of the temporal evolution of the extension of the over-threshold areas within and far away from the epicentral zone. The percentage of pixels (over the total with $\otimes^t$ > 0.6) falling in a circle of 100km of radius around the epicentre , is plotted a few days before and after the earthquake occurrence (black arrow)

f) In order to understand whether or not the spatial distribution of the over-threshold pixels reported in fig. 8 can be put in some relation with seismogenic areas, the following analysis was performed:

-Seismogenic faults (694 pixels on the scene) and source spring sites (167 in the scene) reported in fig. 1 a as well as epicentres of earthquakes of magnitude $M_S > 3$ from 1963 to date (1834 on the scene) reported in fig. 1b, were all considered possible indicators of seismically active zones and a possible location of greenhouse gas discharge.

-For each over-threshold pixel in fig. 7, the distance from the closest of these indicators (and separately for each typology) was computed. The same analysis was performed using a synthetic random distribution of over-threshold pixels having the same spatial density across the scene.

-The histograms and cumulative distributions of the number of over-threshold pixels (resulting from both the actual and random distribution) versus distance were computed and plotted together in fig. 11a-d.
From fig. 11a it is possible to note that more than 95% of the over-threshold pixels are less than 10 km from whatever indicator and quite all of them at less than 15 km. The spatial distribution of over-threshold pixels appears (fig. 11 b) particularly related to epicentres (with a modal value around 7 km and a 90% of probability to find over-threshold pixels at less than 12 km from an epicentre) and less related (fig. 11c) to seismogenic faults distribution.

Thermically anomalous (T > 17 °C) source springs (Albarello and Martinelli, 1997) appear (fig. 11d) systematically shifted with respect to over-threshold pixels whose spatial distribution has a modal value around 20 km with more than a 90% probability of finding them between 20 and 40 km away from the closest spring source. Comparing actual and simulated distributions, it is possible to note how the observed spatial correlation with over- threshold pixels is not fortuitous in the case of epicentres (that give the main contribution to the overall correlation) and, as far as distances shorter than 20 km are concerned, in the case of seismogenic faults. On the other hand, fig. 11d clearly indicates the absence of correlation between over-threshold pixels and source spring sites distribution.

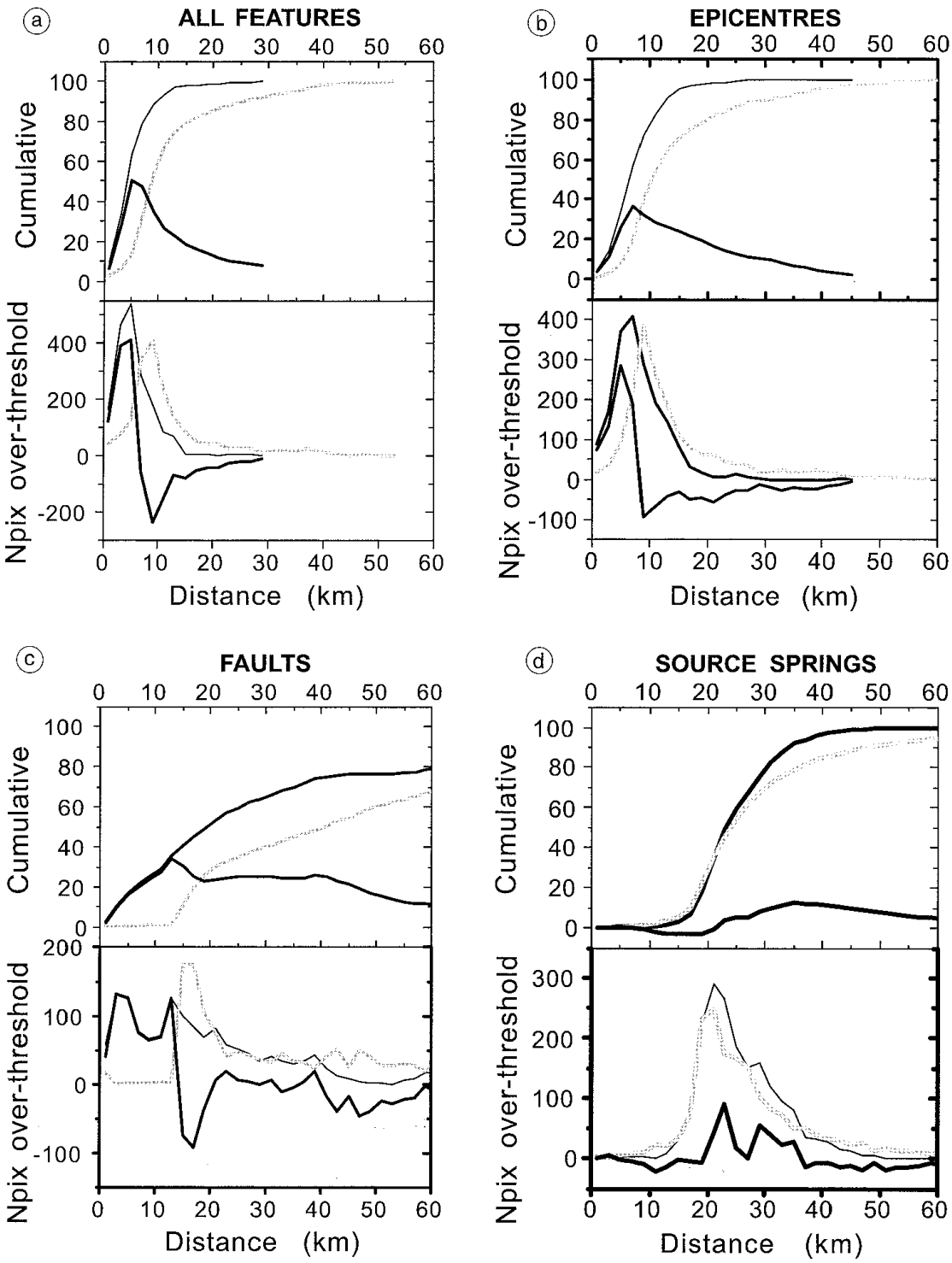

Fig.11a-d.November 1980 : comparative correlation analysis between the actual spatial distribution of over-threshold pixels and a synthetic set (with the same average density) of randomly distributed points , together with the seismogenic indicators over the whole study area : a)all features ; b) epicentres ; c) faults; d) source springs. Top :cumulative distribution ; bottom :histogram. For all cases the actual data (thin black) ,the synthetic set (thick ,light grey) and their difference (thick black) are shown .

3.5.4. Discussion

The main target of this work was to devise a new approach to satellite TIR survey for seismogenic regions monitoring. The RAT approach (Tramutoli, 1998) has been applied in a simplified form mainly aiming at a preliminary estimate of the TIR signal-to-noise ratio in the worst informative context. In particular, only the most simple natural and observational noise sources have been removed both in the temporal and spatial domain, avoiding, at this preliminary stage, the use of any specific model to achieve a further noise level reduction. Results achieved in the case-study of the Irpinia-Basilicata earthquake of November 23, 1980 (M_S = 6.9) show how the observed TIR excesses (defined by $\otimes^t(r, t)$ in the temporal domain) still remain , within the noise level so that a refined noise-removal approach should be applied to reduce the residual natural and observational noise to a statistically acceptable level. Major improvements in this direction can be expected by the use of more refined cloud/ snow detection techniques (e.g., following Derrien et al., 1993) and by the introduction of standard corrections taking into account the llocal variability of atmospheric water vapour content and satellite view angle. At this preliminary stage, we understood that, at least in the time domain (and especially when averaged on a monthly basis as in our case), we are dealing with a very weak llocal signal.

Signal-to-noise ratios higher than 1.5 (open to further improvements as in the previous case) have been achieved for $\otimes^s(r, t)$ after the analysis performed in the spatial domain.

Even with the above-mentioned limitations, the temporal evolution of the areas with higher TIR excesses appears in some relation with the seismogenic areas

distribution and their activation in the case study considered. Also by comparison with the results of the analyses per- formed on relatively unperturbed years, which do not show similar effects, it appears that the observed TIR excesses extend their presence far away (several hundred of kilometres) from the epicentral zone and with a non casual spatial correlation with seismoactive regions marked by the epicentres of recent earthquakes of magnitude $M_S > 3$.

A number of indications emerge from this preliminary study:

a) It seems to confirm, even in a more complex context and using a completely different methodology, the indications from the work of Tronin (1996) who found a correlation between seismic areas activation and the widening of TIR anomalies.

b) It suggests, in the case study of the Irpinia-Basilicata earthquake, the possible presence of large scale (up to several hundred kilometres) effects up to now not otherwise documented even if perfectly compatible with theoretical considerations (e.g., Dobrovolsky et at., 1979; Fleisher, 1981) and observational evidence related to events of similar magnitude in other geographic areas (Qiang Zu-ji et at., 1992b).

c) The observed spatial distribution of over- threshold pixels with respect to thermally anomalous spring sources raises several problems (mainly on the spatial distribution and change with the time of gas emissions) to be better investigated, also in the light of recent studies performed in the same area by Martinelli et at. (1999) -indicating a systematic shift between thermal springs and seismogenic faults distribution -and Italiano et at. (2000) who found a substantial stability with the time (no quick discharge) of gas emission due to the most important spring sources considered in this paper. The poor correlation found in this case, in comparison with the high correlation achieved using epicentres or, to a lesser

extent, seismogenic faults, might indicate (if the claimed origin of TIR anomalies from a localised greenhouse effect is confirmed by further specific studies) a major role to be attributed to occasional rather than permanent gas discharges in the context of seismogenic areas monitoring activities.

3.5.5. SOME EXAMLE OF LATE INTEGRATION

Long term satellite records are used as instrumental test beds in order to evaluate the possible correlation,in the space-time domain,between TIR anomalies and pre/co-seismic phenomena by using different methologies in different geographic scenarios(Italy,Greece,Turkey,Africa,USA).Independent measurements based on GPS(TEC and deformation transients) ,seismometric(seismic and micro-seismic analyses) ,multi-parametric (geothermal , geochemical , geoelectrical) networks, as well as systematic campaigns of magnetotelluric and electromagnetic tomographic survey are analysed in order to verify explanatory physical models which can justify satellite observations.All significant changes in the measured parameters(and particularly,deformation fields,TEC and geoelectrical signals)are compared with both satellite TIR anomaly fields and earthquake occurences, in order to confirm or reject, the proposed models for thermal anomaly occurence explanation.Advanced statistical techniques are implented to extract quantitative dynamics from geophysical observations. On this base of development of suitable physical models describing deep fluids motion and convective heat transport during the preparatory phase of earthquakes must be attemped .

RAT approach could permit to overcome one of the most relevant obstacles to satellite prediction of earthquakes.In fact whatever is the used precursory phenomenon under observation the main problem in this kind of application

remains the high number of environmental factors(independent from any seismic activity) which could affect the possible precursor signal up to comletely mask it.This is the case of observations made in thermal IR AVHRR channels which values, in order to be interpreted, should be preliminarily corrected, at least for the effects of atmospheric absorption(mainly due to the water vapor)superficial emissivity(higly variable over land)and observational conditions(mainly satellite zenithal angle).The use of a RAT approach,as we have seen,could permits to strongly reduce all these effects.Obviously in this case the constuction of an appropriate ALICE should be done taking into account not only the specific time-dynamics of the signal to be used as a precursor but also the space/time dynamics of all the other variables which affect its measure.

Satellite TIR anomaly fields more often are combined with the surface temperature, in order to make our investigations. Lately is tried to achieve detailed and precise conclusions for our work also by the combination of Tir anomaly fields with also other sectors. So we have to consider also apart the surface temperature :

a) the presence of lakes and hydrographic network in the area of interested

b) the presence of springs

c) epicentrals from previous earthquakes in the area of interested

d) the altitude of the area of interested

e) fault scarps that are observed

f) tectonic lineaments

g) external thrusts

3.5.6. PLANNING SUITABLE OBSERVATIONAL STRATEGIES AND NETWORKS

SUMMARY (AND FUTURE PLANS)

Recent results we achieved by applying robust satellite techniques (RAT) to the problem of seismogenic areas monitoring by satellite TIR surveys surely encourage the research in this direction besides indicating that specific observational strategy must be implemented in order to increase the signal-to-noise ratio up to an acceptable level. Improvements of the signal-to-noise (S/N) ratio obtained by progressively introducing correction for atmospheric water vapour and surface emissivity, as well as moving from polar (NOAA) to geostationary satellites (METEOSAT), even though still preliminary (requiring further confirmations by an extended test bed) seems to put on a more firm ground the research in this field. The problem of furtherly reduce the natural/observational noise increasing both RAT sensitivity and robustness against false alarms will greatly benefit of next generation of satellite sounders. Among the others incoming geostationary satellites, which promise (as in the case of MSG/SEVIRI for instance) improved spatial, spectral and temporal resolutions, will be of particular importance in order to further improve TIR S/N ratio achievable by our methodological approach. By the other side, in order to verify suggested explanatory models (like local green-house effects related to abrupt changes in CO_2 and CH_4 gas discharge regimes) for the observed TIR anomalies of great importance will be scientific mission (like ENVISAT to quote only the most recent) highly increasing our present investigation capabilities of atmospheric chemistry.

Variety of plans which exist and which are being developed :

Improving seismically active areas monitoring moving from polar to geostationary satellite TIR packages.

Space-time TIR anomalies, observed from months to weeks before the occurrence of earthquakes, have been suggested, by several authors, as pre-seismic signals.

A robust satellite data analysis approach has been proposed which permits a statistically based definition of TIR anomaly even in the presence of highly variable contributions from atmospheric (e.g. transmittance), surface (e.g. emissivity and morphology) and observational (time/season, but also solar and satellite zenithal angles) conditions. In this paper the actual potential of satellite TIR surveys is evaluated on the basis of several years of NOAA/AVHRR and METEOSAT observations over Europe. TIR anomalies, as an example, possibly associated to the Athens earthquake which occurred on September 7th 1999, have been particularly considered in order to evaluate the capability of the proposed approach to filter-out noisy contributions to the measured TIR signal due to variable, observational and meteorological, conditions. The study demonstrated the capability of the proposed method to isolate (if any) possible pre-seismic anomalous TIR patterns from the most important noisy contributions to the measured signal. The advantages offered by the use of geo-stationary (quite doubling the achievable signal-to-noise ratio) instead than polar satellite TIR packages are particularly discussed together with the further improvements expected by the use of geostationary satellite packages (like MSG-SEVIRI) with enhanced multi-spectral capabilities.

The research project "Earthquakes prediction in active tectonic areas by

space techniques" (1995/97)

CO.RI.S.T.A. has conceived a research programme, commissioned by the European Community, whose primary objective is to evaluate the feasibility of an integrated system of seismicity and ground deformations monitoring, which employs space techniques along with traditional methods. The second, but not less important objective is to develop an accurate seismic-tectonics model of a test area, properly selected among the most active in Southern Italy, which allows to interpret precursory phenomena of an earthquake recorded by the integrated monitoring system.

Method for the Reduction of Signal-Induced Noise in Photomultiplier Tubes

Cynthia K. Williamson, Russell J. De Young

A new method to reduce photomultiplier tube detector signal-induced noise (SIN) in a lidar system is successfully demonstrated. A metal ring electrode placed external to the photomultiplier tube photocathode is pulsed during the intense near-field lidar return with a potential between 15 and 500 V, resulting in a significant reduction in SIN. The effect of the metal ring voltage on the decay time constant and the magnitude of a simulated lidar signal is presented. Optimal experimental conditions for the use of this device in lidar receivers, such that the lidar decay time constant is not affected, are determined. Mechanisms for this SIN suppression system are discussed in detail, and data were recorded to show that the voltage on the metal ring functions by altering the photomultiplier electron optics.

Estimation of the Remote-Sensing Reflectance from Above-Surface Measurements

The remote-sensing reflectance R rs is not directly measurable, and various methodologies have been employed in its estimation. I review the radiative transfer foundations of several commonly used methods for estimating R rs , and errors associated with estimating R rs by removal of surface-reflected sky radiance are

evaluated using the Hydrolight radiative transfer numerical model. The dependence of the sea surface reflectance factor , which is not an inherent optical property of the surface, on sky conditions, wind speed, solar zenith angle, and viewing geometry is examined. If is not estimated accurately, significant errors can occur in the estimated R rs for near-zenith Sun positions and for high wind speeds, both of which can give considerable Sun glitter effects. The numerical simulations suggest that a viewing direction of 40 deg from the nadir and 135 deg from the Sun is a reasonable compromise among conflicting requirements. For this viewing direction, a value of 0.028 is acceptable only for wind speeds less than 5 m s 1 . For higher wind speeds, curves are presented for the determination of as a function of solar zenith angle and wind speed. If the sky is overcast, a value of 0.028 is used at all wind speeds.

Angular Variation of Thermal Infrared Emissivity for Some Natural Surfaces from Experimental Measurements

Multiangle algorithms for estimating sea and land surface temperature with Along-Track Scanning Radiometer data require a precise knowledge of the angular variation of surface emissivity in the thermal infrared. Currently, few measurements of this variation exist. Here an experimental investigation of the angular variation of the infrared emissivity in the thermal infrared (8 14- m) band of some representative samples was made at angles of 0 65 (at 5 increments) to the surface normal. The results show a decrease of the emissivity with increasing viewing angle, with water showing the highest angular dependence (7% from 0 to 65 views). Clay, sand, slime, and gravel show variations of approximately 1 3% for the same range of views, whereas a homogeneous grass cover does not show angular dependence. Finally, we include an evaluation of the impact that these data can produce on the algorithms for determining land and sea surface temperature from double-angle views.

INDEX , EXPLANATIONS :

Brightness Temperature

Definition: The apparent temperature of a non-blackbody determined by measurement with an optical pyrometer or radiometer

Emissivity

Definition: The ratio of the radiation emitted by a surface to the radiation emitted by a perfect blackbody radiator at the same temperature.

Thermal Infrared (TIR)

Definition: Infrared radiation extending approximately from 3.0 to 15.0 micrometers and being part of the emissive infrared.

Infrared Band

Definition: The band of electromagnetic wavelengths lying between the extreme of the visible (approximately 0.70 micrometer) and the shortest microwaves (approximately 100 micrometers).

Aerial Photography

Definition: Photography from airborne platforms.

Altimetry

Definition: The science and techniques involved in making relative or absolute height measurements.

Cartography

Definition: The production of charts and maps representing spatial distributions over various areas of the earth.

Global Positioning System (GPS)

Definition: A satellite-based radio-navigation system comprised of a constellation of twenty-four satellites and their supporting ground stations, used to obtain precise positions of targets on, or near, the surface of the Earth.

Geographic Information System (GIS)

Definition: A computer-based system designed to input, store, manipulate, and output geographically referenced data.

Band

Definition: (1) A selection of wavelengths. (2) Frequency band. (3) Absorption band. (4) A group of tracks on a magnetic drum. (5) A range of radar frequencies, such as X-band, Q-band, etc.

Electromagnetic Spectrum (EMS)

Definition: The total range of wavelengths or frequencies of electromagnetic radiation, extending from the longest radio waves to the shortest known cosmic rays.

Visible Band (VIS)

Definition: The band of the electromagnetic spectrum which can be perceived by the naked eye. This band ranges from 7500 ang. to 4000 ang. Being bordered by the infrared and ultraviolet bands.

Photogrammetry

Definition: The application of photographic principles to the science of mapping. The science of obtaining reliable spatial measurements from imagery.

Imagery

Definition: The products of image forming instruments (analogous to photography).

Infrared Imagery

Definition: A reproduction of an object by imaging the infrared radiation coming from the object or reflected by the object.

Infrared Photography

Definition: The theory and technology of photography employing infrared film.

Microwave Imagery

Definition: A reproduction of an object by imaging the microwave radiation coming from the object.

Multispectral Imagery

Definition: Two or more images taken simultaneously, but each image taken in a different part of the electromagnetic spectrum.

Radar Altimetry

Definition: The science and techniques involved in using a radar altimeter for precise measurements of distance between the sensor and the surface or feature.

Raster Data

Definition: A matrix of measurements ordered by layers, columns and rows with each cell in the matrix being implicitly addressable by its coordinates (x,y).

Ratio Image

Definition: An image created by dividing the mean value of parcels of pixels in two different images of the same area.

Remote Sensing (R/S)

Definition: The science, technology and art of obtaining information about objects or phenomena from a distance (i.e., without being in physical contact with them).

Spatial data

Definition: Data that refers to a location (which may be a specific location on the Earth's surface, or relative to an arbitrary point).

Spatial Analysis

Definition: Study of spatial arrangement of points, lines, objects, etc.., in images.

Vector Data

Definition: The representation of spatial features by explicitly recording their geospatial co-ordinates and their attributes using points, lines, and polygons.

Llocal

Definition: A specific time ***t*** and location ***r*** (i.e. a location (*r,t*)) in the space/time domain *D* x *T* .

Signal to Noise Ratio (SNR, S/N)

Definition: The ratio of the level of the information-bearing signal power to the level of the noise power.

Explanation: Quantitative basis for comparing the relative level of a desired signal, such as a SAR image, to unwanted elements, traditionally taken to be additive noise. The signal-to-noise ratio may be increased (improved) by increasing the amount of signal power.

REFERENCES

Alessio G.,F.Esposito,A.Gorini,S.Porfido(1995):Detailed study of the Potentino seismic zone in the Southern Apennines.

Arno', V., C. Principe, M. Rosi, R. Santacroce, A. Sbrana, and M. F. Sheridan (1987). Eruptive History, in Somma-Vesuvius, Consiglio Nazionale delle Ricerche, Rome.

Ambrosetti P.,C.Bartolini,C.Bosi,F.Carraro,N.Cianranfi,G.Papani,L.Vezzani,A.Zanferrari and N.Zitellini(1987):Neotectonic map of Italy.

Friedemann T. Freund: Toward a Better Understanding of Non-Seismic Pre-Earthquake Phenomena

Gorny V.,Salman G., Tronin A.,Shilin B.(1998):The earth ouygoing IR radiation as an indicator of seismic activity, Proceeding of academy of sciences of the USSR

Guo Ziqi, Hu Guiwen,Qian Shuqing,Spatial detection technology applied on earthquakes impending forecast, 22nd asian conferenceon remote sensing, Singapore .

Martinelli G.,M.Mucciarelli,g.Valensise(1999):Relationship between the location of thermal springs and seismogenic faults in Apennines,Italy.

Martini M.,R.Scarpa(1983):Earthquakes in Italy in the last century

Pantosti D.and G.Valensise :Faulting mechanism and complexity of the November 23,1980,Campania Lucania earthquake,inferred from surface observations.

Pantosti, D., D. P. Schwartz and G. Valensise (1993). Paleoseismology along the 1980 Irpinia earthquake fault and implications for earthquake recurrence in the southern Apennines.

Pantosti D., G. D′Addezio, and F.R. Cinti (1993). Paleoseismological evidence of repeated large earthquakes along the 1980 Irpinia earthquake fault, Annali di Geofisica

Pergola,N and V. Tramutoli(2000):SANA:Sub-pixel Automatic Navigation of AVHRR imagery, Int.J.Remote sensing

Postpischl D. (Editor) (1985). Atlas of isoseismal maps of Italian earthquakes, Quad. della Ricerca Scientifica, Consiglio Nazionale delle Ricerche, Roma.

Qiang Zu-Ji,Dian Chang-Gong,Wang Xuan-Ji and Hu Si-Yi(1992):Satellite thermal infrared anomalous temperature increase and impending earthquake precursor.

Qiang Zu-Ji,Dian Chang-Gong, Xu Xiu-Deng(1991):Thermal infrared anomaly-precursor of impending earthquakes.

Qiang Zu-Ji,Dian Chang-Gong(1992):Satellite thermal infrared impending temperature increase precursor of Gonghe earthquake of magnitude 7.0,Quinghai province.

Stuiver, M., Reimer P. J. and Reimer R. (1998). Calib Radiocarbon calibration program.

S.Pondelli,A.Morelli,E.Boschi,Instituto nazionale di geofisica distribuzione della sismicitae aree sismogenich nel mediterraneo e in Europa

Tramutoli V.,G.Di Bello, N.Pergola,S.Piscitelli(2001):Robust satellite techniques for remote sensing of seismically active areas

Tramutoli V. (1998):Robust AVHHR Techniques for environmental monitoring:theory and applications,in earth surface remote sensing

Tronin A. (1994):Satellite thermal survey- a new tool for the study of seismoactive regions.

Tronin A. (1999): Thermal IR satellite sensor data application for earthquake research in China,Int.J.Remote sensing ,2000

Ulivieri C.,M.Castronuovo,R.Fracioni, A.Cardillo(1994):A split window algorithmfor estimated land surface temperature from satellite,Advances in space research .

Valensise G.,D.Pantosti(2001):Annali di Geofisica,database of potential sources for earthquakes larger than M5.5 in Italy

Valensise G.and D.Pantosti(2001):The investigation of potential earthquakesources in peninsular Italy.

Wang L.,C.Zhu(1984):Anomalous variation of ground temperature before the Tangsan and Haiheng earthquakes

Westaway R.and J.Jackson(1987):The earthquake of 1980november 23 in Campania Basilicata(Southern Italy).

Internet:

http://depts.washington.edu/qil/calib/ .
http//faust.ingv.it/
http://www.ga.gov.au/acres/futurewk/index.htm#NOAA
http://www.io.ingrm.it/sismomed/pingtesto.htm
http://quake.geo. berkeley .edu/ cnss/ catalo g -search.html/
http://www.inqv.it/~wwwpaleo/pantosti/eventsirpmain.html
http://www.anss.org (advanced national seismic system)
http://www.cnss.org (council of the national seismic system)
http://disaster.ceos.org (ceos disaster managemeny support group)
htpp://www.iris.edu (incorporated research institutions for seismology)

ACRONYMS AND ABBREVIATIONS USED IN THE TEXT

IR : infra-red

AVHRR :Advanced Very High Resolution Radiometer

LST : Land Surface Temperature

NOAA : National Oceanic and Atmospheric Administration

RAT : Robust AVHRR Techniques

SEVIRI :Spinning Enhanced Visible and Infrared Imager

TIR : Thermal Infra-red

GIS : Geographic Information System

GPS : Global Positioning System

R/S : Remote Sensing

MSG : Meteosat Second Generation

USGS : US Geological Survey

ESRI : Environmental Systems Research Institute

NASA : National Aeronautics and Space Administration

SAR : Synthetic Aperture Radar

RADAR : **RA**dio **D**etection **A**nd **R**anging

LIDAR : LIght Detection And Ranging

IGIS : Integrated Geographic Information Systems

GOES : The Geostationary Operational Environmental Satellite Program

GMS: Groundwater Modeling System

CEOS : Committee on Earth Observation Satellite

IGOS : Integrated Global Observation Strategy

GESS : Global Earthquake Satellite System

DEMETER : Detection of Electro-Magnetic Emissions Transmitted from Earthquake Regions

SEISMASS : Seismic Area Monitoring By Advanced **Satellite** Systems

S/N : signal-to-noise

CONTENTS